

Aim and Scope

The objective of the *Journal of Residuals Science & Technology* (JRS&T) is to provide a forum for technical research on the management and disposal of residuals from pollution control activities. The Journal publishes papers that examine the characteristics, effects, and management principles of various residuals from such sources as wastewater treatment, water treatment, air pollution control, hazardous waste treatment, solid waste, industrial waste treatment, and other pollution control activities. Papers on health and the environmental effects of residuals production, management, and disposal are also welcome.

Editor-in-Chief

P. Brent Duncan
Department of Biology
University of North Texas
Denton, TX, USA
pduncan@unt.edu

Assistant Editor

James Lee
james.lee3918@gmail.com

Editorial Advisory Board

Muhammad Abu-Orf
AECOM, USA
mohammad.abu-orf@aecom.com

Nafissa M. Bizo
City of Philadelphia Water Department
nafissa.bizo@phila.gov

Richard Dick
Cornell University, USA
rid1@cornell.edu

Eliot Epstein
Epstein Environmental Consultants
epsteinee@comcast.net

Guor-Cheng Fang, Ph.D.
Hungkuang University, Taiwan
gcfang@sunrise.hk.edu.tw

Robert Hale
Virginia Institute of Marine Science, USA
hale@vims.edu

Paul F. Hudak
University of North Texas, USA
hudak@unt.edu

Blanca Jimenez Cisneros
Inst. de Ingenieria, UNAM, Mexico
bjc@mumas.iingen.unam.mx

Julia Kopp
Technische Universitat Braunschweig,
Germany
j.kopp@tu-bs.de

Uta Krogmann
RutgersUniversity, USA
krogmann@aesop.rutgers.edu

D. J. Lee
National Taiwan University, Taiwan
djlee@ntu.edu.tw

Giuseppe Mininni
Via Reno 1, Italy
mininni@irsa.rm.cnr.it

Lynne H. Moss
CDM Smith
mosslh@cdmsmith.com

John Novak
Virginia Tech, USA
jtnov@vt.edu

Nagaharu Okuno
The University of Shiga Prefecture,
Japan
okuno@ses.usp.ac.jp

Jan Oleszkiewicz
University of Manitoba, Canada
oleszkie@ms.umanitoba.ca

Banu Örmeci
Carleton University, Canada
banu_ormeci@carleton.ca

Ian L. Pepper
University of Arizona, USA
ipepper@ag.arizona.edu

Ioana G. Petrisor
Co-Editor-in-Chief
Environmental Forensics Journal, USA
Environmental.Forensics@gmail.com

Bob Reimers
Tulane University, USA
rreimers@tulane.edu

Dilek Sanin
Middle East Technical University,
Turkey
dsanin@metu.edu.tr

Heidi Snyman
Golder Associates Africa (Pty) Ltd.,
South Africa
hsnyman@golder.co.za

Ludovico Spinosa
Consultant at Commissariat
for Env. Energ. in Region,
Puglia, Italy
ludovico.spinosa@fastwebnet.it

P. Aarne Vesilind
Bucknell University, USA
aarne.vesilind@gmail.com


Doug Williams
California Polytechnic State
University, USA
wmsengr@thegrid.net

JOURNAL OF RESIDUALS SCIENCE & TECHNOLOGY—Published quarterly—January, April, July and October by DEStech Publications, Inc., 439 North Duke Street, Lancaster, PA 17602.

Indexed by Chemical Abstracts Service. Indexed/abstracted in Science Citation Index Expanded. Abstracted in Current Contents/Engineering, Computing & Technology. Listed in ISI Master Journal.

Subscriptions: Annual \$219 per year. Single copy price \$60. Foreign subscriptions add \$45 per year for postage.

(ISSN 1544-8053)

 DEStech Publications, Inc.

439 North Duke Street, Lancaster, PA 17602-4967, U.S.A.

©Copyright by DEStech Publications, Inc. 2016—All Rights Reserved

C O N T E N T S

Research

- Study on Heavy Metal Characteristics of Soil in Phosphorus Tail** 1
YUNG-PIAO CHIU, DONG-WEI LI AND YAN-CHYUAN SHIAU
- Optimized Preparation of Directional Modified Attapulgite and its Application to Adsorbance of Humic Acid in Polluted Raw Water Effluent** 9
XIANGJUN ZOU, ZHIHONG WANG and HUI SHI LING
- Effects of Fe²⁺ and Fe³⁺ on Algal Proliferation in a Natural Mixed Algal Colony in Algae-Rich Raw Water in Southern China** 15
TAO ZHOU, ZHIHONG WANG, QUAN HU, LIFAN LIU and KESHU LUO
- Optimization of Geosmin Removal from Drinking Water Using UV/H₂O₂** 23
FENGXUN TAN, HAIHAN CHEN, DAOJI WU, NING WANG, ZHIMIN GAO and LIN WANG
- Microorganism Removal from Ballast Water using UV Irradiation** 31
Z. J. REN, L. ZHANG, Y. SHI, J. C. SHAO, X. D. LENG and Y. ZHAO
- Selective Release of Inorganic Constituents in Broiler Manure Biochars under Different Post-Activation Treatments** 37
ISABEL LIMA, K. THOMAS KLASSON and MINORI UCHIMIYA
- Improvements to Manufactured Tiles using Sewage Sludge Ash Based on Kiln Temperature and Nano-SiO₂ Additive** 49
DENG-FONG LIN, HUAN-LIN LUO, LISA Y. CHEN and SHU-WEN ZHANG
- Comparison of Energy Efficiencies for Advanced Anaerobic Digestion, Incineration, and Gasification Processes in Municipal Sludge Management** 57
A. GEZER GORGEÇ, G. INSEL, N. YAĞCI, M. DOĞRU, A. ERDİNÇLER, D. SANIN, A. FILİBELİ, B. KESKİNLER and E.U. ÇOKGÖR
- Effect of Cadmium Stress on Enzyme Activity and Concentration of Mineral Nitrogen in Soil when Growing *Quercus acutissima* Seedlings** 65
FEI HE, XIURONG GAO, NA CHEN, BAOSHAN YANG, HUI WANG and YIBING MA
- Trace Metals Risk Evaluation and Pollution Identification in Surficial Sediment from the Haikou Bay, South China Sea** 71
PING SHI, JUN SHI, LINGLONG CAO, JIAN XIE, HAITAO TIAN and YANHUI ZHAI

Study on Heavy Metal Characteristics of Soil in Phosphorus Tail

YUNG-PIAO CHIU^{1,2}, DONG-WEI LI^{3,*} and YAN-CHYUAN SHIAU^{4,*}

¹Department of Digital Media Design, Hwa Hsia University of Technology, New Taipei City 23568, Taiwan

²Department of Technology Management, Chung Hua University, Hsinchu 30012, Taiwan

³The Key Laboratory for Coal Mine Disaster Dynamics and Control, Chongqing University, 400044, China

⁴Department of Construction Management, Chung Hua University, Hsinchu, 30012 Taiwan

ABSTRACT: During the last half-century, China has produced a huge amount of mining tailings. Due to past unreasonable rapid development and exploration, these tailings still contain a considerable level of heavy metals which would transfer into surrounding soils and ground water under natural conditions posing a threat to human health and the environment. In this study, tailing samples taken from two different mining areas were analyzed via XRD, XRF, and leaching toxicity analysis. XRF analysis shows that As (Arsenic), Cu (Copper), Cd (Cadmium), Cr (Chrome), Ni (Nickel), and Zn (Zinc) are the main heavy metals in these tailing samples, while in the leachate only Cd and Zn were detected suggesting that Cu (0.0158%), Ni (0.0091%), and Cr (0.0232%) are associated to stable metal bearing-phases and consistent with the XRD analysis. Existing phases of heavy metals in tailing samples vary significantly depending on sampling locations. Our investigation on heavy metal phase and leaching properties in tailings provides clues for heavy metal pollution remediation in mining areas.

INTRODUCTION

CHINA has the second largest amount of phosphate rock resources in the world [1], but past exploitation and processing of these resources has resulted in an immense amount of waste and causes great pressure on the environment. Land application of sludge needs to be properly managed to avoid detrimental effects on micro and macro-organisms in the soil [2]. The tailings which are small in particle size and exposed to the natural environment, especially extremely tiny weathered secondary mineral kernel, can easily react with air, water, and living things [3]. Phosphate rocks are rich in heavy metals and are spreading by groundwater or rain into soil [4,5]. Therefore, the tailing deposits are a main source of soil heavy metal pollution [6]. These tailings characterized by high heavy metal content occupy a vast area of land and cover pre-existing vegetation. The spread of heavy metals also affects human health ultimately through the food chain and causes

damage to residents living in the surrounding area. The problem of soil heavy metal pollution has become severe and garnered more and more attention from researchers due to continuous exploitation of phosphate rock resources driven by local socio-economic factors [7–10]. Therefore, a better understanding of the basic characteristics of soils in a phosphorus mining area is fundamental and helpful for prevention of heavy metal pollution and to evaluate impacts on human health [11].

MATERIAL AND METHODS

Sampling

Considering that the Yunnan province has the largest amount of phosphate rock in China, samples investigated in this study were taken from both Haikou and Jinning cities in Yunnan, respectively. Regarding Haikou, tailings passed through the tank by a pressurized conveyor and eventually flowed into the tailing pond. Within this area five sampling sites were selected in a triangle zone around the end of flowing. The Jinning tailing pond is open terrain and emission of tailings were at the end of the tailing pond. In this area five soil tailing samples were selected from the tailings. Samples were collected, prepared, and analyzed

*Authors to whom correspondence should be addressed.

Dong-Wei Li: Email: litonwei@cqu.edu.cn; litonwei@qq.com; Address: College of Resource and Environmental Science, Chongqing University, No. 174 Shazhengjie, Shapingba, Chongqing, 400044, China; Phone: +86-13983379386, +86 15826021906
Yan-Chyuan Shiau: Email: ycshiau@chu.edu.tw; Address: Department of Construction Management, Chung Hua University, No. 707, Wufu Rd., Sec. 2, Hsinchu 30012, Taiwan, Phone: +886-916047376

according to methods established/recommended by the Ministry of Environment Protection, The People’s Republic of China [12].

Mineral Phase Analysis by XRD

A D8 advance X-ray diffractometer (Bruker Corporation) was used to characterize sample phases. Tailing and soil samples were first dried at room temperature and sieved to 200 mesh at least before a XRD test. By

using XRD, diffraction pattern analysis was performed to obtain composition, internal structure, and other sample information. Samples were placed into a XRD-1800 (Shimadzu Corporation) to collect X-ray Fluorescence spectra. Finally, each part of a sample was fully analyzed.

Leaching Toxicity Analysis

Leaching toxicity experiments were conducted

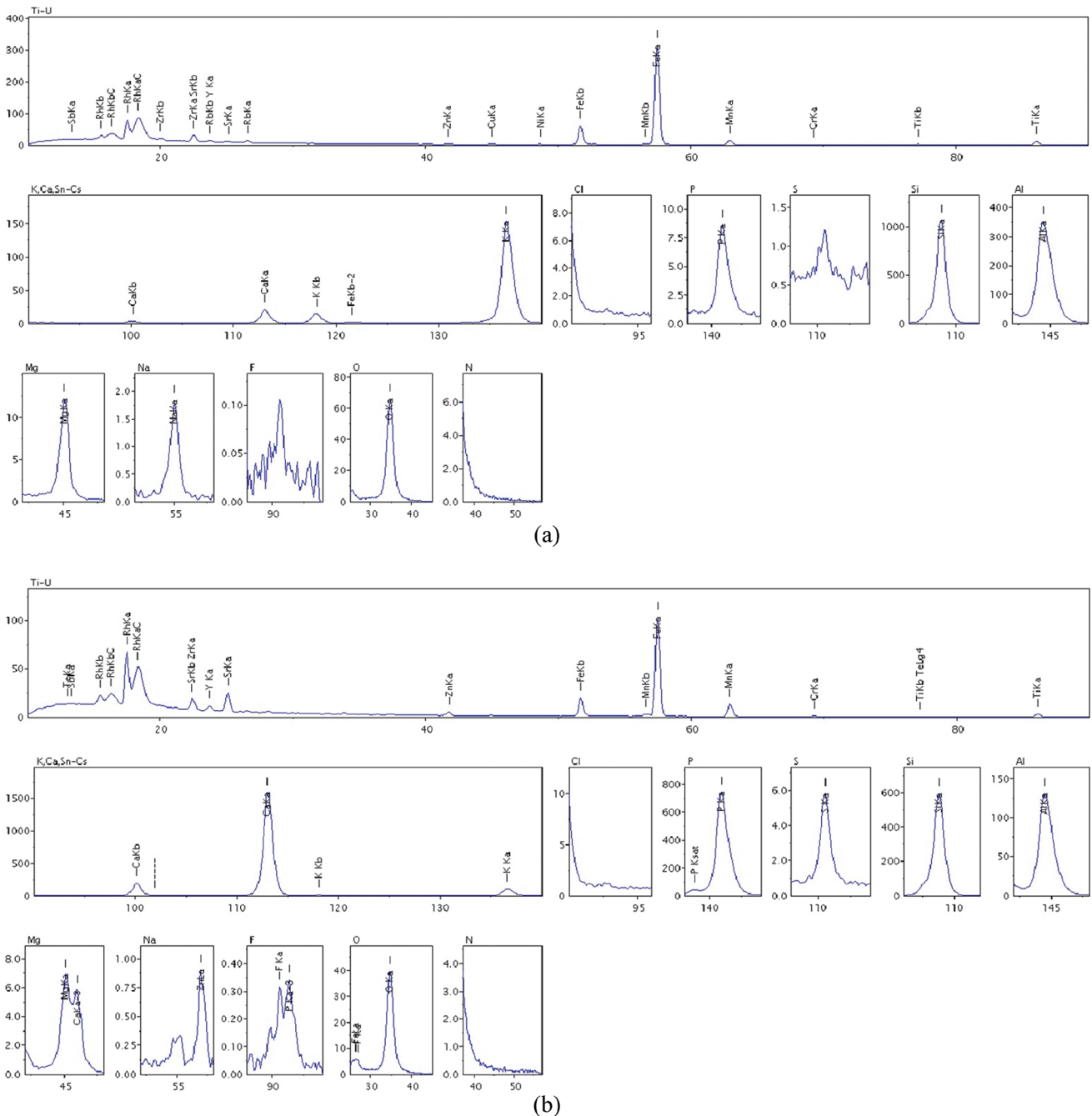


Figure 1. XRF results. (a) XRF results for Haikou samples and (b) XRF results for Jinning samples.

Table 1. The Sample in Haikou Tailings and the Sample in Jinning Tailings.

Sample in Haikou Tailings		Sample in Jinning Tailings	
Element	Percentage of Element	Element	Percentage of Element
O	40.5170%	O	47.4744%
Ca	24.2024%	Si	35.4248%
Si	15.7582%	Al	8.5428%
P	10.7975%	Fe	3.1891%
Al	3.0181%	K	2.4589%
Fe	1.5377%	Mg	1.0832%
F	1.5087%	Ti	0.5828%
K	1.3064%	Na	0.3835%
Mg	0.6148%	Ca	0.3580%
Mn	0.2682%	P	0.1904%
Ti	0.2070%	Mn	0.1789%
S	0.0978%	Zr	0.0369%
Sr	0.0560%	Cr	0.0232%
Zn	0.0265%	Cu	0.0158%
Cr	0.0264%	Rb	0.0155%
Zr	0.0182%	Zn	0.0103%
Pb	0.0133%	Ni	0.0091%
Y	0.0119%	Sr	0.0072%
As	0.0090%	Y	0.0066%
Cu	0.0050%	As	0.0056%
		Pb	0.0030%

following solid waste-extraction procedures using a leaching toxicity-sulphuric acid and nitric acid method [13]. Concentrations of heavy metals in the leachate such as As, Cu, Cd, Cr, Ni, and Zn were measured using a SK-2002B atomic fluorescence spectrometer.

RESULTS AND DISCUSSION

XRF Analysis

The XRF analysis results are seen in Table 1 and Figure 1. XRF results indicate that soil tailing samples collected near tailings contain complex components with a variety of harmful heavy metals creating a unpredictable toxic matrix. Different tailings may contain different elements [14]. According to results, all samples show high concentrations of As, Cd, Cr, Cu, Pb, and Zn. Considering their toxicities and huge amounts

of tailing materials present on the land the environmental issue of heavy metal pollution cannot be ignored.

Leaching Toxicity Analysis

To assess toxicity of tailings, ten samples from the tailings in both Haikou and Jinning were analyzed. The experiment was conducted using a sulphuric acid and nitric acid method [15]. Results are presented in Table 2.

First, As, Cu, and Pb were not detected in the leachate that used a SK-2002B atomic fluorescence spectrometer suggesting these metals reside in tailings in the form of stable (acid-resistant) phases not easily dissolved and extracted by acid solution.

Results also demonstrate leaching of other heavy metals was insignificant implying content of those exchangeable heavy metals in tailings was low. Due to decades of leaching in nature a part of heavy metals in tailings has already migrated into surrounding soils or dissolved in groundwater. Thus, the leftover exchangeable fractions of heavy metals correspondingly decreased [16–18]. Based on our experimental data and the national “Identification standard for hazardous waste leaching toxicity identification” (GB5085.3-2007) these tailing samples are not hazardous waste with negligible leaching toxicity [19]. However, considering the huge amount of the tailings particular attention should still be paid to the tailings for potential threat to the human health.

XRD Analysis

Figure 2 shows XRD patterns for studied samples. Analysis was conducted using a MDI Jade 5.0 and then searching in four PDF card libraries for comparison as follows: inorganic materials, minerals, ICSD inorganic materials, and ICSD minerals.

Major phases in tailing samples found in XRD data are as follows: (1) quartz (SiO_2) existed both in Haikou and Jinning samples (See Figure 3); (2) berlinite (AlPO_4) both in Haikou and Jinning samples as the secondary and trace phases (See Figure 4); (3) hematite (Fe_2O_3), copper oxide (CuO), lanarkite ($\text{Pb}_2(\text{SO}_4)\text{O}$), cadmium cyanide ($\text{Cd}(\text{CN})_2$), and claudetite (As_2O_3) only in Haikou (See Figure 5); (4) zinc sulfide (ZnS),

Table 2. Samples from the Tailings in Both Haikou and Jinning.

Sample	H-1	H-2	H-3	H-4	H-5	SK-1	SK-2	SK-3	SK-4	SK-5
Cd	0.08	0.39	0.07	0.14	0.09	0.2625	0.22	0.6325	0.08	0.3825
Zn	28.825	22.5	24.3	8.425	49.65	74.775	47.25	43.225	288.375	59.2

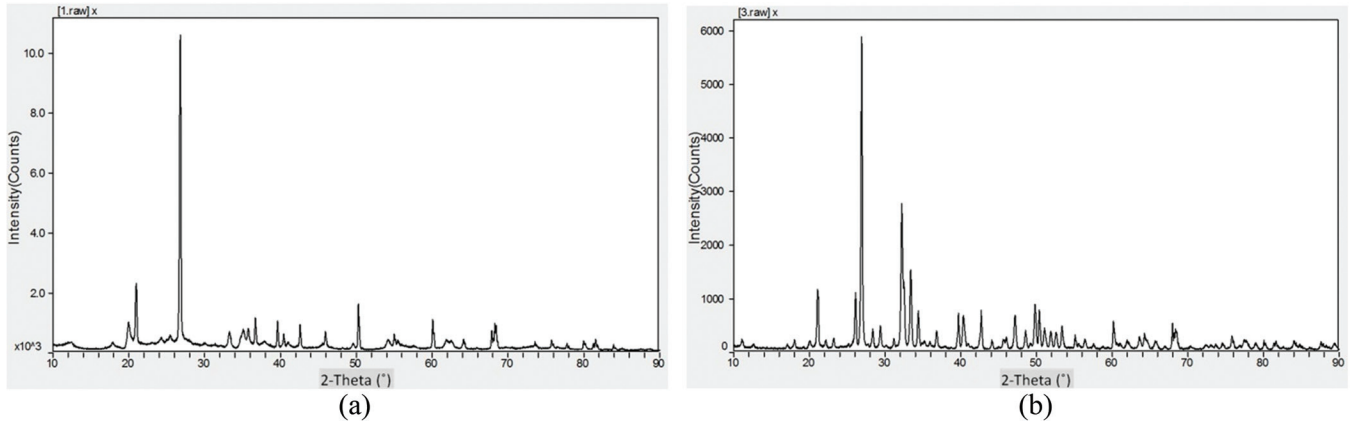


Figure 2. (a) XRD pattern for Haikou samples and (b) XRD pattern for Jinning samples.

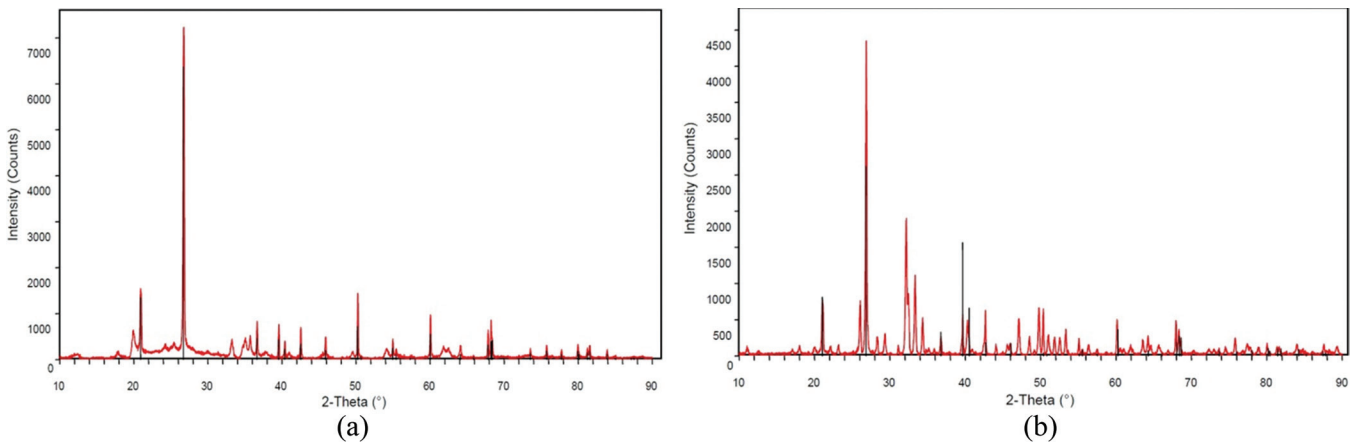


Figure 3. (a) XRD patterns of SiO_2 for Haikou samples and (b) XRD patterns of SiO_2 for Jinning samples.

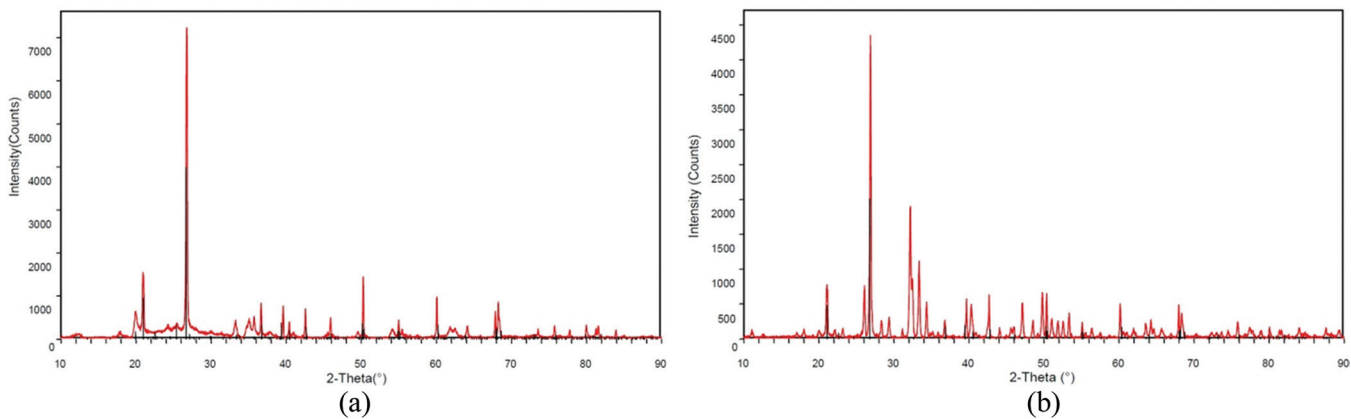


Figure 4. (a) XRD patterns of AlPO_4 for Haikou samples and (b) XRD patterns of AlPO_4 for Jinning samples.

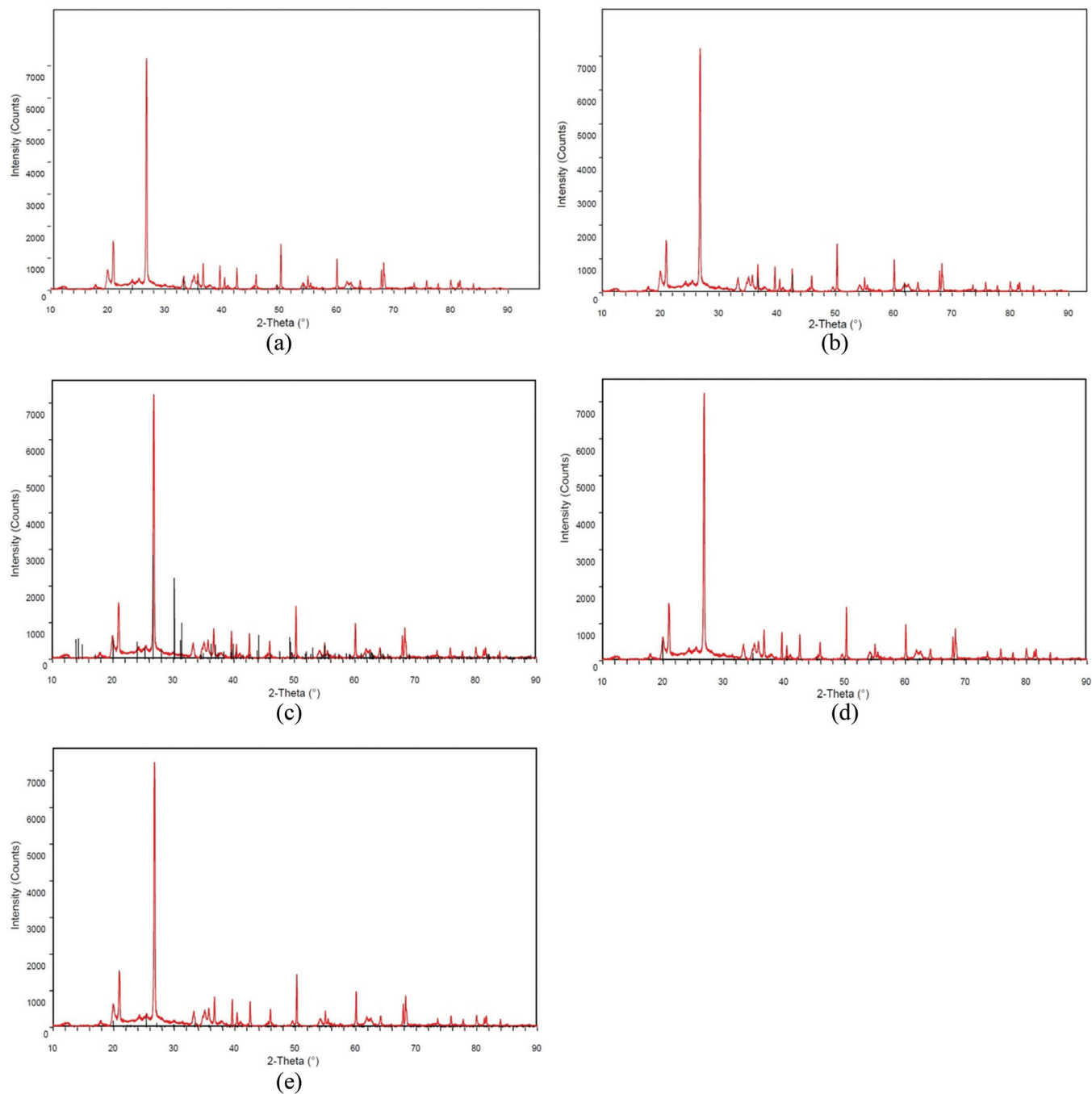


Figure 5. (a) XRD patterns of Fe_2O_3 ; (b) XRD patterns of CuO ; (c) XRD pattern of $\text{Pb}_2(\text{SO}_4)\text{O}$; (d) XRD pattern of $\text{Cd}(\text{CN})_2$ and (e) XRD pattern of As_2O_3 .

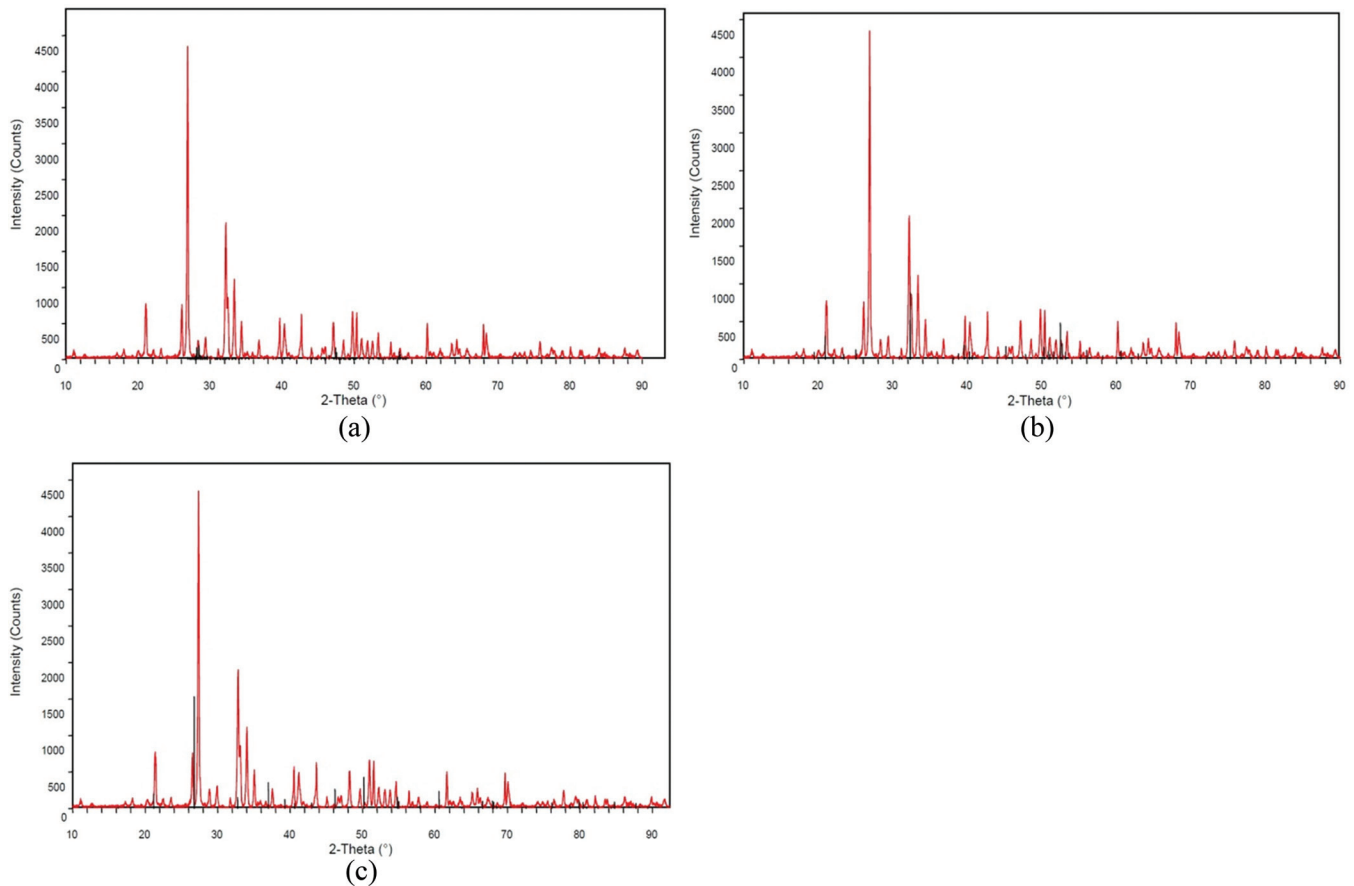


Figure 6. (a) XRD pattern of ZnS; (b) XRD pattern of FeP₄ and (c) XRD pattern of Pb(As₂O₆).

iron phosphide (FeP₄), lead diarsenate (Pb(As₂O₆)), and hydroxylapatite (Ca₅(PO₄)₃(OH)) only in Jinning samples (See Figure 6). It is evident samples contain complex phases related to local geological structure and composition related to the tailings' composition.

CONCLUSION

Three main conclusions were drawn from this study. First, XRF analysis indicates compositions of soil samples from phosphorus tailings are complicated. Although different tailings contain some different elements, all samples contained Cd, Zn, Pb, Cr, and As. Second, analysis of leaching toxicity and further investigation provided understanding that samples in tailings are not hazardous waste due to leaching toxicity based on experimental data and the national standard.

Finally, XRD analysis showed the major phase of the soil sample in tailings was quartz. Due to the large amount of tailings in the mining field they also posed potential hazards to downstream residents, farmland, livestock, food security, and drinking water. Our study reveals major phases and heavy metals in these tail-

ings which may be helpful for future environmental remediation or for understanding local pollution-related health issues.

ACKNOWLEDGEMENTS

This study was supported by the project "Investigation on Heavy Metals Polluted Biological Treatment Technology for Phosphorus Excavating Soil" from National Phosphorus Resource Development and Utilization Engineering Technology Research Center (No. 2012, National Phosphorus Center k002). The work was completed in National Key Laboratory on Coal Mine Disasters Power Science and Control, College of Resources and Environmental Science, Chongqing University.

REFERENCES

1. Li X. S. and Li Y. J., "Phosphate rock resources exploitation status and prospect in our country: Retrospect and prospect acquisition of technology in China for ten years", 2012, pp. 20–23.
2. Dindar E., Topac Sagban F. O. and Baskaya H. S., "Effects of Waste-water Sludge Amendments on Soil Enzyme Activities in Earthworm

- Cast", *Journal of Residuals Science & Technology*, Vol. 11, No. 1, 2014, pp. 9–14.
3. Zhao Y. H., Zhang T. and Cheng X. X., "Heavy Metals at a Tailing Reservoir of Sulfide Ores", *Journal of Residuals Science & Technology*, Vol. 11, No. 4, 2014, pp. 131–135.
 4. Liu D. J., Jiang S. Z. and Luo H. B., "Phosphate rock resources depletion trend and countermeasures in China", Vol. 20, No. 1, 2005.
 5. Mo X. P., Hu S. Y. and Shen J. Z., "The development of phosphorus resources industry in China", *Mineral and chemical processing*, Vol. 34, No. 8, 2005.
 6. Dudka S. and Adriano D. C., "Environmental impacts of metal ore mining and Processing: a review", *Journal of Environmental Quality*, Vol. 26, 1997, pp. 590–602. <http://dx.doi.org/10.2134/jeq1997.00472425002600030003x>
 7. Machender G., Dhakate R. and Prasanna L., "Assessment of heavy metal contamination in soils around Balanagar industrial area", *Hyderabad, India, Environment Earth Sciences*, Vol. 10, 2010, pp. 325–334.
 8. Zhuang P., Zou B. and Li N. Y., "Heavy metal contamination in soils and food crops around Dabaoshan mine in Guangdong, China: implication for human health", *Environmental Geochemistry and Health*, Vol. 31, 2009, pp. 707–715. <http://dx.doi.org/10.1007/s10653-009-9248-3>
 9. Bhattacharyya P., Tripathy S. and Chakrabarti K., "Fractionation and bioavailability of metals and their impacts on microbial properties in sewage irrigated soil", *Chemosphere*, Vol. 72, 2008, pp. 543–550. <http://dx.doi.org/10.1016/j.chemosphere.2008.03.035>
 10. Soriano-Disla J. M., Speir T. W. and Gómez I., "Evaluation of different extraction methods for the assessment of heavy metal bioavailability in various soils", *Water, Air and Soil Pollution*, Vol. 213, 2010, pp. 471–483. <http://dx.doi.org/10.1007/s11270-010-0400-6>
 11. Li D. W., Yang K. and Ke B. Q., "Review: The Prevention & Control Technology of Heavy Metal Pollution", *Disaster Advances*, Vol. 16, No. S1, 2012.
 12. Ministry of Environment Protection, The People's Republic of China, Website: <http://english.mep.gov.cn/>, 2015/09/25.
 13. Mills C., Sc M., and Eng P., "Metal Leaching Text Procedures", *Mining Intelligence & Technology*, Website: http://technology.infomine.com/enviromine/ard/Acid-Base%20Accounting/metal_leaching.htm, 2015/09/19.
 14. Liao G. L., "Heavy metals contamination characteristics in soil of different mining activity zones", *Transactions of Nonferrous Metals Society of China*, Vol. 18, No. 1, 2008, pp. 207–211. [http://dx.doi.org/10.1016/S1003-6326\(08\)60037-0](http://dx.doi.org/10.1016/S1003-6326(08)60037-0)
 15. Liu J., Wang Q. and Li D. W., "Study on Environmental Properties of the Waste Residues in Pyrite Smelting by Indigenous Method", *Research Journal of Chemistry and Environment*, Vol. 15, No. 2, 2011.
 16. Blaser P., Zimmermann S., Luster J. and Shotyk W., "Critical examination of trace element enrichments and depletions in soils: As, Cr, Cu, Ni, Pb, and Zn Swiss forest soils", *The Science of the Total Environment*, Vol. 249, No. 1-3, 2000, pp. 257–280. [http://dx.doi.org/10.1016/S0048-9697\(99\)00522-7](http://dx.doi.org/10.1016/S0048-9697(99)00522-7)
 17. Facchinelli A., Sacchi E. and Mallen L., "Multivariate statistical and GIS-based approach to identify heavy metal sources in soils", *Environmental Pollution*, Vol. 114, 2001, pp. 313–324. [http://dx.doi.org/10.1016/S0269-7491\(00\)00243-8](http://dx.doi.org/10.1016/S0269-7491(00)00243-8)
 18. Lamy L., Boutgeviset S. and Bermond A., "Soil cadmium mobility as a consequence of sewage sludge disposal", *Journal of Environmental Quality*, Vol. 22, 1993, pp. 731–737. <http://dx.doi.org/10.2134/jeq1993.00472425002200040014x>
 19. Jiao B. Q., Li D. W. and Xiao Z. J., "Analysis and Identification of the Toxicity of the Solid Waste in Chemical Industry", *Disaster Advances*, Vol.1-2, 2010, pp. 457–461.

Optimized Preparation of Directional Modified Attapulgite and its Application to Adsorbance of Humic Acid in Polluted Raw Water Effluent

XIANGJUN ZOU, ZHIHONG WANG* and HUIISHI LING

Guangdong University of Technology, Higher Education Mega Center, Panyu District, Guangzhou, Guangdong Province, China

ABSTRACT: Natural attapulgite modified using acid activation, heat treatment, and organic modification was investigated as a humic acid adsorbent and an optimal modification method was confirmed. Results suggest that acid activation should be performed first and followed by organic modification. Optimum dosage of modified attapulgite was 0.7 g/L and the humic acid removal rate reached 97%. Optimum modification conditions were as follows: acid concentration at 3 mol/L, sodium chloride concentration at 0.5 mol/L, sodium treatment duration was 2 h, modifier amount was 3%, and microwave modification time was 9 min. Modified attapulgite prepared as such may be beneficial for water treatment processes.

INTRODUCTION

In raw water, the humic acid (HA) concentration is approximately 1–12 mg/L. Humic acid is a type of negatively charged macromolecular organic matter that is soluble in alkaline conditions but insoluble in water and acidic conditions. It is important to effectively control and remove HA because it is harmful to waterworks operation and human health. For instance, HA may impart undesirable color and taste to water. Greater concern is HA may react with chlorine disinfectants to form carcinogenic by-products during chlorination of drinking water [1–5].

Currently natural inorganic minerals are a hot research topic. Most natural minerals have a high surface activity and large specific surface area displaying good adsorption during water treatment. Attapulgite is a type of natural one-dimensional nanomaterial with a special structure. Also, it is alkaline with a pH of 8–9 with abundant reserves in China. With a special fiber structure and good colloidal properties such as unique dispersibility, temperature, salt tolerance, and higher adsorption capacity, attapulgite is used to remove heavy metals and organic pollutants in the water [6–9].

Natural attapulgite clay generally cannot act as an adsorbent for removing organic material during water treatment. Its use as an adsorbent must be promoted by physical or chemical modification [10]. The objective

of modification is to remove impurities from natural attapulgite, increase its surface area and organic load, and enhance its ability to remove organic material.

During recent years the number of studies on modification of attapulgite has gradually increased in China and abroad. Attapulgite treated by coupling thermal treatment and acid activation has been studied by Frini-Srara who reached the conclusion that lengthy acid modification time requires a low optimal thermal treatment temperature. Internal structure will be broken and the gap will be closed reducing specific surface area when thermal treatment temperature exceeds 750°C [11]. Acid activation may increase attapulgite specific surface area, but excessive acid concentrations lead to a decrease in the specific surface area because newly generated pores in attapulgite will be plugged by impurities [12]. Ma used a 1 mol/L NaCl solution to exchange Ca²⁺ and Mg²⁺ cations in attapulgite, improving efficiency of exchanging surfactant for cation in attapulgite before modifying attapulgite by organic means [13]. Song reported organic modified means reduces microstructure properties of attapulgite significantly and the only loaded organic modifier on the surface of attapulgite. It did not change the internal structure of the attapulgite [14].

Existing research has shown attapulgite modified with different methods will have different adsorption effects for different organic pollutants. The goal here was to determine an optimum modification method for efficient adsorption of humic acid in slightly polluted water.

*Author to whom correspondence should be addressed.
E-mail: gdwzhihong@126.com

EXPERIMENTAL

Equipment and Materials

Equipment used in this study included a T6 series UV/vis spectrophotometer (Puxi Co., Beijing), a portable turbidimeter (Shanghai), an acidimeter (Leici Co., Shanghai), a PHS-3C (Hongyi Co., Shanghai), a DHG electrothermostatic blast oven (Jinghong Co., Shanghai), a high-temperature calcination furnace, a constant-temperature vibrator (Fuhua Co.), a microwave oven, and a low-speed centrifuge (Anhui).

Materials used included natural attapulgite (Xuyi, Jiansu, China), octadecyl trimethyl ammonium chloride (OTAC, AR), humic acid (H108498 Aladdin Industrial Corporation, Shanghai, China), kaolin, NaOH (AR), HCl (AR), and NaCl (AR).

Preparation of Modified Attapulgite

To accomplish acid activation, 45 g of natural attapulgite was added to 100 mL of HCl and vibrated for 3 h under a constant temperature of 25°C. Concentrations of HCl used were 1, 2, 3, and 4 mol/L. Attapulgite was then washed until a neutral pH was reached. It was dried for 12 h in a drying oven and then ground and passed through a 200-mesh sieve for storage. Regarding heat treatment, the attapulgite was calcined at 350°C for 3 h.

Regarding organic modification, in order to make Na⁺ exchange cation in the structure of the attapulgite improving efficiency of exchanging surfactant for cation in the structure of attapulgite sodium was first on attapulgite. The attapulgite was added to 100 mL of sodium chloride in a conical flask and then vibrated at a constant temperature of 100°C. Concentrations of NaCl were 0.5, 1, 1.5, and 2 mol/L and reaction times were 2, 4, 6, and 8 h. Attapulgite was subjected to centrifugal washing five times after sodium modification. It was then added to the 50 mL organic modifier solution and microwaved in a microwave oven. Modifier dosage was 1, 2, 3, and 4% of attapulgite. The attapulgite was microwaved for 3, 6, 9, and 12 min at a frequency of 100 Hz. It was dried for 12 h after modification and then ground and passed through a 200-mesh sieve for storage.

Sorption Experiments

Regarding preparation of standard humic acid solution, humic acid was added to a NaOH solution (pH

> 12) and then heated in a water bath at 60°C until the humic acid was completely dissolved. The solution was adjusted to a neutral pH using an HCl solution.

Regarding humic acid adsorption experiments, 100 mL of a 10 mg/L standard solution of humic acid was added to a 250 mL beaker to which an addition of 50 mg of modified attapulgite was added. The supernatant was filtered after mixing the solution at a speed of 6.7 s⁻¹ (400 rpm). It was determined to be humic acid residue and was used to calculate humic acid removal rate.

RESULTS AND DISCUSSION

Optimization of Modification Methods

Comparison of Single Modifications

According to the experimental method described here, attapulgite was activated with 3 mol/L HCl to obtain an acid-modified attapulgite. It was then calcined at high temperature to obtain heat-modified attapulgite and treated with 100 mL of 0.5 mol/L sodium chloride to obtain sodium attapulgite. It was then subjected to microwave modification with OTAC whose dosage was 3% of the attapulgite.

Under different dosages of modified attapulgite, the effect of the three types of modified attapulgite on adsorption efficiency of humic acid was investigated. Results are displayed in Figure 1.

The organic-modified attapulgite exhibited the best adsorption of humic acid at a dosage of 0.7 g/L. The removal ratio of the organic-modified attapulgite was 97.2%. However, removal rates of the acid- and

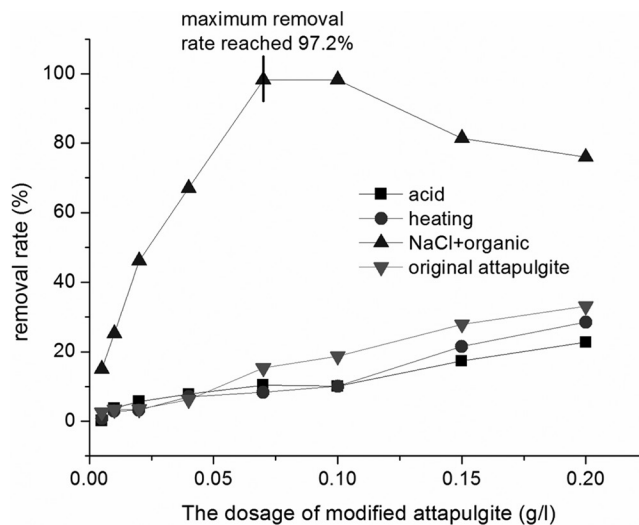


Figure 1. Effect of modified attapulgite on removal rate of humic acid.

heat-modified attapulgite were only 10.4% and 8.3%, respectively. They were even lower than the removal rate of the original clay. The function of acid modification is mainly to remove some large particles and cations in the natural clay, decrease attapulgite crystal fiber length, change crystal morphology, and increase specific surface area of the attapulgite [15] and also to remove carbonate impurities in the original clay [16].

The water of crystallization of attapulgite lies in channels on the surface. Thus, it is easy to form hydrogen bonds with the adsorbate within the channels. This creates many activation points on the attapulgite surface to which polar molecules are preferably adsorbed. Due to water molecules' strong polarity during adsorption of the liquid phase, attapulgite adsorbs water molecules first [17]. Attapulgite loses most of its water of crystallization after high-temperature calcination at 350°C [18,19]. This not only increases specific surface area, but it also increases hydrophobicity of attapulgite which improves its affinity for organic matter [17]. When the modified attapulgite dosage is greater than 1 g/L the heat-modified attapulgite is better than the acid-modified attapulgite in terms of adsorption of humic acid. See Figure 1.

To reiterate, acid and heat modification may increase specific surface area of attapulgite, but its effect on adsorption of humic acid is lower than that of the original clay. The reason is thought to be that although modified attapulgite has many microchannels and large specific surface area, adsorption properties of humic acid are restricted by crystal structure. Humic acid is a type of macromolecular organic material. Particle size is greater than 1 nm and internal channel size of attapulgite is approximately 0.37 nm × 0.64 nm. Because humic acid particles are larger than the attapulgite channel size, humic acid cannot be adsorbed into the channel surface area [20]. Surface adsorption is divided into inner and outer surface adsorption. Therefore, authors think attapulgite adsorption of humic acid is based on outer surface adsorption. Therefore, after heat and acid modification because of removal of impurities and water of crystallization the specific surface area increased while total volume decreased due to channel collapse. Thus, adsorption of humic acid was lower than that of the original clay.

Attapulgite surface is negatively charged and not conducive to adsorbing humic acid which has the same charge. By OTAC cationic surfactant modification, large-molecular-weight organic groups replace original inorganic cations improving hydrophobic properties of attapulgite [21]. This also greatly improves ad-

sorption ability of attapulgite on humic acid. Organic modification had the best adsorption performance for humic acid among the three modification methods. The sodium organic modification method was determined to be the core of modified attapulgite.

Comparison and Optimization of Combined Modification Methods

After confirming effectiveness of the organic modification method, the attapulgite was treated with a combination of three or four methods. Influence of these combined methods on adsorption properties of attapulgite on humic acid was investigated. See Figure 2.

Figure 2 suggests that combining the three types of modified methods had a very good effect on removal of humic acid when dosage of the "acid + hot + sodium organic modification" and the "acid + sodium organic modification" was 0.4 g/L. Respective removal rates were 89.5% and 86.9% showing that the two methods are equal in removal capability. Figure 1 suggest removal rate was 67.1% with the same dosage of "sodium organic modification" attapulgite which increased by 22.4% and 19.8%, respectively. Removal rates of "acid + hot + sodium organic modification" and "acid + sodium organic modification" are better than that of attapulgite treated with only one method. The combination of methods may reduce dosage.

The reason may be that acid treatment not only removed some large particles in ore and metal ions outside the structure (mainly Ca⁺ and Na⁺), but also at the same time an ionic exchange between H⁺ and hydrated cations in attapulgite was realized. This improved efficiency of sodium in the subsequent process. This in

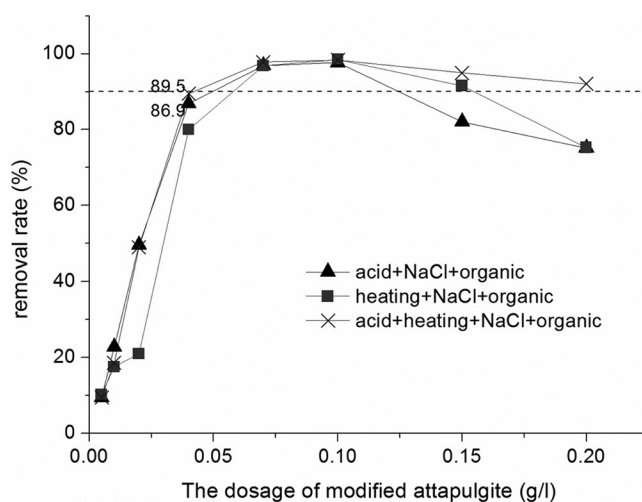


Figure 2. Effect of modified attapulgite on removal rate of humic acid.

turn improved the surfactant exchange efficiency of cations in the structure of attapulgite [22], increased attapulgite surface adhesion rate of OTAC, and finally achieved the goal of improving removal for humic acid.

Considering saving energy by reducing heat consumption, the “acid + sodium organic modification” of attapulgite was chosen.

Design of Orthogonal Experiment and Result Analysis

To determine optimal modification conditions of multiple modification methods a design using an orthogonal experiment of five factors and four levels was chosen.

Optimum modification of attapulgite conditions was decided using five factors: (1) acid concentration, (2) concentration of NaCl, (3) sodium time, (4) the dosage of modifier, and (5) modification time at four levels (See Table 1) [23]. Orthogonal experimental results are displayed in Table 2.

Evaluation index for the orthogonal experiment is removal of humic acid. See Table 2. Humic acid removal rate of the 16th group was highest at 99.77%. According to factors affecting modified attapulgite removal rate of humic acid occurs in the following order: sodium modifier dosage > sodium time > modification time > NaCl concentration > acid concentration. Combination of the process conditions is A3B1C1D3E3.

Variance Analysis and Optimal Design of Orthogonal Experiment

Further investigating significance of each factor, fluctuation of experiment data is reflected by changes of this column level and variance analysis was performed on orthogonal experiment data. See Table 3.

Table 3 shows that sodium time and dosage of the modifier have a significant impact on adsorption capacity of modified attapulgite and that acid concentration, concentration of NaCl, and modification time

Table 1. Orthogonal Design Factor Levels.

Level	Factors				
	A (mol/L)	B (mol/L)	C (h)	D (%)	E (min)
1	1	0.5	2	1	3
2	2	1	4	2	6
3	3	1.5	6	3	9
4	4	2	8	4	12

Table 2. Orthogonal Test Results and Range Analysis.

No.	Factors					Removal Rate (%)
	A	B	C	D	E	
1	1	1	1	1	1	86.83
2	1	2	2	2	2	82.66
3	1	3	3	3	3	87.14
4	1	4	4	4	4	97.26
5	2	1	2	3	4	97.05
6	2	2	1	4	3	99.27
7	2	3	4	1	2	59.38
8	2	4	3	2	1	78.14
9	3	1	3	4	2	88.33
10	3	2	4	3	1	95.76
11	3	3	1	2	4	97.80
12	3	4	2	1	3	78.96
13	4	1	4	2	3	95.02
14	4	2	3	1	4	68.12
15	4	3	2	4	1	94.06
16	4	4	1	3	2	99.77
K_1	354	367	384	293	355	
K_2	354	346	353	354	330	
K_3	361	338	322	380	360	
K_4	357	354	347	379	360	
R	6.75	7.21	15.48	21.61	7.56	

also have a significant influence. The best condition of modified attapulgite is an acid concentration of 3 mol/L, an NaCl concentration of 0.5 mol/L, a sodium time of 2 h, a modifier dosage of 3%, and a modification time of 9 min.

Effect of pH

By changing pH of the humic acid solution, effect of pH on the removal rate of humic acid was observed.

pH is an important factor affecting modified attapulgite adsorption of humic acid. Figure 3 suggest

Table 3. Orthogonal Experiment Analysis.

Source	Sum of Squares S	Freedom f	MSE S/f	Threshold F	Significance
A	107.1	3	35.68	49.91	
B	114.8	3	38.27	53.53	
C	484.5	3	161.5	225.9	#
D	1235	3	411.7	575.8	#
E	155.6	3	51.87	72.55	
Error	2.145	3	0.715		
Sum	2099	18			

Note: $F_{0.99}(3,3) = 29.46$.

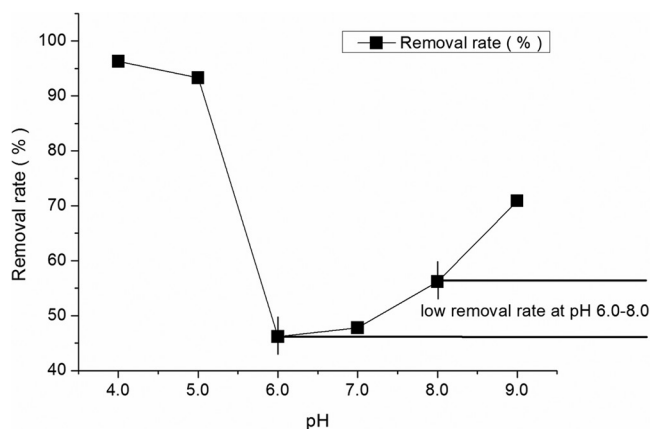


Figure 3. Removal rate of humic acid for different pH values.

that when the pH is less than 5 the humic acid removal rate may reach more than 93%. The poorest results observed were those under neutral conditions. As pH increases, humic acid removal rate again increases slowly.

A possible reason is that pH affects some organic states of existence thus changing the acid value of humic acid [24]. Zeta potential is one of the important factors that influence the stability of colloidal solutions. It is generally believed the higher the zeta potential the greater the stability of the colloidal solution. The lower the pH value the higher the electric potential of the humic acid solution [25] and the greater the stability of the colloidal solution. Nevertheless, because of the fraction of humic substances insoluble under acidic conditions, the high removal rate at acidic pH is caused by aggregation and precipitation of humic acid under acidic conditions. With increasing pH, the solubility of humic acid gradually increased. Thus, the humic acid removal rate showed a gradual downward trend as seen in the pH range of 6–8 (See Figure 4). Whereas, under alkaline conditions, humic acid possesses an increasing negative zeta potential and can therefore interact with attapulgite electrostatically with removal rate showing a slowly increasing trend.

The modified attapulgite adsorption of humic acid is best at pH values less than 5 (i.e., under acidic conditions). Under neutral conditions adsorption capacity is poor. Results correspond to the conclusions reported by Anirudhan [26] who used the modified bentonite adsorption of humic acid in water versus Wang who used the modified attapulgite adsorption of humic acid [27,28].

Modified Attapulgite Subsidence

We investigated the settling property of modified at-

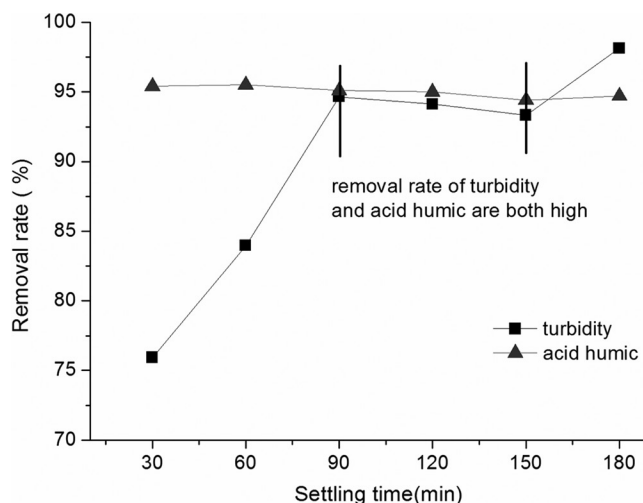


Figure 4. Settling properties of modified attapulgite.

tapulgite by detecting changes in NTU and humic acid content after 30, 60, 90, 120, 150, and 120 min standing. See Figure 4. Turbidity occurs with the addition of modified attapulgite. Therefore, to some extent the turbidity removal rate represents settling property of the modified attapulgite.

Seen in Figure 4 that within 30–90 min turbidity removal rate obviously increased with increasing settling time. Within 90–150 min, the turbidity removal rate remained at 90–95%. After 150 min turbidity removal rate increased. Therefore, the optimum settling time of modified attapulgite clay is 90 min. Effect of settling time on humic acid removal rate is very small at $\pm 1\%$. When modified attapulgite is used in a water treatment plant to strengthen the coagulation process, allowing subsidence for 90 min may have a positive effect on humic acid removal.

CONCLUSIONS

To remove natural organic matter in form of humic acid from water a comparison was made between three different methods for modifying attapulgite: acid activation, heat treatment, and sodium modification. Sodium organic modification was found to be the most effective method. Effectiveness of combined modification methods was determined and “acid + sodium organic modification” was the best modification method. Dosage of modified attapulgite was 0.7 g/L and humic acid removal rate reached 97%. Based on the orthogonal experiment, best conditions for modified attapulgite included an acid concentration of 3 mol/L, a NaCl concentration of 0.5 mol/L, a sodium time of 2 h, a modifier dosage of 3% attapulgite weight, and a modi-

fication time of 9 min. Modified attapulgite adsorption of humic acid was best under acidic conditions. Under neutral conditions, adsorption capacity was poor. The modified attapulgite showed positive settlement at 90 min conducive to improving natural organic matter removal rate in the coagulation sedimentation process.

REFERENCES

1. Yingxue Sun, Yuan Tian. 2005. "The water treatment theory of slightly polluted source and its application," M. Beijing Chemical Industry Press. (in Chinese)
2. Katsumata H., Kaneco S., Matsuno R., *et al.* 2003. "Removal of organic polyelectrolytes and their metal complexes by adsorption onto xonotlite," *Chemosphere*, 52(5): 909–915. [http://dx.doi.org/10.1016/S0045-6535\(03\)00285-6](http://dx.doi.org/10.1016/S0045-6535(03)00285-6)
3. Kam S. K., Gregory J. 2001. "The interaction of humic substances with cationic polyelectrolytes," *Water Research*, 35(15): 3557–3566. [http://dx.doi.org/10.1016/S0043-1354\(01\)00092-6](http://dx.doi.org/10.1016/S0043-1354(01)00092-6)
4. J. Wang, Y. Zhou, A. Li, L. Xu. 2010. "Adsorption of humic acid by bi-functional resin JN-10 and the effect of alkali-earth metal ions on the adsorption," *J. Hazard. Mater.*, 176: 1018–1026. <http://dx.doi.org/10.1016/j.jhazmat.2009.11.142>
5. S. Deng, R.B. Bai. 2003. "Aminated polyacrylonitrile fibers for humic acid adsorption: behaviors and mechanisms, *Environ.*" *Sci. Technol.*, 37: 5799–5805. <http://dx.doi.org/10.1021/es034399d>
6. Liya Hou. 2011. "Removal Methods and Harms of Humic Acid in Water," *Water Conservancy Science and Technology and Economy*, 17(9):68–70. (in Chinese)
7. Potgieter J. H., Potgieter-Vermaak S. S., Kalibantonga P. D. 2006. "Heavy metals removal from solution by palygorskite clay," *Mineral Engineering*, 19(5): 463–470. <http://dx.doi.org/10.1016/j.mineng.2005.07.004>
8. A. Neaman, A. Singer. 2004. "Possible use of the Sacalum (Yucatan) palygorskite as drilling muds," *Appl. Clay Sci.*, 25: 121–124. <http://dx.doi.org/10.1016/j.clay.2003.08.006>
9. J. Zhang, S. Xie, Y.S. Ho. 2009. "Removal of fluoride ions from aqueous solution using modified attapulgite as adsorbent," *J. Hazard. Mater.*, 165: 218–222. <http://dx.doi.org/10.1016/j.jhazmat.2008.09.098>
10. B. Sarkar, Y. Xi, M. Megharaj, G.S.R. Krishnamurti, R. Naidu. 2010. "Synthesis and characterisation of novel organo palygorskites for removal of p-nitrophenol from aqueous solution: isothermal studies," *J. Colloid Interface Sci.*, 350: 295–304. <http://dx.doi.org/10.1016/j.jcis.2010.06.030>
11. Frini-Srasra N, Srasra E. 2008. "Effect of heating on palygorskite and acid treated palygorskite properties," *Surface Engineering and Applied Electrochemistry*, 44(1): 43–49. <http://dx.doi.org/10.3103/S1068375508010092>
12. Barrios M S, Gonzalez V F, Rodriguez A V. 1995. "Acid activation of a palygorskite with HCl: development of physico-chemical, textural and surface-properties," *Appl. Clay Sci.*, 10(3): 247–251. [http://dx.doi.org/10.1016/0169-1317\(95\)00007-Q](http://dx.doi.org/10.1016/0169-1317(95)00007-Q)
13. Hongrui Ma, Xiaojing Han, Jiahong Wang. 2012. "Adsorption behavior of humic acid by organic modified attapulgite," *Ion exchange and adsorption*, 28 (1): 46–53 (in Chinese).
14. Yan Song, Hailing Wang, Zhaolian Zhu, Jin Sun. 2012. "Preparation and characterization of modified attapulgite and its adsorption to 4-chlorophenol," *Chin. J. Environ. Eng.*, 6(12): 4481–4486 (in Chinese).
15. Liu, Y., S. Zheng, and X. Yu. 2009. "Effect of sulfuric acid treating on properties of attapulgite clay," *Non-Metallic Mines*, 32(1): 58–59 (in Chinese).
16. Zheng, M. and A. Wang. 2007. *The Application Research of Attapulgite Clay*, Beijing, China: Beijing Chemical Industry Press (in Chinese).
17. Chen, T. 2000. "A discussion on the adsorption mechanism of palygorskite clay to pollutants in wastewater," *Geol. J. China Univ.*, 6(2): 265–270 (in Chinese).
18. Hu, S., H. Zhou, and D. Tian. 2013. "Effect of heat treatment on structure and morphology of attapulgite in Xuyi," *New Chemical Materials*, 41(6): 143–145 (in Chinese).
19. He, X., Z. Wang, and J. Nie. 2014. "Preparation of attapulgite modified by heat treatment and surfactant," *Mater. Rev.*, 28(4): 79–82 (in Chinese).
20. Chen, T., J. Wang, and C. Qing. 2006. "Effect of heat treatment on structure, morphology and surface properties of palygorskite," *J. Chin. Ceram. Soc.*, 34(11): 1406–1410 (in Chinese).
21. Zhou, Y., S. He, and H. Fan. 2008. "Research progress for adsorbing the organic pollutants in water by attapulgite," *J. Water Res. Water Eng.*, 19(2): 72–75 (in Chinese).
22. Han, X. and H. Ma. 2012. "Adsorption behaviors and mechanism of humic acid in source water on surface-functionalized-attapulgite composite," Shanxi University of Science and Technology. (in Chinese).
23. Li, L., H. Tang, and Y. Sun. 2010. "Effect of preparation on compressive strength of foamed concrete by orthogonal test," *Concrete*, 17(8): 23–24 (in Chinese).
24. Zhu, L., Y. Li, J. Zhang, and J. Wang. 1997. "The properties for organ bentonites to adsorb naphthylamine, naphthol and its application in wastewater treatment," *J. Environ. Sci.*, 17(2): 19–22 (in Chinese).
25. Guo, X. 1999. "Effects of different ions on humic acid particles potential at different pH values," *J. Humic Acid*, 7: 25–26 (in Chinese).
26. Anirudhan, T. S. and M. Ramachandran. 2007. "Surfactant modified bentonite as adsorbent for the removal of humic acid from wastewater," *Appl. Clay Sci.*, 35(3): 276–281. <http://dx.doi.org/10.1016/j.clay.2006.09.009>
27. Wang, M., L. Liao, and X. Zhang. 2012. "Adsorption of low concentration humic acid from water by palygorskite," *Appl. Clay Sci.*, 67–68: 164–168. <http://dx.doi.org/10.1016/j.clay.2011.09.012>
28. Wang, J., X. Han, and H. Ma. 2011. "Adsorptive removal of humic acid from aqueous solution on polyaniline/attapulgite composite," *Chem. Eng. J.*, 173: 171–177. <http://dx.doi.org/10.1016/j.cej.2011.07.065>

Effects of Fe²⁺ and Fe³⁺ on Algal Proliferation in a Natural Mixed Algal Colony in Algae-Rich Raw Water in Southern China

TAO ZHOU^{1,*}, ZHIHONG WANG¹, QUAN HU^{1,2}, LIFAN LIU¹ and KESHU LUO¹

¹*School of Civil Engineering and Transportation, Guangdong University of Technology, Guangzhou, Guangdong 510006, People's Republic of China*

²*Environmental Protection Engineering Research and Design Institute of Guangdong Province, Guangzhou, Guangdong 510635, People's Republic of China*

ABSTRACT: As a necessary micronutrient for algal growth, iron (Fe) has important effects on the physiological metabolism and enzymatic reactions of algae. There are various forms of iron in nature, and soluble iron exists mainly in two forms: Fe²⁺ and Fe³⁺. In this study, a series of experiments were designed to compare the effects of Fe²⁺ and Fe³⁺ on the growth of natural mixed algal colonies and single-species colonies of *Scenedesmus quadricauda*. The results show that Fe²⁺ and Fe³⁺ have different effects on the reproductive processes of these two algal populations. The optimal growth concentration of both Fe²⁺ and Fe³⁺ for natural mixed algae is 0.3 mg/L; at that concentration, algal biomass reaches its peak, with values of 1.74 × 10⁶ cells/L and 6.82 × 10⁵ cells/L for the two iron forms, respectively. At the same time, the average growth rates of these algae also reach their maximum, which are 0.3620 d⁻¹ and 0.3398 d⁻¹, respectively. The optimal growth concentrations of Fe²⁺ and Fe³⁺ for *S. quadricauda* are about 0.4 mg/L. We propose that Fe²⁺ exhibits higher biological time-effectiveness than Fe³⁺ for algal reproduction, and while Fe²⁺ and Fe³⁺ exhibit similar facilitation in the growth of both natural mixed algae and *S. quadricauda*, differences exist between their facilitation effects. The results of the study further suggest that problems involving iron uptake priority and inter-specific competition could arise during the reproductive process in mixed algal colonies.

INTRODUCTION

IN China, eutrophication and algal blooms in lakes and reservoirs have been one of the major focuses and challenges for environmental researchers. Over the last few years, severe algal blooms that strongly affect people's daily lives have broken out frequently in some intensively monitored lakes including Taihu, Chaohu, the Dian Lake, and Erhai. [1,2]. Guangdong Province, one of the most important provinces in southern China, considers algal blooms in lakes and inshore red tides as critical environmental issues. Climate features of Guangzhou include many hot days and abundant sunshine. Additionally, the surface and ground water in the Southern China has high iron content [3,4]. Induction effects and impact mechanisms of high-iron-content

fresh water on eruption of algal blooms are important research subjects needing greater understanding.

A number of studies show nutrient elements nitrogen and phosphorus in natural water is the key to affect the growth of microorganisms and total group structure [5]. However, with limited theory of iron is put forward, more and more researchers focus on how metallic elements (Fe, Cu, Zn, etc.) affect the microbial growth. Metal concentration in natural water is increasing at present due to industrial wastewater discharge and the widely application of pesticides. Different microorganisms have different demand and tolerance of metal elements [6], resulting in the change of microbial community structure and the dominant population in natural water, so a series of problems of water environment, such as blue-green algae blooms are bound to appear. Iron (Fe) is an essential micronutrient necessary for the growth of algae, and it is also an important component of plankton respiratory chains and photosynthetic electron transfer chains [7–9]. Influence of Fe on the growth of algae has also become a topic of special interest in algal bloom studies [10,11]. In natural waters, iron ex-

*Author to whom correspondence should be addressed.

Tel.: +86-020-3932-2517; Fax: +86-020-3932-2511; Postal address: The West Living District, Guangdong University of Technology, Higher Education Mega Center, Panyu District, Guangzhou, Guangdong Province 510006, China; E-mail: zhoutaoty@163.com

This work is supported by National Natural Science Foundation of China (Nos. 51308131) and Natural Science Foundation of Guangdong Province (Nos. 9151009001000048)

ists mainly in three forms: soluble iron, colloidal iron, and particulate iron. Soluble iron includes Fe^{2+} , Fe^{3+} , $\text{Fe}(\text{OH})_2^+$, $\text{Fe}(\text{OH})_2^{2+}$, $\text{Fe}(\text{OH})_3$, and the hydrolysate of Fe^{3+} . Most of the soluble Fe^{3+} exists in an organic complexing state, and most of the soluble Fe^{2+} exists in the form of hydrate; $\text{Fe}(\text{OH})_2$ and FeSO_4 account for about 4% of all soluble Fe. Fe^{2+} and most of the salt ions are soluble [12,13]. Colloidal iron, including organic complexing state iron and colloidal ferric hydroxide, as well as particulate iron, exist in biological forms and inorganic forms. Various forms of iron transmute into each other through complexation, photochemical degradation, biological absorption, decomposition, and polymerization [14]. The ionic radius of Fe^{2+} is larger than Fe^{3+} . Fe^{2+} has redox properties, and its activity is the highest among all the iron valence states [15]. The mechanisms by which algae absorb iron in different forms and different valences are not yet clear, because the forms and valences of iron in water are quite complicated. For this reason, Wang *et al.* and Fujii *et al.* carried out related studies of the valences and forms of iron on the growth of algae. Their results revealed that iron with different organic complex states and valences have different impacts on algae, and different forms of iron can transform into each other [16,17]. In natural water, soluble Fe^{3+} either formed colloidal complex iron through the process of hydrolysis and complexation, or was reduced to soluble Fe^{2+} through photodegradation, thermodynamic reduction, and enzymatic degradation, and was then absorbed and utilized by the algae. Soluble Fe^{2+} is a form that can be utilized by algae directly, while other forms need to be converted into soluble iron before being absorbed and consumed [18,19]. The above studies indicate that Fe^{2+} and Fe^{3+} can transmute into each other in natural waters, and that both of them are closely related to the growth of algae. However, we still lack intensive studies into the effects of these iron forms on algae. Researchers have been more focused on the influence of Fe^{2+} and Fe^{3+} on single species of algae. There are a great variety of algae in natural waters, and different species have different Fe acclimation ranges [11,20]. Understanding more about causes of algal blooms in waters with high iron content are needed as well as the influence of various valences of iron on growth of mixed algae in natural waters.

The natural mixed algae communities in Guangdong Province was taken as the study object to investigate the impacts of iron with different valences on the reproduction of natural mixed algae, and comparisons will be made between the results of this experiment and that of the *Scenedesmus quadricauda*. The rela-

tionship between different valences of iron and growth of algae is used to estimate effects of these iron forms on algal blooms.

MATERIALS AND METHODS

Experimental Materials

This research was conducted from July 2011 to April 2012. Natural algae groups were sampled from natural waters in the landscape lake of Guangdong University of Technology in Guangzhou Higher Education Mega Center (the center of the lake is located at 23°02'N, 113°23'E). Number of algae in raw water ranges from 4×10^4 cells/L to 5×10^5 cells/L. Dominant algal types were green algae and blue-green algae which accounted for about 48% and 40%, respectively, of the total number of algae in raw water. Proportion of algae species in raw water remained stable throughout the experimental period.

To better ascertain distribution of Fe^{2+} and Fe^{3+} in the experimental lake, continuous water quality monitoring was conducted from April 2011 to October 2012. Sampling from month to month, the research group found that Fe^{2+} content is higher in lake water samples and makes up about 60% of the total iron. The pH fluctuated around 7.0 (weakly acidic or weakly alkaline) and was thus conducive to the presence of Fe^{2+} . Samples from the lake showed stable characteristics that provided a good foundation for this experiment with natural raw water.

Main Instruments and Equipment

Experimental instruments and manufacturers are provided in Table 1.

Experimental Design and Methods

Natural mixed algae species. Using a self-designed

Table 1. Instruments and Manufacturers.

Instrument Name	Model	Manufacturer
Biological Microscope	BK5000	Chongqing Ott Optical Instrument Co., Ltd.
New Century UV-vis Spectrophotometer	T6	Beijing Puxi General Instrument Co., Ltd.
3 Fluorescence Spectrophotometer	F96PRO	Shanghai Leng Guang Technology Co., Ltd.
Low Speed Centrifuge	SC-3610	Anhui Zhongjia Scientific Instrument Co., Ltd.

and self-processed micro-universe artificial cultivation water tank for algae, the volume of water was maintained between 150–300 L and the initial biomass was set to about 5×10^4 cells/L. Culture medium was based on Zhu improved No. 10, with initial total nitrogen content of 2.0 mg/L and total phosphorus content of 0.1 mg/L. Ferrous chloride and ferric chloride were chosen as the sources of Fe²⁺ and Fe³⁺, and their initial concentrations were set at 0.2~0.7 mg/L. The major nutrients nitrogen and phosphorus were injected all at once, at the same time, researchers added 15 mL Zhu improved No. 10 culture solution to the tank each day to simulate natural water conditions.

S. quadricauda. We adopted the Algal Growth Potential Test (AGP) as our experimental method. *S. quadricauda* was seeded in 250-ml Erlenmeyer flasks using improved BG-11 medium as a culture medium. Throughout this experiment, total nitrogen (TN) and total phosphorus (TP) values were 2.5 mg/L and 0.1 mg/L, respectively. The initial algal biomass of *S. quadricauda* was about 10^6 cells/L.

Counting methods. During the experimental period we collected samples for dilution in triplicate daily at 09:00 and placed three 0.5-ml samples of diluted algae on slides. After staining, we counted the algal cells. The algal biomass was expressed using their average number (N).

The specific growth rate was calculated by following formula.

$$\mu = (\ln N_2 - \ln N_1) / (t_1 - t_2) \quad (1)$$

μ = the specific growth rate per day

t_1 and t_2 = the culture time in days

N_1 and N_2 = the algal biomass values at t_1 and t_2

RESULTS AND DISCUSSION

Comparison of Cultures with Fe²⁺ and Fe³⁺

Seen in Figure 1, significant differences exist between the experimental results using iron ions with various valences. Curves of each experiment show that the group with Fe²⁺ as its iron source (the ferrous or Fe²⁺ group) has a larger peak biomass value than the group using Fe³⁺ as its iron source (the ferric or Fe³⁺ group). The algae in the Fe²⁺ group exhibited stronger growth status.

Explanation for the aforementioned results may lie in the algae's absorption patterns of iron. In general there are two such patterns. The first is absorption at the transport points on the cell surface. Morel

et al. suggested that *Bacillariophyta* and eukaryotic autotrophs absorb soluble Fe²⁺ and Fe³⁺ through the complexation of the ligand on the cell surface [19,21]. Soluble Fe²⁺ and Fe³⁺ diffuse to the cell surface and then the complexation takes place at the transport point in the cell membrane; next, soluble iron is transferred into the cells. Among all the valences of iron, Fe²⁺ is the most active, which could be the result of its faster complexation speed compared with that of Fe³⁺. For this reason, Fe²⁺ can be better absorbed by algae and thus can accelerate their growth. The second absorption pattern is siderophore complexation absorption. Siderophores come into being when bacteria, fungi, and Gramineae plants isolate iron from the external environment; siderophores are low-molecular-weight compounds that show strong affinity for Fe³⁺ [22]. The siderophores secreted by algae will compete with other complexing agents for Fe³⁺ and draw it into the siderophore complex; next, the siderophore complex will be transferred into the cells, and the Fe³⁺ will then be released and deoxidized to form Fe²⁺; finally, the Fe²⁺ will be absorbed by the algae [14]. The direct addition of Fe²⁺ in this experiment eliminates the transformation process from Fe³⁺ to Fe²⁺, which reduces energy consumption and further promotes the growth of algae; in this experiment, Fe²⁺ complexes with siderophores directly and is then transferred into cells and released.

Comparing Effects of Fe²⁺ and Fe³⁺ on the Growth of Natural Mixed Algae

Algae exhibited differences in the concentration threshold of different iron valences. Our experiment primarily investigated the effects of Fe²⁺ and Fe³⁺ on the peak biomass and the average growth rate of the algae when the initial iron concentration was within the range of 0.2~0.7 mg/L, thus associating the correlation of the peak and the growth rate of mixed algae species with the initial concentration. See Figures 2 and 3.

Seen in Figure 2, effects of Fe²⁺ and Fe³⁺ on the growth of algal biomass were similar. Algal biomass first increased to a peak and then decreased with increasing Fe concentration. However, the range was different. Figure 3 shows that the curve of the Fe²⁺ group is higher than the curve of the Fe³⁺ group at all Fe concentrations. This shows that the average growth rate of algae in the Fe²⁺ group was higher than Fe³⁺ group: when the initial iron form was Fe²⁺, the algal biomass and the growth rate reached their highest levels at a concentration of 0.3 mg/L, when they were about 1.74×10^6 cells/L and 0.3620 d^{-1} , respectively. When the

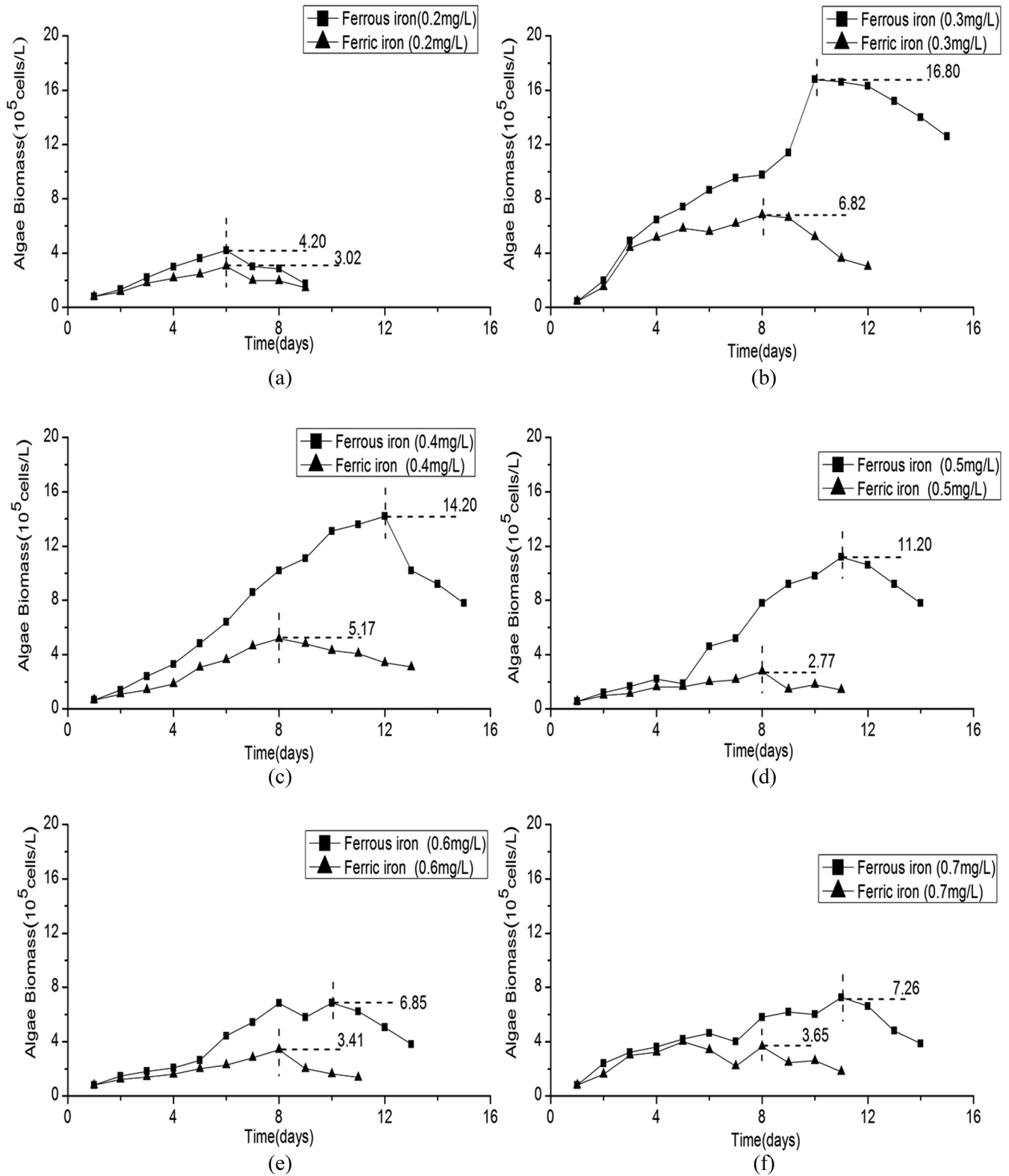


Figure 1. Effects of Fe^{2+} (ferrous iron) and Fe^{3+} (ferric iron) on the growth of algae.

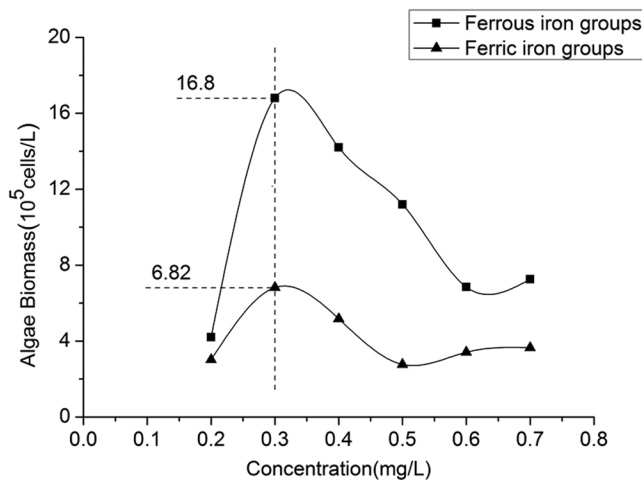


Figure 2. Effects of Fe^{2+} , Fe^{3+} , and different initial concentrations on algal biomass peak.

initial concentration of Fe^{2+} was > 0.3 mg/L, the biomass levels and the growth rate decreased slightly with increasing Fe concentration. When the initial concentration of Fe^{2+} reached 0.6 mg/L, the biomass level was about 6.85×10^5 cells/L. Similarly, when the initial iron form was Fe^{3+} , the biomass peak also occurred at a concentration of 0.3 mg/L with about 6.82×10^5 cells/L. It reached its maximum growth rate of 0.3398 d^{-1} at the same time. After that, biomass decreased slowly as the Fe concentration increased to 0.5 mg/L, with about 2.77×10^5 cells/L.

It was clear that the change in algal biomass showed a trend of “promoting-inhibiting-slowly promoting” in the presence of different forms of iron. The change thresholds for growth were 0.3 mg/L and 0.6 mg/L in culture conditions with Fe^{2+} , and 0.3 mg/L and 0.5 mg/L in culture conditions with Fe^{3+} . This shows that trace metal elements have a double effect on algae pro-

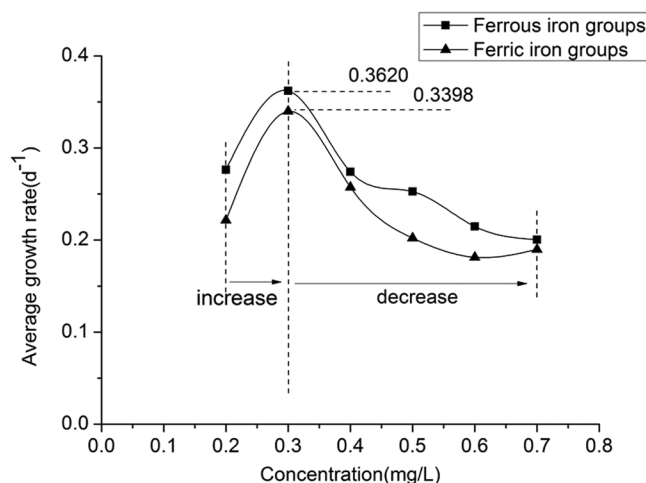


Figure 3. Effects of Fe^{2+} , Fe^{3+} , and different initial concentrations on average algal growth rate.

liferation. At low concentrations (less than 0.3 mg/L), iron is a key inhibitory factor on the multiplication process of algae, and it affects the absorption of other nutrients. Thus, the growth rate and algal biomass were small at low concentrations [23]. As the concentration of iron reached 0.3 mg/L, trace elements, nutrients, and algae achieved a dynamic balance between supply and demand, and the average growth rate of the algae and the algal biomass reached a maximum. At that point, the mass ratio of TN:TP:TFe was 20:1:3, and the molar ratio was 79:1:3. Nonetheless, the proliferation of algae was inhibited when the concentration was higher than a certain level.

Comparison of the AGP Results with Results from Pure *S. quadricauda*

The investigation also explored the impacts of Fe^{2+} and Fe^{3+} in various initial concentrations on the algal biomass value of *S. quadricauda* and on that species’ average growth speed. These results are shown in Figures 4 and 5.

According to Figure 4 iron forms with different valences and initial concentrations have different effects on the algal biomass of *S. quadricauda*. When the initial iron form was Fe^{2+} and its concentration was increasing, the general trend of algal biomass first increased and then decreased; algal biomass reached its maximum (2.90×10^8 cells/L) when the concentration of Fe^{2+} was 0.4 mg/L. When the initial iron form was Fe^{3+} , the algal biomass values exhibited no significant variability during the entire experiment; the peak value (3.74×10^7 cells/L) occurred when the Fe^{3+} concentration was 0.4 mg/L.

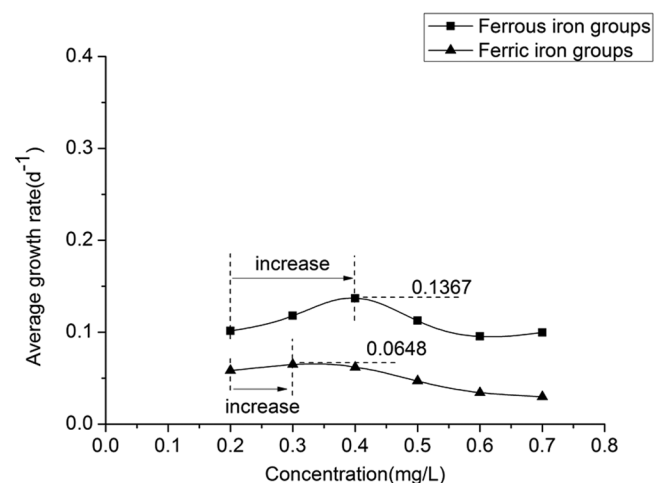


Figure 4. Effects of Fe^{2+} , Fe^{3+} , and different initial concentrations on average growth rate of *Scenedesmus quadricauda*.

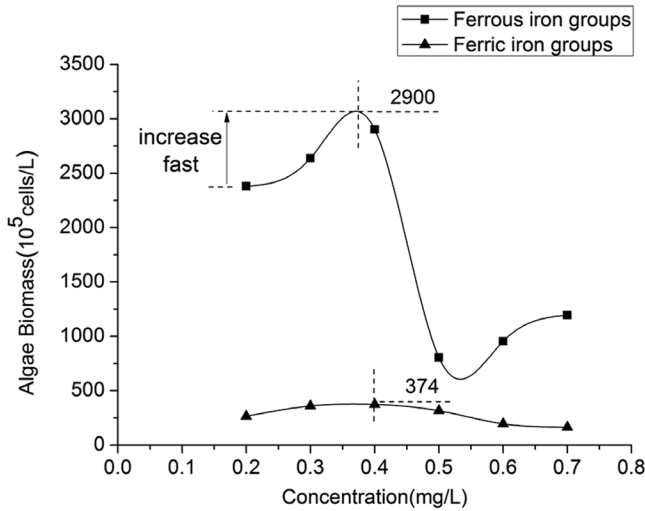


Figure 5. Effects of Fe^{2+} , Fe^{3+} , and different initial concentrations on growth of algal biomass of *Scenedesmus quadricauda*.

Figure 5 shows that the maximum average growth rate (0.1367 d^{-1}) of the Fe^{2+} group occurred when the concentration was 0.4 mg/L ; for the Fe^{3+} group, the maximum growth rate was about 0.0648 d^{-1} when the concentration was 0.3 mg/L (the rate at 0.4 mg/L was about 0.0618 d^{-1}). Based on Figures 4 and 5, the optimal Fe concentration for *S. quadricauda* was about 0.4 mg/L , at which concentration of the average growth rate and the biomass value reach their maxima.

Through a comprehensive comparison of the data presented in Figures 2, 3, 4, and 5, we can see that within the range of experimental concentrations, the algal biomass and average growth rate curves of both natural mixed algae and of *S. quadricauda* were consistent: the curve of the Fe^{2+} group was always above the curve of the Fe^{3+} group. In other words, at the same concentration, the algal biomass and average growth rate of the Fe^{2+} group were always larger than that of the Fe^{3+} group. This means that for natural mixed algae, Fe^{2+} surpassed Fe^{3+} in its effects, and the same was true for *S. quadricauda* [24]. This can be explained by the complicated and variable character of natural mixtures of algae. Since each algal species differs in its preferred living conditions and encounters different initial valences and concentrations of Fe [25,26], competition among the species has been magnified. Under different culture conditions, differently advantaged algal species will accumulate and play a leading role, and will reproduce at different rates compared with a single-species algal colony. For example, *Chlamydomonas* and *Oscillatoria tenuis* are sensitive to low Fe concentrations, while *S. quadricauda* and *Microcystis aeruginosa* survive well in high concentrations, and

this may be the main reason behind the difference of threshold between natural mixtures of algal species and *S. quadricauda* alone.

Discussion of Algae Iron Absorption Mechanisms

In light of the different effects of different iron valence states on algal growth, our research group conducted a further study of the iron absorption patterns of algae using the Franklin separation method [27], and we chose *S. quadricauda* with an initial Fe^{2+} concentration of 0.4 mg/L as the experimental condition. Fe was divided into solution iron, adsorption iron, and adsorption iron, and the relationships between algal biomass and the different forms of iron during the experimental period are shown in Figure 6.

According to Figure 6, during the early stage of cultivation the concentration of solution iron was sharply reduced from 0.3712 to 0.0608 mg/L , and this reduction slowed after the 10th day. Previous research has shown that algae use iron in two main processes: replacement of iron and protein trafficking. There is a divalent metal ion transporter in the algal cytomembrane, and it has two binding sites for iron. Therefore, a possible explanation for our observations is that during the earlier stage of cultivation, *S. quadricauda* was absorbing divalent metal ions mainly through membrane protein transport. The sharp reduction of solution iron was because the transport protein binding sites were abundant enough for solution iron to enter the algal cells smoothly through the transport proteins. On the 13th day, *S. quadricauda* entered the logarithmic growth phase with a rapid increase of algal biomass from $1 \times 10^5 \text{ cells/L}$ to $2.5 \times 10^8 \text{ cells/L}$. However, the concen-

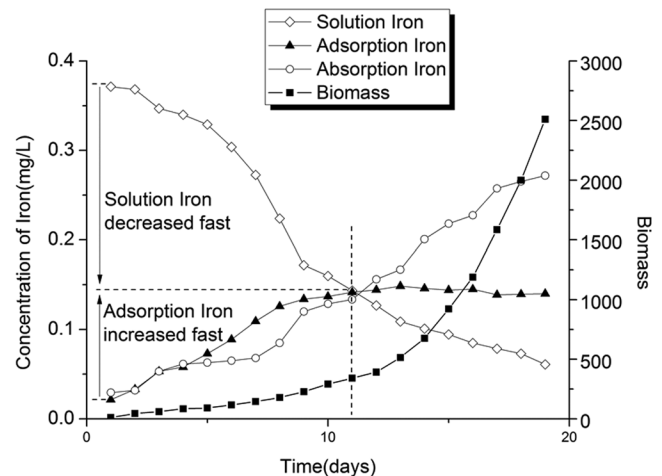


Figure 6. Relationships between different forms of iron and algal biomass.

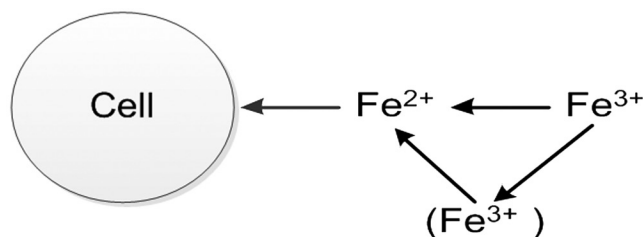


Figure 7. Diagram of Shaked's iron absorption model.

tration of adsorption iron became smooth and steady after the 12th day when it reached 0.14 mg/L, while the concentration of absorption iron kept increasing with increasing biomass. The reason for this result seems to be that the algae's need for nutrients was greater during the logarithmic phase. However, the transfer rate of the membrane was limited by the quantity of translocator molecules and not enough iron could be transported to support the algae's growth. At that point, the absorption of iron gradually gave way to iron removal. When adsorption iron and absorption iron reached a dynamic balance, the transfer rate of the membrane proteins stabilized.

According to the iron absorption model for phytoplankton suggested by Shaked *et al.* [28], seen in Figure 7, the absorption and utilization of iron is accomplished by converting Fe^{3+} to Fe^{2+} and then absorbing and utilizing the Fe^{2+} . However, it doesn't give a clear description of the iron uptake and conversion process inside algae's cytomembrane. Based on the changing relationship of intracellular and extracellular iron concentrations in *Scenedesmus*, shown in Figure 6, our research group attempted to further revise this iron absorption model. As shown in Figure 8, algal iron utilization consists of two processes: the replacement of iron and protein trafficking. The replacement of iron is centered on sulfur (S) and involves a replacement reaction with an outside iron complex before the combined FeS is transported into the cell. The second process, protein trafficking, can be divided into Fe^{3+} reduction and Fe^{2+} transshipment: different forms of iron are converted to Fe^{2+} through biochemical action and chemical reduction reactions, and then the Fe^{2+} is

transported into the cells by means of divalent metal ion transporters. When there was Fe^{2+} in the water, protein trafficking was the main absorption method. When extracellular absorption of Fe^{2+} became steady, iron replacement was the main absorption method.

CONCLUSION

In this experiment, the optimum iron concentration for the growth of natural mixed algae was found to be 0.3 mg/L. At this optimum concentration, algal biomass of the Fe^{2+} group and Fe^{3+} group reached 10^6 cells/L and 10^5 cells/L, and the average growth rate reached $0.3620 d^{-1}$ and $0.3398 d^{-1}$, respectively. Compared with Fe^{3+} , Fe^{2+} is more advantageous to algal growth. Algae proliferated faster, had a higher biomass peak and a faster average growth rate, and the growth cycle extended 2 to 3 days longer with Fe^{2+} . The algal biomass levels showed a trend of "promoting-inhibiting-slowly promoting" in different concentrations of iron. On the basis of our experimental data, we recommend modifications to the phytoplankton iron absorption model, and suggest that the absorption and utilization of iron by algae involves two main processes: protein transport and iron replacement. The absorption and utilization of Fe^{2+} is mainly by means of protein transport.

ACKNOWLEDGMENTS

The financial support of the National Natural Science Foundation of China (No. 51308131) and the Natural Science Foundation of Guangdong Province (No. 9151009001000048) are appreciated.

REFERENCES

- Jiang, G. Z., and Y. Li. 2009. "Research Progress of Water Bloom Cause and Preventive Measures," *Journal of Environmental Science and Engineering*, 12(3):15–20.
- Shi, D. 2005. "The problems and countermeasures of prevention and control of lakes Eutrophication," *Resource development and market*, 21(1):17–18.
- Huang, G., J. C. Sun, J. H. Jing, S. Wang, X. Chen, Y. X. Zhang, and

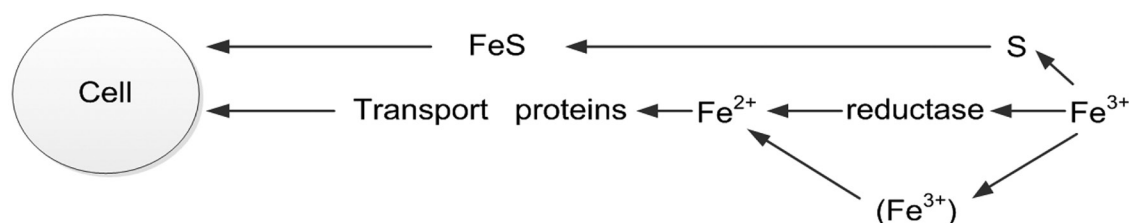


Figure 8. Revised diagram of the iron absorption model.

- X. B. Di. 2008. "Distribution and origin of iron in groundwater of the Pearl River Delta region," *Geology in China*, 135:531–538.
4. Zhang, Y., J.C. Sun, G. X. Huang, J. H. Jing, X. Chen, J. T. Liu, and Y. X. Zhang. 2011. "A preliminary study on the background value of groundwater environment in the Pearl River Delta region," *Geology in China*, 38:190–196.
 5. Chao, Y., J. Zhang, L. Wu, Y. Z. Liu, and G. Ge. 2015. "Effects of Heavy Metal and Nutrients on Benthic Microbial Communities in Freshwater Sediment of Poyang Lake (China)," *Journal of Residuals Science & Technology*, 12(2):105–111. <http://dx.doi.org/10.12783/issn.1544-8053/12/2/11>
 6. Wu, Q. Q., G. Q. Liu, X. L. Zheng, and J. G. Ren. 2015. "Screening of Heavy Metal Tolerant Microbes in Sludge and Removal Capability of Lead," *Journal of Residuals Science & Technology*, 12(2):85–91. <http://dx.doi.org/10.12783/issn.1544-8053/12/2/7>
 7. Chappell, P. D., J. W. Moffett, A. M. Hynes, and E. A. Webb. 2012. "Molecular evidence of iron limitation and availability in the global diazotroph *Trichodesmium*," *The ISME Journal*, 6:1728–1739. <http://dx.doi.org/10.1038/ismej.2012.13>
 8. Fraser, J. M., S. E. Tulk, J. A. Jeans, D. A. Campbell, T. S. Bibby, and A. M. Cockshutt. 2013. "Photophysiological and photosynthetic complex changes during iron starvation in *Synechocystis* PCC 6803 and *Synechococcus elongatus* PCC 7942," *PLoS ONE*, 8(3): e59861. <http://dx.doi.org/10.1371/journal.pone.0059861>
 9. Xu, H., G. W. Zhu, B. Q. Qin, and H. W. Paerl. 2013. "Growth response of *Microcystis* spp. to iron enrichment in different regions of Lake Taihu," *Hydrobiologia*, 700: 187–202. <http://dx.doi.org/10.1007/s10750-012-1229-3>
 10. Chen, S. G., and Z. H. Wang. 2009. "Study on the incentive trend of typical trace metal elements in algae," *Environmental Science & Technology*, 12:166–170.
 11. Yao, B., B. D. Xi, C. M. Hu, J. T. Ding, J. T. Zhang, Q. G. Xu, and H. L. Liu. 2010. "Summary of effects of iron limitation on phytoplankton growth and community composition," *Ecology and Environmental Sciences*, 19(2): 459–465.
 12. Xing, W. June 2007. "Ecophysiological Effects of Iron on Bloom-forming Cyanobacteria," Graduate School of the Chinese Academy of Sciences, Beijing.
 13. Fernandez-Otero, E., and C. Pohl. 2012. "Iron distribution and speciation in oxic and anoxic waters of the Baltic Sea," *Marine Chemistry*, 145(147):1–15.
 14. Kong, Y., P. Zou, L. M. Song, Z. Wang, J. Q. Qi, L. Zhu, and X. Y. Xu. 2014. "Effects of iron on the algae growth and microcystin synthesis," *Chinese Journal of Applied Ecology*, 25(5):1533–1540.
 15. Hinsinger, P. 1999. "Bioavailability of trace elements as related to root-induced chemical changes in the rhizosphere," presented at *Proceedings of extended abstracts of 5th international conference on the biogeochemistry of trace elements*, Vienna, Austria, 1999.
 16. Wang, M. H., N. Wang, X. F. Yuan, J. J. Geng, Y. C. Li, and X. R. Wang. 2007. "Effects of Different Forms of Iron on Growth of *Microcystis aeruginosa* and Bioavailability of Iron," *Journal of Agro-Environment Science*, 26(3):1029–1032.
 17. Fujii, M., A. L. Rose, T. Omura, and T. D. Waite. 2010. "Effect of Fe (II) and Fe (III) transformation kinetics on iron acquisition by a toxic strain of *Microcystis aeruginosa*," *Environmental Science & Technology*, 44:1980–1986. <http://dx.doi.org/10.1021/es901315a>
 18. Yang, M. June 2008. "A preliminary study on available iron abundance in relation to the formation of blue algae bloom in Taihu Lake," Zhejiang University, Hangzhou.
 19. Morel, F. M. M., A. B. Kustka, and Y. Shaked. 2008. "The role of unchelated Fe in the iron nutrition of phytoplankton," *Limnology and Oceanography*, 53:400–404. <http://dx.doi.org/10.4319/lo.2008.53.1.0400>
 20. Sun, X. W., H. X. Weng, and J. F. Chen. 2007. "Potential effect of sedimentary iron-phosphorus accumulation on frequent algal bloom in the Pearl River Estuary," *Science in China, Series D: Earth Sciences*, 50(3):453–461. <http://dx.doi.org/10.1007/s11430-007-2042-0>
 21. Morel, F. M. M., R. J. M. Hudson, and N. M. Price. 1991. "Limitation of productivity by trace metals in the sea," *Limnology and Oceanography*, 36:1742–1755. <http://dx.doi.org/10.4319/lo.1991.36.8.1742>
 22. Hider, R. C., and X. Kong. 2010. "Chemistry and biology of siderophores," *Natural Product Reports*, 27:637–657. <http://dx.doi.org/10.1039/b9066679a>
 23. Philip, B. 2004. "Ironing out algal issues in the southern ocean," *Ocean Science*, 304(5669):396–397.
 24. Hu, Q., Z. H. Wang, L. F. Liu, D. Gao, and Y. Guo. 2014. "Study of effect of different valence states of iron on the growth of *Scenedesmus quadricauda* and mechanism," *Water Supply and Drainage*, 40(1):115–120.
 25. Liu, J., H. J. Shen, Y. Q. Xu, and K. Feng. 2008. "Effect of Fe on the growth of *Scenedesmus quadricauda*," *Environmental Pollution and Control*, 30(8): 61–64.
 26. Wang, P., and Z. L. Hu. 2009. "Mechanism of Heavy Metal Tolerance and Binding Properties in *Chlamydomonas*," *Environmental Science & Technology*, 32(2):84–89.
 27. Franklin, N. M., J. L. Stauber, and S. J. Matkovich. 2000. "pH dependent toxicity of copper and uranium to a tropical freshwater alga (*Chlorella* sp.)," *Aquatic Toxicology*, 48:275–289. [http://dx.doi.org/10.1016/S0166-445X\(99\)00042-9](http://dx.doi.org/10.1016/S0166-445X(99)00042-9)
 28. Shaked, Y., A. B. Kustka, and F. M. M. Morel. 2005. "A general kinetic model for iron acquisition by eukaryotic phytoplankton," *Limnology and Oceanography*, 50:872–882. <http://dx.doi.org/10.4319/lo.2005.50.3.0872>

Optimization of Geosmin Removal from Drinking Water Using UV/H₂O₂

FENGXUN TAN¹, HAIHAN CHEN, DAOJI WU, NING WANG, ZHIMIN GAO and LIN WANG

¹School of Municipal and Environmental Engineering, Shandong Jianzhu University, Jinan250101, China

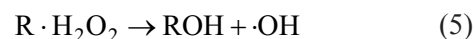
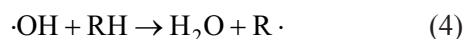
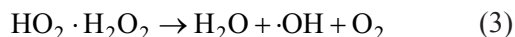
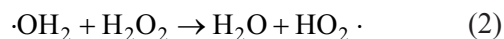
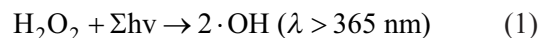
ABSTRACT: Geosmin (GSM) is a common odor-causing compound in drinking water with a low odor threshold (10 ng/L). Since conventional treatment processes cannot effectively remove it, both laboratory experiments and pilot trials were performed in this study to evaluate UV/H₂O₂ advanced oxidation process in GSM removal from drinking water. Results demonstrated removal efficiency of GSM increased with an increase in H₂O₂ concentration. GSM was reduced from 582 ng/L to below the detection limit (5 ng/L) after 8 min of reaction with 3.92 mg/L of H₂O₂. GSM was reduced from 514 ng/L to 8 ng/L after 8 min of reaction with 1.93 mg/L of H₂O₂. Degradation of GSM conformed to first-order kinetics. Data obtained from pilot trials were analyzed with Design-Expert software and optimal operation conditions were determined (H₂O₂ concentration of 7.5 mg/L, UV intensity of 400 mJ/cm², and GSM concentration of 300 ng/L) for the highest GSM removal percentage of 97.14%. Reaction rate between UV/H₂O₂ and GSM was determined using the same software fitting experimental data.

INTRODUCTION

AGRICULTURAL, municipal, or industrial waste discharge may cause eutrophication in natural waters promoting growth of cyanobacteria and actinomycetes [1], both of which can generate geosmin (GSM) which is one of the most common odor-causing compounds in drinking water [2]. GSM severely reduces drinking water quality and is difficult to remove by conventional treatment processes [3]. Once over the odor threshold (10 ng/L) it gives off an earthy smell in water [4]. Even aeration (air stripping) which is generally effective for volatile compounds is in this case not the treatment of choice due to a low Henry's coefficient (6.66×10^{-5} m³/mol) for GSM [5]. Molecular geometry of GSM is a kind of saturated bicyclic alcohol with two methyls [6]. The structure of a tertiary alcohol like GSM highly resists common disinfectants and oxidants such as chlorine, chlorine dioxide, and potassium permanganate [7–10]. One solution to this problem is ozone/activated carbon treatment. However, it increases cost and does not perform well in many cases [11].

As a potential alternative, advanced treatment UV/H₂O₂ technology was originally used in organic wastewater treatment and began application to drinking wa-

ter treatment in 1980s [12]. It has been widely studied in treating organic pesticides, disinfection byproducts (DBPs), and endocrine disruptors but rarely in removal of GSM. Photochemical oxidation process of UV/H₂O₂ is summarized with Equations (1)–(5) [13].



H₂O₂ absorbs ultraviolet light and the O–O bond is cleaved, generating free hydroxyl radicals. With an oxidation potential of 2.8 V, ·OH is the second strongest oxidizing agent in nature after fluorine. It can eventually mineralize organic matter into water, carbon dioxide, and inorganic salts. This is also the mechanism related to how GSM is degraded using UV/H₂O₂ technology [14]. Compared to ozone/activated carbon treatment, UV/H₂O₂ works under mild reaction conditions and occupies smaller space without producing byproducts [15–16].

Design-Expert (Version 9, Stat-Ease, Inc. 2015) is a

*Author to whom correspondence should be addressed.
Email: 530431028@qq.com

statistical experimental design software that may help to optimize the process. It can establish a continuous variable surface model, it can evaluate influence for the process of factors and their interactions, it can determine optimal level range, and it has a required test group which is relatively few. It is more intuitive than orthogonal design and better reflects the dependent variable excellent value [17].

In this study, the feasibility of using UV/H₂O₂ to remove GSM and the effects of UV intensity and H₂O₂ concentration on GSM removal from drinking water was investigated. It was analyzed with Design-Expert software and optimal operation conditions were determined.

MATERIALS AND METHODS

Materials and Equipment

Raw water (See Table 1) used in this study was taken from charcoal and sand filter effluent from the Yuqing Drinking Water Treatment Plant in Jinan, Shandong, China.

The plant is facing a seasonal odor problem with GSM concentrations ranging from 50–150 ng/L. The GSM and catalase used in this study was purchased from Wako Pure Chemical Industries with a purity over 98%.

Devices used in laboratory experiments included a UV system (Trojan Technologies Inc., Canada using a

Table 1. Characteristics of raw water taken from Yuqing Drinking Water Treatment Plant.

pH	Turbidity (NTU)	TOC (mg/L)	UV254 (cm ⁻¹)	UVT
8.05	0.624	1.9	0.036	0.92

low pressure UV lamp with a wavelength of 254 nm, power of 70 W, and influence of 86 mJ/cm²), circulating pumps, storage tanks and a piping distribution system. Devices used in the pilot trial included a UV system (low pressure UV lamps with a wavelength of 254 nm, a total power of 2000 W, and influence of 250–450 mJ/cm²), dosing pumps, suction pumps, and piping as seen in Figure 1.

GSM and DBPs were determined using solid phase extraction-gas chromatography/mass spectrometry (SPE-GC/MS). The automatic SPE (Thermo) system was equipped with a C18 column with a water sample volume of 1 L. Analysis was performed using an Agilent 7000B tandem mass spectrometer. H₂O₂ (detection limit 0.01mg/L) and UV₂₅₄ (detection limit 0.001 cm⁻¹) were determined using a TU1901 double-beam UV spectrophotometer.

Experimental Procedures

Two sets were run in the laboratory with 582 ng/L GSM and 3.93 mg/L H₂O₂ for one set and 514 ng/L



(a)



(b)

Figure 1. Pilot trial devices.

Table 2. Factors and Experimental Design Levels Used.

Factor	Code Identification	Level		
		-1	0	+1
H ₂ O ₂ concentration (mg/L)	A	2.0	250	50
UV intensity (mJ/cm ²)	B	6.0	350	275
GSM initial concentration (ng/L)	C	10.0	450	500

GSM and 1.92 mg/L H₂O₂ for the other. GSM was first added to the storage tank and then H₂O₂ was added. Next, the water pump was started. After 2 min of thorough mixing the UV lamp was turned on. Each time two water samples were taken from the sampling port one catalase was immediately added to resolve residual H₂O₂, to make it no longer produce ·OH and another was to detect H₂O₂ concentration.

During the pilot trial the raw water was fed into the lamp reactor and UV lamps at the desired influence were turned on for 15 min of preheating. Then the dosing pump was turned on and GSM and H₂O₂ were added simultaneously.

Box-Behnken Design (BBD)

The pilot trial adopted a three-level three-factorial Box-Behnken experimental design with 17 sets of experiments (See Table 2). In the BBD the GSM removal efficiency (γ_1) responds to H₂O₂ concentration (A),

UV intensity (B), and GSM initial concentration (C). A quadratic polynomial equation was developed using response surface methodology (RSM). Design-Expert 8.0 was employed for data analysis.

RESULTS AND DISCUSSION

Laboratory Experiments

Figures 2–4 display GSM and H₂O₂ concentration changes in the treated water over time.

As seen in Figures 2 and 3, when 514 ng/L of GSM was treated with 1.93 mg/L of H₂O₂ at UV intensity of 86 mJ/cm² the concentration of GSM decreased to 315 ng/L after 2 min and further to 8 ng/L after 8 min. Degradation efficiency of GSM was 98.44% at the 8th min and 99.03% at the 10th min. When 582 ng/L of GSM was degraded by 3.93 mg/L of H₂O₂ at a UV intensity of 86 mJ/cm² the concentration of GSM decreased to 295 ng/L after 2 min and further to below the detection limit after 8 min. Degradation efficiency was 99.99% at the 8th min. Results suggested that UV/H₂O₂ was effective for GSM removal.

During GSM degradation, concentration of H₂O₂ showed a slowly decreasing trend. The main reason was UV irradiation and H₂O₂ produced hydroxyl radicals which consumed some H₂O₂. When the initial concentration of H₂O₂ was 1.93 mg/L, then after 8 min H₂O₂ concentration decreased by 9.33% to 1.75 mg/L.

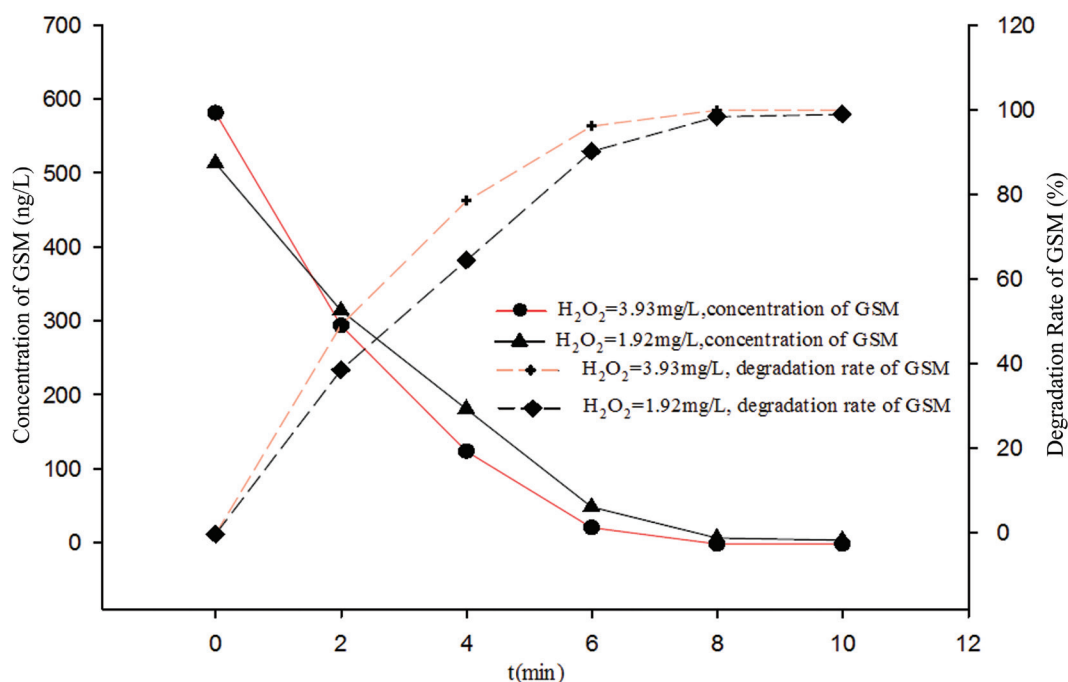


Figure 2. GSM concentration and degradation rate changes with time.

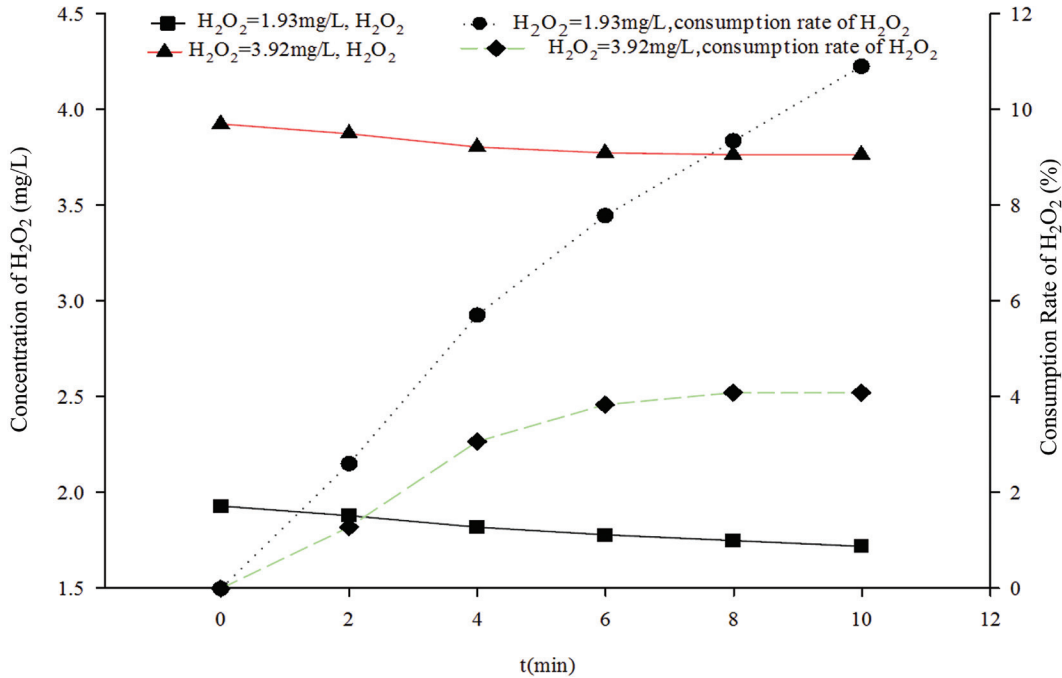


Figure 3. H_2O_2 concentration and consumption rate changes with time.

When the initial concentration of H_2O_2 was 3.92 mg/L after 8min then the H_2O_2 concentration decreased by 4.08% to 3.76 mg/L.

As seen in Figure 4, degradation of GSM conformed to first-order kinetics. When the initial concentration of H_2O_2 was 1.93 mg/L the first-order kinetic equation was $\ln C = 6.6638 - 0.5064x$ ($R^2 = 0.9538$). When the

initial concentration of H_2O_2 was 3.92 mg/L, the first-order kinetic equation was $\ln C = 6.901 - 0.6809x$ ($R^2 = 0.9695$). The reaction rate constant increased to 0.6809 for H_2O_2 concentration of 3.92 mg/L from 0.5064 for an H_2O_2 concentration of 1.93 mg/L. Recent researches reported that GSM removal by UV/ H_2O_2 conforms to first-order kinetics. The constant (0.0332~0.505)

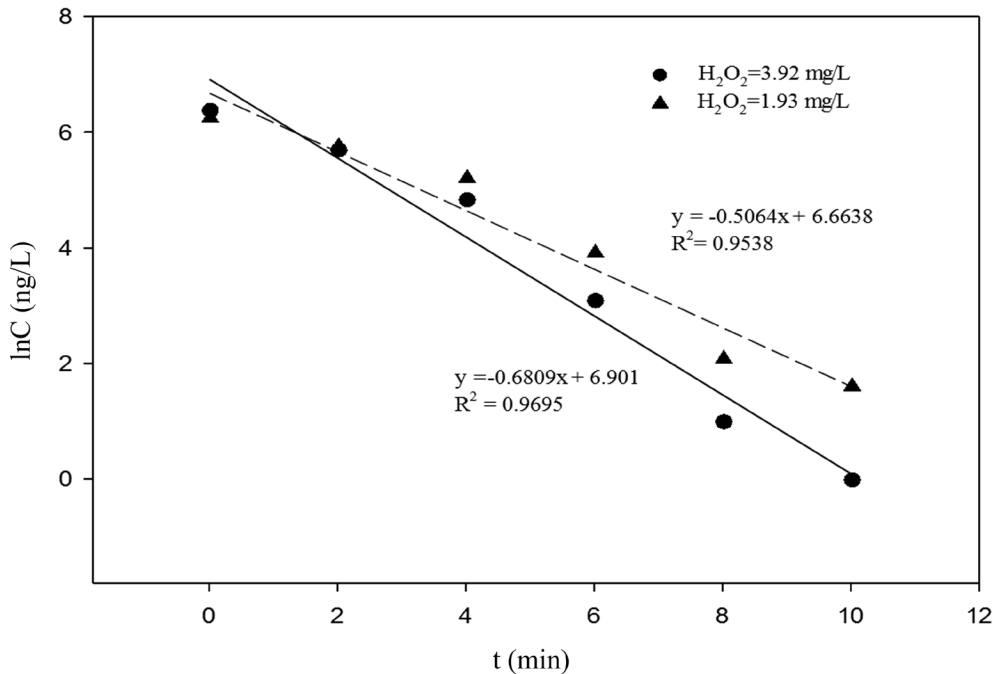


Figure 4. Kinetic equation of GSM degradation.

Table 3. Box–Behnken Design and Results (actual versus predicted).

Experiment No.	Factor (A)		Factor (B)		Factor (C)		y ¹ /%	
	Code	Values (mg/L)	Code	Values (mg/cm ²)	Code	Values (mg/L)	Actual Value	Predicted Value
1	0	6	0	350	0	275	87.24	87.86
2	1	10	0	350	-1	50	99.99	100
3	0	6	1	450	-1	50	99.99	100
4	0	6	0	350	0	275	87.16	87.86
5	0	6	-1	250	1	500	66.25	66.02
6	0	6	-1	250	-1	50	88.32	88.67
7	1	10	0	350	1	500	99.15	100
8	-1	2	1	450	0	275	65.43	66.28
9	0	6	1	450	1	500	88.62	88.27
10	-1	2	0	350	-1	50	78.16	77.09
11	0	6	0	350	0	275	88.24	87.86
12	1	10	1	450	0	275	99.99	100
13	-1	2	-1	250	0	275	41.21	41.94
14	1	10	-1	250	0	275	90.65	89.80
15	-1	2	0	350	1	500	43.27	42.77
16	0	6	0	350	0	275	88.20	87.86
17	0	6	0	350	0	275	88.48	87.86

varied with different test conditions (water quality, UV lamp model, and H₂O₂ concentration) [18–20].

Pilot Trial

The UV/H₂O₂ pilot trial simulating an actual water treatment process was performed to explore optimum parameters used for GSM removal.

Results and Regression Equation Development

According to BBD, 17 sets of experiments were carried out as seen in Table 3.

Based on data in Table 3, the quadratic polynomial fitting result of RSM is displayed as Equation (6) which was used to predict GSM removal efficiency (y_1):

$$y_1 = \left[\begin{array}{l} 87.86 + 20.21A + 8.45B - 8.65C - 3.72AB \\ + 8.51AC + 2.68BC - 9.60A^2 - 3.95B^2 + 1.88C^2 \end{array} \right] \quad (6)$$

As seen in Table 3, differences between actual and predicted values were found to be within $\pm 1.07\%$, indicating the regression model fit the data very well.

Table 4 displays results from an analysis of variance of the regression model. P -value of the model was less than 0.0001 indicating the model was statistically significant. Arguments A, B, C, B², AB, and AC were highly significant items ($P \leq 0.001$) while A², C², and BC are significant items ($P < 0.05$) indicating

that H₂O₂ concentration, UV intensity, and GSM initial concentration affected GSM removal. Lack of fit F -value indicates a difference between the model and the experiment was only 4.94. The lack of fit P value was 0.0784 and greater than 0.05 indicating lack of fit is not significant.

The R-squared of the regression model y_1 as seen in Table 5 was 99.87% and the adjusted R-squared was 99.69% and both of which are greater than 80% demonstrating the model fit the data well.

Table 4. Analysis of Variance for Response Surface Quadratic Model (y_1).

Source	Sum of Squares	DF	Mean Square	F Value	P Value
Model	5288.77	9	587.64	575.43	< 0.0001
A	3268.77	1	3268.77	3200.84	< 0.0001
B	571.22	1	571.22	559.35	< 0.0001
C	598.06	1	598.06	585.63	< 0.0001
AB	55.35	1	55.35	54.2	0.0002
AC	289.85	1	289.85	283.83	< 0.0001
BC	28.62	1	28.62	28.03	0.0011
A ²	387.9	1	387.9	379.84	< 0.0001
B ²	65.55	1	65.55	64.19	< 0.0001
C ²	14.83	1	14.83	14.52	0.0066
Residual	7.15	7	1.02		
Lack of fit	5.63	3	1.88	4.94	0.0784
Pure error	1.52	4	0.38		
Cor. total	5295.92	16			

Note: $P \leq 0.0001$ indicates highly significant; $P \leq 0.05$ indicates significant; $P > 0.05$ indicates not significant.

Table 5. Regression Analysis.

Model	Std. Dev %	R-Squared %	Adj. R-Squared %
y ₁	1.01	99.87	99.69

Response Surface Model Analysis

To evaluate all factors and interactions, Design Expert 8.0 software was used for response surface model analysis. Results are displayed as 3D plots in Figures 4–6. Figure 5 shows GSM removal efficiency increased significantly with increasing H₂O₂ concentration and then tended to be stable when H₂O₂ concentration was higher than 7.5 mg/L. Effect of UV intensity was similar but not as significant as H₂O₂.

Figure 6 displays that H₂O₂ concentration affected removal efficiency more than GSM concentration did and both promoted GSM removal. Figure 7 suggests that GSM removal efficiency increased with increasing UV intensity but decreased with increasing GSM concentration.

Three factors were in the following descending order in terms of their influence on GSM removal by UV/H₂O₂:H₂O₂ concentration > UV intensity > initial concentration of GSM (See Figures 5–7).

Optimum Conditions and Model Validation

Based on the aforementioned model analysis and consideration of actual water quality, optimum parameters for GSM removal were selected. H₂O₂ concentration was 7.5 mg/L, UV intensity was 400 mJ/cm², and

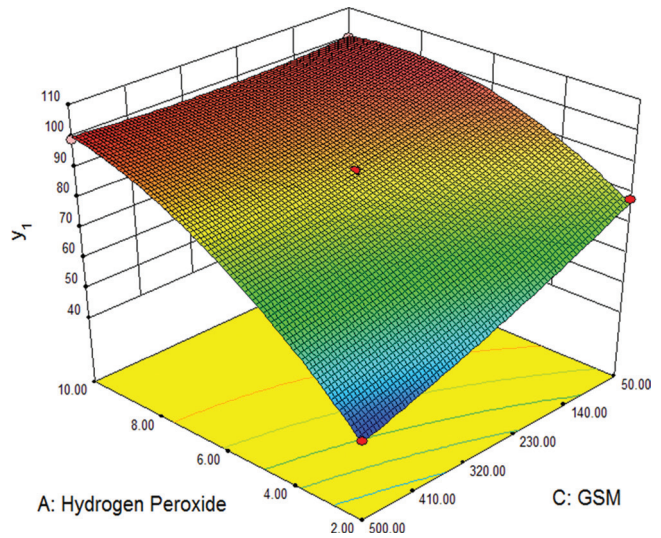


Figure 6. 3D response surface plot showing relative effects of A and C on y₁.

GSM initial concentration was 300 ng/L. Under these conditions experiments were carried out three times and average GSM removal rate was 97.14%. This is close to the predictive value of 96.20%. This indicated the response surface model was reliable and optimization of process parameters was reasonable.

Water Quality after Treatment using a UV/H₂O₂ Advanced Oxidation Process under Optimum Conditions

Cl may easily substitute Br in a reaction with organic matter in water. Cl more closely combines with C in organic matter so chlorinated THMs is more stable.

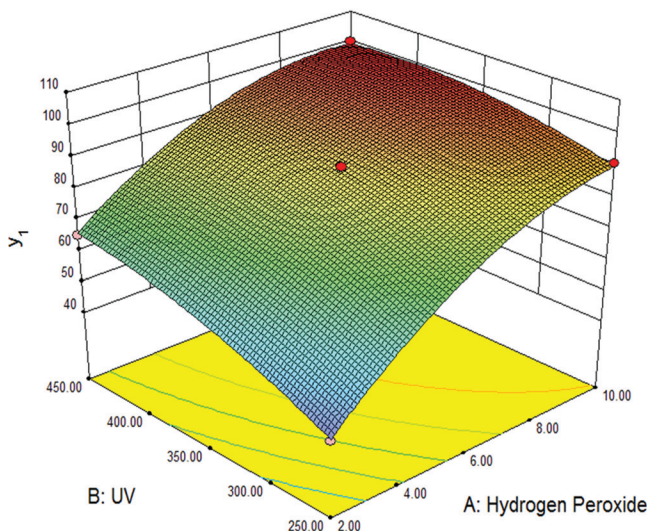


Figure 5. 3D response surface plot showing relative effects of A and B on y₁.

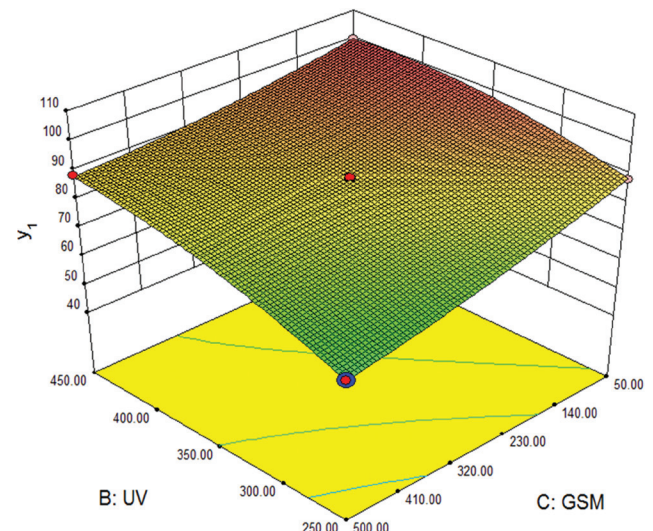


Figure 7. 3D response surface plot showing relative effects of B and C on y₁.

Table 6. Water Quality After Treatment Under the Optimum Conditions.

	TOC	UV ₂₅₄	CHCl ₃	CHCl ₂ Br	CHClBr ₂	CHBr ₃	GSM
Unit	mg/L	cm ⁻¹	mg/L	mg/L	mg/L	mg/L	ng/L
Measured Value	2.1	0.016	0.024	0.0236	0.0017	< 0.0014	8.58
detection Limit	0.0014	0.001	0.0014	0.0014	0.0014	0.0014	5.00
Standard	—	—	0.060	0.0600	0.1000	0.1000	10

Added coagulant is PAFC (Polymeric aluminum ferric chloride; Jiangxi Hui Hai Environmental Protection Technology Co., Ltd.) so Cl concentration is higher in water. Therefore, chlorinated THMs formed higher than brominated THMs.

As seen in Table 6, after water was treated using a UV/H₂O₂ advanced oxidation process under these optimized conditions its quality met requirements for “drinking water health standards” (GB5749-2006).

CONCLUSIONS

In laboratory experiments, removal efficiency of GSM increased with increasing H₂O₂ concentration. 582 ng/L of GSM was reduced below the detection limit and the odor threshold for humans after 8 min of reaction with 3.92 mg/L of H₂O₂. 514 ng/L of GSM was reduced to 8 ng/L after 8 min of reaction with 1.93 mg/L of H₂O₂. Degradation of GSM conformed to first-order kinetics. GSM was significantly removed by the process.

Design-Expert software was used to analyze pilot trial data and a fitted equation was obtained between GSM degradation efficiency and factors. According to the equation the optimum conditions for GSM removal were an H₂O₂ concentration of 7.5 mg/L, a UV intensity of 400 mJ/cm² and a GSM initial concentration of 300 ng/L. Under these conditions actual GSM removal rate was 97.14% and water after treatment met drinking water quality requirements. The fitted equation may be used to determine optimum conditions for removal of GSM at other concentrations in drinking water to meet the requirement of less than 10 ng/L.

REFERENCES

- P. Omür-Ozbek, J.C. Little, and A.M. Dietrich., “Ability of humans to smell geosmin, 2-MIB and nonadienal in indoor air when using contaminated drinking water”, *J. Water Science & Technology A Journal of the International Association on Water Pollution Research*, Vol. 55, No. 5, 2007, pp. 249–256.
- G.A. Burlingame, R.M. Dann, G.L. Brock., “A case study of 2-methylisoborneol in Philadelphia’s water”, *J. Am. Water Works Assoc.*, Vol. 78, No. 8, 1986, pp. 56–61.
- Paerl, H.W., Hall, N.S., Calandrino, E.S., “Controlling harmful cyanobacterial blooms in a world experiencing anthropogenic and climatic-induced change”, *J. Sci. Total Environ.*, Vol. 409, No. 10, 2011, pp. 1739–1745. <http://dx.doi.org/10.1016/j.scitotenv.2011.02.001>
- Jirong Ping, Lv Xiwu, Li Xianning., “Oxygen-enriched water taste and odor compounds in water removal techniques”, *J. water supply and drainage*, Vol. 30, No. 6, 2004, pp. 8–12.
- S. Lalezary, M. Pirbazari, M.J. McGuire, S.W. Krasner., “Air stripping of taste and odor compounds from water”, *J. Am. Water Works Assoc.*, Vol. 76, No. 8, 1984, pp. 83–87.
- Chen Beibei, Gao Nai-yun, Ma Xiaoyan., “Taste and odor compounds in drinking water for 2-methylisoborneol and 2-methylisoborneol Removal”, *J. Sichuan Environment*, Vol. 26, No. 7, 2007, pp. 87–93.
- Zhang Zhao, Yin Baoguo., “Explore the taste and odor problems of urban water supply system”, *J. urban water supply*, Vol. 4, No. 10, 2003, pp. 14–17.
- D. Bruce, P. Westerhoff, A. “Brawley-Chesworth, Removal of 2-methylisoborneol and 2-methylisoborneol in surface water treatment plants in Arizona”, *J. Water Supply Res. Technol. Aqua*, Vol. 51, No. 8, 2002, pp. 183–197.
- S. Lalezary, M. Pirbazari, M.J. McGuire., “Oxidation of five earthy-musty taste and odor compounds”, *J. Am. Water Works Assoc.*, Vol. 78, No. 8, 1986, pp. 62–69.
- W.H. Glaze, R. Schep, W. Chauncey, E.C. Ruth, J.J. Zarnoch, E.M. Aieta, C.H. Tate, M.J. McGuire., “Evaluating oxidants for the removal of model taste and odor compounds from a municipal water-supply”, *J. Am. Water Works Assoc.*, Vol. 82, No. 5, 1990, pp. 79–84.
- Sun, A., Xiong, Z., Xu, Y., “Removal of malodorous organic sulfides with molecular oxygen and visible light over metal phthalocyanine”, *J. Journal of Hazardous Materials*, Vol. 152, No. 1, 2008, pp.191–195. <http://dx.doi.org/10.1016/j.jhazmat.2007.06.105>
- Lekkerkerker-Teunissen, K., A.H. Knol, J.G. Derks., “Performance comparison of LP vs MP UV lamps for advanced oxidation process”, C, 2010.
- Han, Do Hung, S. Y. Cha, and H. Y. Yang., “Improvement of oxidative decomposition of aqueous phenol by microwave irradiation in UV/H₂O₂ process and kinetic study”, *J. Water Research*, Vol. 38, No. 11, 2004, pp. 2782–2790. <http://dx.doi.org/10.1016/j.watres.2004.03.025>
- Theodora Fotiou, Theodoros M. Triantis, Triantafyllos Kaloudis, Elias Papaconstantinou, Anastasia Hiskia., “Photocatalytic degradation of water taste and odour compounds in the presence of polyoxometalates and TiO₂: Intermediates and degradation pathways”, *J. Journal of Photochemistry and Photobiology A: Chemistry*, Vol. 286, 2014, pp. 1–9. <http://dx.doi.org/10.1016/j.jphotochem.2014.04.013>
- James M, Kevin L Worley., “An advanced oxidation process for DBP control”, *J. JAWWA*, Vol. 11, No. 8, 1995, pp. 66–75.
- Behnjady, M. A., N. Modirshahla, and H. Fathi., “Kinetics of decolorization of an azo dye in UV alone and UV/H₂O₂ processes”, *J. Journal of Hazardous Materials*, Vol. 136, No. 3, 2006, pp. 816–821. <http://dx.doi.org/10.1016/j.jhazmat.2006.01.017>
- Jo, C.H., Dietrich, A.M., Tanko, J.M., “Simultaneous degradation of disinfection byproducts and earthy-musty odorants by the UV/H₂O₂ advanced oxidation process”, *J. Water Res.*, Vol. 45, No. 8, 2011, pp. 2507–2516. <http://dx.doi.org/10.1016/j.watres.2011.02.006>
- Zheng cheng, Zhang Xinqiang, Wei Yunlu, Mao Taoyan, Zhou Yongqiang., “Microwave synthesis, structure and properties of methylidihydroxyethylbenzyl ammonium chloride”, *J. CIESC Journal*, Vol. 60, No. 1, 2009, pp. 244–253.

19. Peter, A., von Gunten, U., "Oxidation kinetics of selected taste and odor compounds during ozonation of drinking water", *J. Environ. Sci. Technol.*, Vol. 41, No. 2, 2007, pp. 626–631. <http://dx.doi.org/10.1021/es061687b>
20. Zoschke, K., Dietrich, N., Börmick, H., Worch, E., "UV-based advanced oxidation processes for the treatment of odour compounds: Efficiency and by-product formation", *J. Water Res.*, Vol. 46, No. 16, 2012, pp. 5365–5373. <http://dx.doi.org/10.1016/j.watres.2012.07.012>

Microorganism Removal from Ballast Water using UV Irradiation

Z. J. REN^{1,*}, L. ZHANG¹, Y. SHI², J. C. SHAO¹, X. D. LENG¹ and Y. ZHAO¹

¹*School of Aerospace and Civil Engineering, Harbin Engineering University, Harbin, China*

²*College of Power and Energy, Harbin Engineering University, Harbin, China*

ABSTRACT: *Staphylococcus aureus* (*S. aureus*) and *Chlorella* were selected as two different reference microorganisms in ballast water. Water treatment static- and dynamic-experiments were conducted for microorganism removal via a UV process. The purpose was to better understand UV irradiation technology potential for microorganism removal. Static results showed UV irradiation is better for *S. aureus* and *Chlorella* removal and a UV dosage of 36mJ/cm² can achieve removal rates as high as 97.6% and 73.1%, respectively. Differences in microbial ecological characteristics and species created different removal curves. A higher UV dose for *Chlorella* removal was needed compared to *S. aureus* removal. Turbidity of the raw water also had great influence on UV irradiation. When turbidity was raised from 1–108NTU the removal effect of UV is reduced significantly to approximately 32.2% and 44.2%, respectively. Dynamic experiments suggested the microbial removal rate could reach more than 90% at a low flow rate (15L/h).

INTRODUCTION

CONSIDERING the rate of rapid development within industry and shipping the problem of marine organisms' intrusion via ships' ballast water has brought serious problems to the marine environment, marine ecological health, and sustainable development [1–2]. Among ballast water treatment technologies, ultraviolet radiation has attracted wide attention for its characteristics of high efficiency, broad spectrum, no secondary pollution, safe and reliable, and good for continuous large amounts of water disinfection [3–4]. However, UV irradiation for ballast water treatment could be affected by a variety of factors such as microorganism species, particle matters, and other considerations [5].

To better understand the UV irradiation process for ballast water treatment, *Chlorella* and *S. aureus* were selected as reference microorganisms. Effects of UV irradiation for different microorganism's removal were considered and effect of particle matters on ultraviolet radiation for microbial removal were also evaluated. Performance based on flow rate regarding microorganism removal by UV was evaluated.

*Author to whom correspondence should be addressed.
Email: renzhijun2003@126.com, Tel: 13115557461

MATERIALS AND METHODS

Experimental Devices

Both static and dynamic experiments were carried out. Static experiments were conducted to study effect of UV dose on microorganism removal. The experimental reactor is displayed in Figure 1. The apparatus utilized a collimated beam system constructed by two low-pressure and low-intensity UV lamps in a horizontal copper pipe (90 mm ID). A collimating tube extended downward from the horizontal pipe to achieve collimation of UV light (length: diameter ratio was 15). At the point of application a radiometer was used to measure intensity of UV light. A sterilized Bunsen beaker (250 mL) containing a spin bar was loaded with 10 mm of water sample. An opaque sheet of cardboard was used to cover the collimating tube and vertical position of beaker was controlled to vary exposure rate. Mixing was initiated, cardboard was removed, and the irradiation timer started simultaneously. The cardboard was inserted between the collimating tube and the Bunsen beaker when a specified amount of irradiation time had passed.

The dynamic experiment was conducted to study effect of flow rate on microorganism removal by UV irradiation. The dynamic experimental reactor is not presented. The flow rate is control from 0 to 100 L/h.

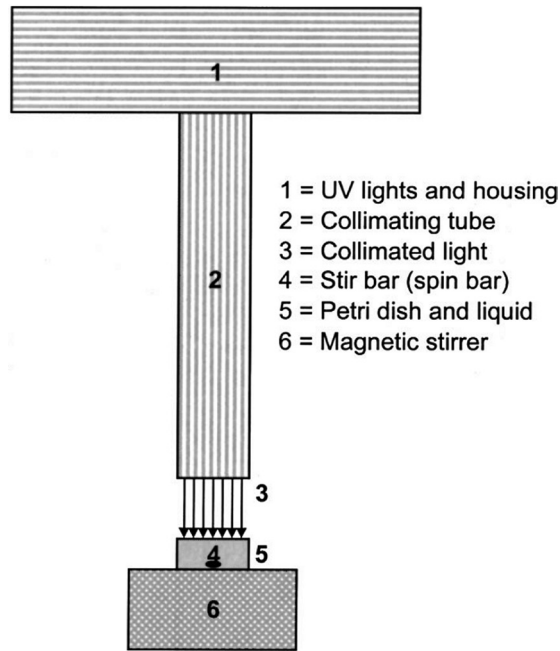


Figure 1. Collimated beam apparatus.

Experimental Methods

Seawater was prepared according to biological indicators from the International Ships' Ballast Water and Sediments Management and Control of the Convention. Physical and chemical indicators of experimental water was used to simulate an average water quality for coastal sea in China. The pH was 7.5 to 8.0, temperature was 16 ~ 26°C, and salinity was 35 psu according to the global average salinity of seawater. The ratio of sodium chloride, magnesium chloride, and potassium chloride is 3:2:1. All experiments were carried out at room temperature with a range from 18–22°C and performed in triplicate.

Chlorella and *S. aureus* were selected as reference microorganisms. A spectrophotometer method was used to test the population of *Chlorella*. The population of *Chlorella* was determined using an optical density method according to Shen's research [6] in which cell density and its related OD had a linear relationship. *S. aureus* was taken from China's Microbe Preservation Center and the strain Number was 1.2465. The population of *S. aureus* was tested according to a test-tube doubling dilution method. Removal rate was used to judge performance of UV irradiation for these two kinds of microorganism removal.

UV intensity was set between 10–600 $\mu\text{W}/\text{cm}^2$ and UV radiation intensity was measured by UV-B Dual UV radiometer (Photoelectric Instrument Factory of Beijing Normal University, China).

Turbidity was measured according to the ISO 7027 "Water Quality: Determination of Turbidity" and a turbidity meter (LP2000, China) with 10mm cell was used to test turbidity [7].

RESULTS AND DISCUSSION

Effect of UV Dose on Microbial Removal

Removal experiments of *S. aureus* and *Chlorella* under different UV doses are conducted. The UV dose for *S. aureus* and *Chlorella* removal is from 0–180 mJ/cm^2 and from 0–540 mJ/cm^2 , respectively. Average initial concentration of *S. aureus* and *Chlorella* were about 1.5×10^{12} cfu/mL and 8×10^7 cfu/mL, respectively. Removal performance for two kinds of microorganisms at different UV doses is displayed in Figure 2.

Figure 2 suggests that a higher removal rate was achieved when UV irradiation was at a lower dose and

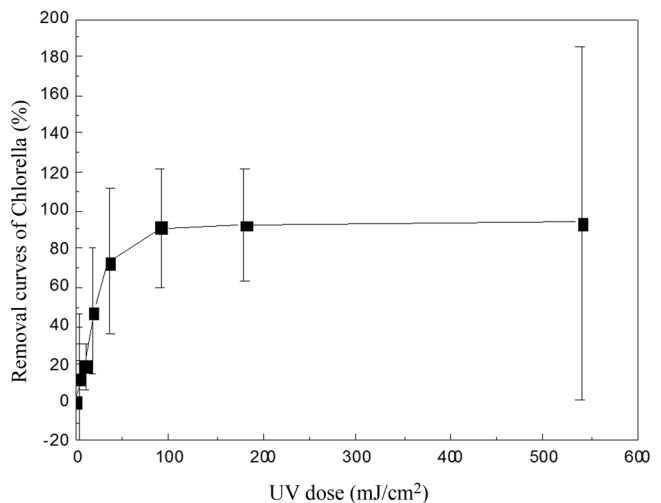
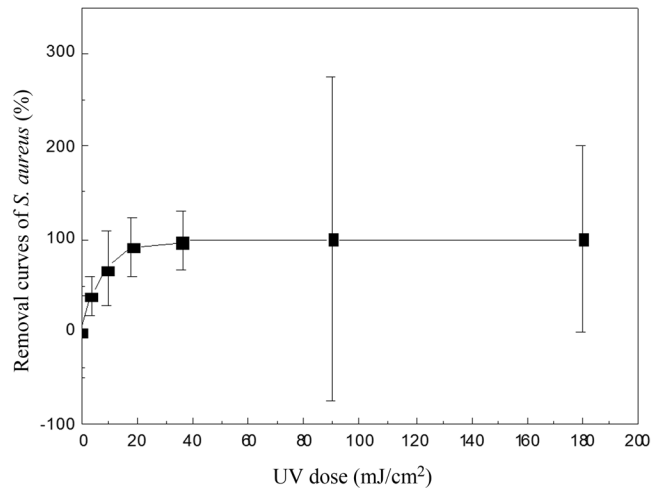


Figure 2. Effect of UV dose on *S. aureus* and *Chlorella* removal.

a reduction of removal rate of microorganisms with increasing UV dose. Considering *S. aureus* for example when the UV dose was 36 mJ/cm² removal rate could reach 97.6%. With UV dose increasing removal rate increased only 2% with UV dose at 90 mJ/cm².

The microbial removal curve by UV irradiation can be divided into three regions: a lag region, a first order region, and a tailed region according Tchobaninglous's research [8]. UV dose at a critical stagnation area and a tailed area are IT_{lag} and IT_{tail} , respectively. When UV dose (IT) is lower than IT_{lag} removal rate for microorganism is lower. When IT value is between IT_{lag} and IT_{tail} and continuously increasing removal rate increases gradually and follows a first-order reaction. Finally, when IT is more than IT_{tail} then it falls into the tailed region.

Figure 2 suggested removal curves for *S. aureus* and *Chlorella* were different. Removal curve of *S. aureus* by UV irradiation included the first order reaction region and a tailed region. The IT_{tail} value of the tailed region was 18mJ/cm² when the IT value was in a range from 0 to 18 mJ/cm², the removal curve of *S. aureus* was in the first order region, and the removal rate rapidly increased with UV dose increase. Kinetic equations for the first order reaction region was $y = 6 \times 10^{-5}x + 0.0027$ ($R^2 = 0.9951$) where y and x represent removal rate and UV dose, respectively. When the IT value reached a critical UV dose for the tailed region, the removal rate of UV irradiation for *S. aureus* could reach 91.6%.

Removal curve for *Chlorella* by UV irradiation included a lag region, the first order reaction region, and a tailed region. When the UV dose was less than IT_{lag} value at 12 mJ/cm², removal of *Chlorella* was only 20–30%. When UV dose was between 12–60 mJ/cm² the removal curve for *Chlorella* was in the first order region, the kinetic equation of the first order reaction area was $y = 2 \times 10^{-5}x + 0.1294$ ($R^2 = 0.9823$), and the critical IT_{tail} value of UV dose in the tailing region was 60 mJ/cm². When IT value reached the IT_{tail} value removal rate of *Chlorella* could reach 91.5%.

Figure 2 also suggested when the UV dose was greater than IT_{tail} value the microbial removal rate would increase slowly with UV dose increasing and the tailed phenomenon occurred. This phenomenon suggested that even if UV dose was increased inactivation rate would not rise and mainly related to the structure of the microorganism itself [9–10].

Compared with the IT_{lag} value of these two tested microorganisms in the first-order reaction region, the IT_{lag} value (60 mJ/cm²) for *Chlorella* was much higher

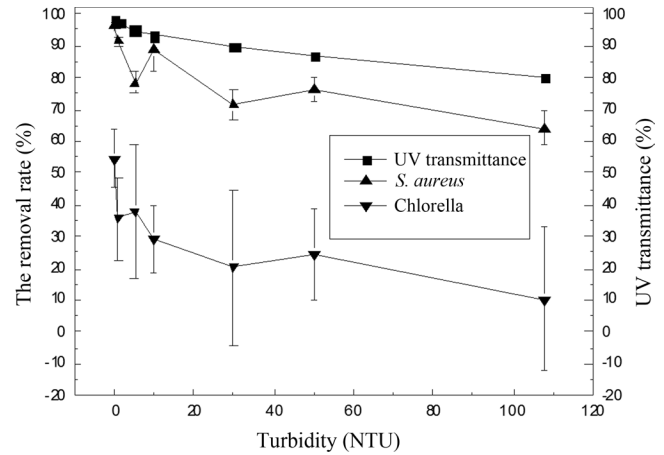


Figure 3. Effect of turbidity on microorganism removal by UV irradiation.

than for *S. aureus* (12 mJ/cm²). The main reason is the differences in physiological characteristics of tested organisms resulting in different resistances to UV radiation. The first order reaction rate constant (K) is used as an indicator for resistance to radiation. The K value of *Chlorella* (0.00002) was significantly less than the K value of *S. aureus* (0.00006). The smaller the K value was the greater the microorganism's resistance to UV. More UV dose would be needed to achieve the same inactivation rate.

Effect of Turbidity on Microorganism Removal by UV Irradiation

Turbidity is the cloudiness or haziness of a fluid caused by large numbers of individual particles generally invisible to the naked eye and similar to smoke in air. Particulate matter present in water may effect efficiency of UV penetration in water [11]. Diatomite was used to prepare the suspending liquid and the range of turbidity was from 0–150 NTU. The effect of different turbidity on microorganism removal by UV irradiation was studied at a constant UV dose of 24 mJ/cm². See Figure 3.

Seen in Figure 3 under the condition of a fixed UV dose a small dose increase in turbidity could significantly effect performance of ultraviolet irradiation for microorganism removal. When turbidity increased from 1–5 NTU removal rate for *S. aureus* and *Chlorella* fell by 18.2% and 16.7%, respectively. With increasing turbidity UV removal rate continued to decrease. When turbidity increased to 108 NTU the removal rate for *S. aureus* and *Chlorella* decreased from 96.6–64.2% and from 54.5–10.3%, respectively, which was consistent with results from other researchers [12].

Effect of turbidity on microorganism removal by UV irradiation is mainly manifested in two aspects. Particulate matter is an important influence factor on the performance of UV penetration. Light scattering by particles is a process by which small particles such as ice crystals, dust, planetary dust, and blood cells cause observable phenomena such as rainbows, color of the sky, and halos. When light hits small particles light scatters in all directions (Rayleigh scattering) as long as particles are small compared to wavelength (below 250 nm). Figure 3 suggested that with increasing turbidity increasing UV transmittance for both *S. aureus* and chlorella removal rates decreased. When turbidity increased from 1–108 NTU UV transmittance values decreased from 97.5–80.9% and removal rate of *S. aureus* and Chlorella declined 32.2% and 44.2%, respectively. This means particulate matter can cause energy loss in the UV dissemination process and then indirectly impact UV dose received influencing UV removal rate of a microbe [13]. However, turbidity may be combined with microorganisms and have a shielding effect on themselves thus making the UV removal rate lower [14].

Dynamic Experiment of UV Irradiation for Microbes Removal

Flow rate or contact time is an important factor for UV irradiation. The flow rate was controlled from 0 to 100 L/h. Performance of the UV process for microbial removal at different flow rates is provided in Figure 4.

Seen in Figure 4, when flow rate increases the microorganism removal rate gradually decreased. Most

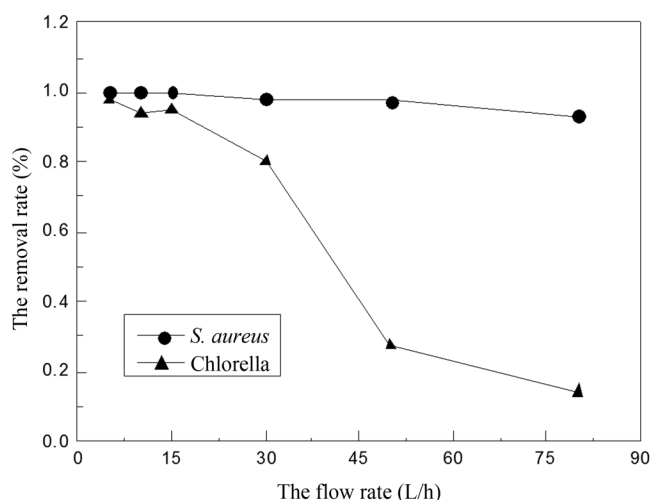


Figure 4. Effect of flow rate on UV irradiation for microorganism removal.

microorganisms can be effectively removed at experimental conditions and removal rate was above 90% when flow rate was at a low flow rate (15 L/h). Additionally, Figure 4 clearly displayed that the removal effect by UV was different for different microorganisms. When a flow rate was 50 L/h the removal rate of *S. aureus* was up to 95%. Yet, when the flow was 15 L/h the removal rate of Chlorella could achieve the same level.

CONCLUSIONS

Effect of UV irradiation on microorganism removal in ballast water was evaluated according to both static and dynamic experiments and results were as follows:

First, UV radiation is an effective way for microorganism removal. When UV dose is at a lower dose (36 mJ/cm²) the removal rate of *S. aureus* and Chlorella could reach more than 70%.

Next, the removal curves of *S. aureus* and Chlorella were different. The curve from the former included the first order reaction region and tailing region while the curve of the latter included a lag region, the first order reaction region, and a tailing region.

Also, turbidity had a significant influence on UV irradiation for microorganism removal. When turbidity increased from 1–108 NTU the removal rate of *S. aureus* decreased from 96.6–64.2% and removal rate for Chlorella decreased from 54.5–10.3%.

Finally, dynamic experimental results suggested UV technology for microbial removal efficiency could reach more than 90% under a condition using a low flow rate (15 L/h).

ACKNOWLEDGEMENTS

This work was supported by the National Science Foundation of China (No. 51179037 and No. 51209053).

REFERENCES

- Lewis. Marine introductions in the Southern Ocean: an unrecognized hazard to biodiversity. *Marine Pollution Bulletin*, 2003, 46(2): 213–223. [http://dx.doi.org/10.1016/S0025-326X\(02\)00364-8](http://dx.doi.org/10.1016/S0025-326X(02)00364-8)
- Niimi, A. Role of container vessels in the introduction of exotic species. *Marine Pollution Bulletin*, 2004,49(9/10): 778–782. <http://dx.doi.org/10.1016/j.marpolbul.2004.06.006>
- David, A. Wright. & Rodger Dawson. A test of the Efficacy a Ballast Water Treatment System aboard the Vessel Coral Princess. *Marine Technology*, 2007, 44(1): 57–67.
- Nam, S, W. Yoon, Y. & Choi, D, J. Degradation characteristics of metoprolol during UV/chlorination reaction and a factorial design optimization. *Journal of Hazardous Materials*, 2015, 285(21): 453–463. <http://dx.doi.org/10.1016/j.jhazmat.2014.11.052>
- Cao Guiping, Lu Jilai, & Wang Gongying. Photolysis kinetics and influencing factors of bisphenol S in aqueous solutions. *Journal of Envi-*

- ronmental Sciences*, 2012, 24(5): 846–851. [http://dx.doi.org/10.1016/S1001-0742\(11\)60809-7](http://dx.doi.org/10.1016/S1001-0742(11)60809-7)
6. Shen Pingping, Wang zhaohui, Qi yuzao, et al. An optical density method for determination of microalgal biomass. *Journal of Jinan University (Natural Science)*, 2001, 22(3):115–119.
 7. Song, W. C.; Li, X.; Sun, S. H. Test Study of Enhanced Coagulation for Conventional.
 8. Tchobaniglous G Burton F L, Stensel H D. *Wastewater Engineering Treatment and Reuse*. New York: McGraw-Hill Inc., 2004, 1231–1254.
 9. Gehr, R. Wagner, M. & Veerasubramanian, P. Disinfection efficiency of peracetic acid, UV and ozone after enhanced Primary treatment of municipal wastewater. *Water Research*, 2003, 37(19): 4573–4586. [http://dx.doi.org/10.1016/S0043-1354\(03\)00394-4](http://dx.doi.org/10.1016/S0043-1354(03)00394-4)
 10. Dong, L. Cralk, S, A. & Smith, D, W. The assessment of Particle association and UV disinfection of wastewater using indigenous spore-forming bacteria. *Water Research*, 2009, 43(2): 481–489. <http://dx.doi.org/10.1016/j.watres.2008.10.025>
 11. Qi, Y. & Kleeman, M, J. Effects of aerosol UV extinction on the formation of ozone and secondary particulate matter. *Atmospheric Environment*, 2003, 37(36): 5047–5068. <http://dx.doi.org/10.1016/j.atmosenv.2003.08.007>
 12. Madge, B, A. Evaluation of wastewater Solids and Their Relevance in Ultraviolet.
 13. Junjiao, W & Lvjian. Research on application of ultraviolet ray in disinfection of recycle-water. *Shanxi Architecture*, 2006, 32(4): 186–187.
 14. Zhang Yongji, Liu Wenjun. Inactivation of Microbe in Drinking Water Using Ultraviolet Irradiation. *China Water and Wastewater*, 2005, 21(9): 1–4.

Selective Release of Inorganic Constituents in Broiler Manure Biochars under Different Post-Activation Treatments

ISABEL LIMA*, K. THOMAS KLASSON and MINORI UCHIMIYA

¹USDA ARS Southern Regional Research Center, 1100 Robert E. Lee Blvd, New Orleans, LA 70124

ABSTRACT: Poultry-litter activated biochars (PLAB) with enhanced metals adsorption may contain significant amounts of inorganic material. This study traces key elements (Ca-Fe-K-Mg-Na-P) from litter to PLAB and selective fate upon acid/water treatments. Samples were pyrolyzed 1 hr/700°C, steam-activated 45 min/800°C, and acid washed/rinsed. Mineral composition concentrated during pyrolysis/activation. Acid wash/water treatments removed unbound inorganics with highest extraction for K (37–100%) and Na (27–49%) and lowest for Fe (0–0.02%). Remaining elements leached significantly less indicating selective removal as influenced by composition and pyrolysis/activation effects on solubility. Heavy metals concentrated upon activation with negligible leaching regarding treatment. Post-activation treatments may improve usability of PLAB in wastewater applications by avoiding unwanted elemental leaching without compromising functionality.

INTRODUCTION

THERMO-CHEMICAL conversion of biomass into renewable fuels and byproducts is now a very well recognized platform with strong economic potential as well as long-term carbon sequestration [1,2]. Amount of available agriculture and forest residues for conversion and utilization into value-added products and fuels is immense. Animal manures in particular are mass produced in concentrated areas with the largest poultry producing states in the south east of the U.S. responsible for one third of total U.S. poultry production [3]. Surplus manures lead to water and air quality issues as well as public health impacts. This has further prompted the need for viable conversion and reuse solutions. Within the thermo-chemical platform, pyrolysis generates biochar as the main product and then synthesis gas and bio-oil from the non-condensable fraction of the gas with a split between liquid, biochar, and gas being governed to a certain degree by variation in process conditions [4]. Slow pyrolysis in particular is feedstock-flexible which has resulted in the research of a multitude of biomass materials as possible precursors due to their lower cost and availability as well [5,7].

Biochars may be further upgraded into activated biochars or activated carbons for improved adsorption potential especially important in remediation applications [8]. World demand for activated carbon was 650,000 metric tons in 2007 and is projected to rise annually at 5% through 2015 [9]. Due to a rapid increase in the price of coal and limited availability of coconut shell there is much monetary incentive for identifying alternative resources for manufacturing affordable activated carbon. Considering the average price of activated carbon is \$2,500 per metric ton [10] while the value of poultry litter as organic fertilizers in land application is \$0–10 per metric ton [11], utilization of poultry litter as a feedstock to generate activated carbon may be a value-added and potentially environment-benign strategy for recycling organic waste. Depending on the source there can be significant ash fractions that are commonly removed via acid washing. Animal manures also contain significant amounts of inorganic elements due to animal feed enrichment using Ca, P, Na, Cl, K, Mg, and S as macro minerals and As, Co, Cr, Cu, Fe, I, Mn, Mo, Se, Zn, and others as trace minerals [12]. These constituents occur as oxides, silicates, carbonates, sulfates, chlorides, and phosphates [13]. In addition to supplementation, manure is treated with chemical additives to control odor, adjust pH, precipitate suspended solids, or enhance biological treatment [14] and poul-

*Author to whom correspondence should be addressed.
Email: isabel.lima@ars.usda.gov, Phone: 504/286-4515, Fax: 504/286-4367

try producers may choose from several amendments (alum, phosphoric acid, TSP, lime, gypsum, Fe salts, and others) to minimize NH_4 volatilization by altering pH or inhibiting microbial-aided uric acid decomposition. Past studies [8,15,16] have demonstrated presence of these inorganic elements may be beneficial for adsorption of positively charged species such as copper, cadmium, and zinc. It is known that small amounts of inorganic material in biomass are sufficient to alter pyrolysis behavior along with organic composition to a large extent and can contribute to higher biochar yields [13]. However, high ash content is normally not desirable and is considered an impurity because it can reduce carbon hardness [17]. Furthermore, upon leaching it can interfere with carbon adsorption through competitive adsorption, catalysis of adverse reactions, and blockage of carbon pores [18]. Fitzmorris *et al.* [19] studied leaching of various species under different pH conditions from poultry carbons both before and after adsorption and determined that leaching was pH dependent occurring readily under highly acidic conditions but minimally under pH conditions usually seen in contaminated water or wastewater (i.e., neutral pH). Ash has also been reported to lead to partial fusion and swelling during the carbonization stage of eucalyptus kraft lignin and pre-treatment methods used to wash inorganic matter with dilute acidic solutions prior to carbonization were established [20]. It is important to understand how their mineral content influences their usability and how effective post-pyrolysis/activation treatments are at alleviating those issues in order for biomass sourced biochars and activated carbons to be competitive with activated carbons sourced from more traditional feedstock materials (coal, wood, and coconut shells). Biomass composition is complex involving six major elements in the organic phase and at least 10 other elements not including heavy metals in the inorganic phase important to ash characterization [21]. Post pyrolysis/activation treatments involving use of dilute acids and/or water can ameliorate negative effects associated with mineral content of manure based activated biochars while maintaining surface functionality. Two different post-pyrolysis/activation treatments were explored (acid wash, AW or water-rinse, RO) in order to investigate their effect on partial removal of mineral content in activated biochars produced from two poultry manures (cake and litter) and activated at different activation levels. Furthermore, the fate of key elements was traced from the feedstock to the activated biochars and to the acid and wash solutions and their respective influence during the adsorption process.

MATERIALS AND METHODS

Sample Preparation

Broiler litter and broiler cake samples were obtained from the USDA-ARS, Genetics and Precision Agriculture Research Unit (Mississippi State, MS). Litter and cake are made of broiler manure with bedding material with up to 30% wood shavings in litter and less than 5% in cake. Air dried samples were milled in a Retsch cross-beater mill (Glen Mills, Clifton, NJ) to less than 1 mm particle size and pelletized in a PMCL5 Lab pellet mill (CPM, Merrimack, NH) equipped with a 3/16 in (4.8 mm) die plate. Pellets were cylinders with a 4.8 mm diameter and a length of approximately 6.5 mm. Pellet moisture content was monitored using a Sartorius Moisture Analyzer model MA 51 (Sartorius, Brentwood, NJ).

Production of Activated Carbons and Post-Activation Treatments

Pelletized samples were placed in a ceramic evaporating dish and placed in a Lindberg bench furnace (Lindberg/Blue M, Waterton, WI) equipped with a retort. Pellets were pyrolyzed at 700°C under nitrogen gas (flow rate of 1.6 L/min) for 1 hr prior to steam activation. Steam activation involved injecting water at three flow rates (1, 3 or 5 ml/min) using a peristaltic pump into the nitrogen gas flow entering the heated retort for 45 min at 800°C. Activated biochar samples were allowed to cool to room temperature overnight under a stream of nitrogen. Then, using an overhead stirrer samples were either (1) used as is (unwashed; NW), (2) water rinsed with deionised water for 1 hr (2% w/v ratio) and dried overnight at 80°C (rinse only, RO), or (3) acid washed with 0.1 M HCl (2% w/v ratio) for 1 hr with two subsequent 1 hr deionised water rinses (2% w/v ratio) and dried overnight at 80°C (acid wash, AW). Overhead stirring was used to enhance sample wetting as well as for improving contact time between acid, water, pore structure, and ash deposits. Washing methods are detailed in Lima *et al.* [8]. Resulting yields were measured as percent yield from initial dry weight.

Chemical Measurements: pH, Ash Content, Ultimate Analysis, Elemental Composition

A Thermo Orion pH meter (Beverly, MA) was used to measure pH where 0.5 g of sample was placed in

50 mL of deionized water, then covered with parafilm, and finally allowed to equilibrate by stirring at 300 rpm for 72 h. Ash content in activated biochar samples was determined by heating 1 gram of sample to 650°C under a flow of air for 6 hr increments until no change in weight was observed and was calculated as a percentage of initial dry sample weight. Ultimate analysis (CHNSO) was determined by dry combustion using a Perkin Elmer model 2400 Series II CHNS/O analyzer (Perkin Elmer, Shelton, CT). Elemental analysis was performed on digested samples using a Milestone Ethos EZ microwave digestion system (Shelton, CT). One mL of concentrated HCl, 4 mL of concentrated HNO₃, and 1 mL of 30% H₂O₂ were added to 0.1 g of sample and placed in a QS-50 Quartz vessel insert, then capped, finally placed onto a Teflon vessel containing 8 mL of DI water and 2 mL of 30% H₂O₂. Vessels were sealed and digestion was carried out using a 25 min ramp to 200°C and a 40 min hold at 200°C. Multiple digestion cycles were performed if necessary until complete digestion was determined by absence of turbidity and solid particles. Diluted digested aliquots were analyzed by inductively coupled plasma (ICP) spectroscopy using a Leeman Labs Profile ICP-AES (Leeman Labs, Hudson, NH) for the following elements: P, Fe, Ca, Mg, K, S, Na, Cu, Cd, Ni, Zn, and As. All reagents were ultra-pure ICP-grade.

Elemental Leaching Studies

One mL aliquots of acid wash and water rinse suspensions were drawn off at 1, 5, 10, 30, and 60 min during post-activation treatments in a disposable syringe and filtered through a 0.22 µm Millipore filter (Millipore Corp., Bedford, MA) to remove any particulates for determining individual key element leaching during post pyrolysis/activation acid wash or rinse treatments. Aliquots were diluted 1:10 and analyzed by inductively coupled plasma spectroscopy (ICP, Leeman Labs Profile ICP-AES, Leeman Labs, Hudson, NH) for Ca, Fe, K, Mg, Na, and P.

Surface Characterization

Surface characterization on activated biochars was done by viewing samples under an Environmental Scanning Electron Microscope (E.S.E.M., Philips, XL 30). Working distance was set to 10 mm with a magnification of 250–2,500×. Acceleration voltage of the electron beam was 17 kV. Prior to analysis and samples were coated with gold/palladium.

Statistical Analysis

Experimental design was a split block design where the main unit is a randomized complete block design in a 2 × 3 factorial arrangement for two manure types (broiler litter and broiler cake) using three steam activation flow rates (FR: 1, 3, and 5 mL/min). Subunit treatments are three post-furnace treatments (PFT): wash (W), no wash (NW), or RO. SAS PROC MIXED was used for analysis of variance and statistical analysis was done using SAS 9.2 for Windows.

RESULTS AND DISCUSSION

Inorganic Composition of Activated Biochars

Previous studies [8] have determined that animal manures as opposed to plant based materials as precursors to activated biochar can yield a significant inorganic material fraction with ash content values ranging from 51.7–73.9% and pH values ranging from 8.3–9.8. Also, a three-fold increase in fixed carbon content is present. Tables 1 and 2, respectively, display concentration of major and minor inorganic elements in raw litter and cake as well as their respective activated biochars as a function of activation flow rate. Because these inorganic constituents can leach when using activated biochar as a remediation agent in aqueous applications post-treatment options involving use of dilute acids and water for partial removal may be a solution. It is well known that functional groups make activated biochar surface's chemically active and ultimately affect their adsorptive properties, particularly for charged species. In their study [8] it was determined that broiler cake activated biochars adsorbed between 37.8–49.1 mg/g copper ion and broiler litter activated biochars adsorbed between 63.0–104.1 copper ions. Mineral composition of both cake and litter was concentrated with pyrolysis and activation but there was no correlation between concentration of an element in the original feedstock (litter or cake) and the respective concentration in final activated biochars. This indicates original feedstock composition affected pyrolysis and activation reactions differently (Table 1 and 2). Overall, a 2.4–3.4 fold increase in concentration of total inorganic material from raw material to activated biochars was observed. Mineral composition of the precursor plays a major role as formation of surface groups occurs during activation by interaction of free radicals on the carbon surface with oxygen, nitrogen, and sulfur from within the precursor and from

Table 1. Elemental Composition in mg/g in Unwashed (NW), Acid Washed (AW) and Rinse-only (RO) Samples for Select Elements (P, Ca, Mg, K, Na, Fe, S) in Litter and Cake and Respective Activated Biochars as Function of Flow Rate (FR) and Post-treatment.

	FR (ml/min)	PFT ¹	P	Ca	Mg	K	Na	Fe	S
Litter Activated Biochar	1	AW	62.2 ± 3.6	101 ± 7.4	87.1 ± 7.0	34.4 ± 0.7	29.3 ± 4.8	4.61 ± 0.01	24.2 ± 0.7
		RO	71.1 ± 1.2	119 ± 5.5	30.8 ± 0.4	45.2 ± 0.1	29.0 ± 0.7	4.46 ± 0.30	22.0 ± 2.2
		NW	51.5 ± 1.7	93.5 ± 0.2	31.8 ± 0.2	136 ± 6.5	40.4 ± 6.2	4.02 ± 0.51	25.0 ± 1.2
	3	AW	66.6 ± 8.5	129 ± 7	40.6 ± 3.7	46.7 ± 2.1	39.1 ± 2.8	5.05 ± 0.51	27.1 ± 1.7
		RO	54.0 ± 8.4	124 ± 17	34.7 ± 3.1	47.7 ± 6.4	34.1 ± 2.5	4.12 ± 0.21	23.7 ± 1.6
		NW	48.5 ± 0.4	106 ± 13	28.4 ± 5.6	86.7 ± 3.6	45.8 ± 3.2	4.31 ± 1.78	17.1 ± 1.4
	5	AW	59.2 ± 10	140 ± 10	36.4 ± 3.5	29.7 ± 12.3	47.0 ± 9.6	5.65 ± 0.78	17.0 ± 1.7
		RO	61.4 ± 8.5	144 ± 28	38.0 ± 7.7	40.3 ± 16.6	49.9 ± 12	5.98 ± 1.57	17.0 ± 2.6
		NW	45.5 ± 4.2	80.4 ± 5.8	31.4 ± 6.3	102 ± 24.7	51.7 ± 9.3	5.06 ± 1.22	16.2 ± 1.0
Cake Activated Biochar	1	AW	46.2 ± 1.3	77.8 ± 1.5	25.1 ± 3.8	23.2 ± 4.0	24.1 ± 0.9	8.38 ± 0.65	8.44 ± 1.3
		RO	44.2 ± 0.6	74.8 ± 1.2	28.2 ± 0.8	78.4 ± 6.4	27.4 ± 0.3	8.85 ± 0.50	6.24 ± 0.79
		NW	40.6 ± 6.7	81.2 ± 10	26.4 ± 4.1	161 ± 8.4	34.4 ± 0.5	7.57 ± 0.58	8.22 ± 0.09
	3	AW	50.4 ± 4.1	85.2 ± 7.1	32.2 ± 2.4	68.4 ± 0.4	26.4 ± 0.2	8.48 ± 0.14	9.57 ± 0.27
		RO	54.7 ± 2.1	92.0 ± 4.2	31.6 ± 5.1	31.1 ± 0.0	33.8 ± 6.3	8.28 ± 0.53	9.83 ± 1.25
		NW	47.6 ± 1.7	79.4 ± 4.5	26.4 ± 1.4	129 ± 4.3	43.5 ± 1.3	7.80 ± 0.59	9.27 ± 0.65
	5	AW	55.9 ± 0.8	95.0 ± 1.1	28.2 ± 0.3	55.6 ± 2.5	33.0 ± 1.1	7.44 ± 0.10	10.3 ± 0.7
		RO	56.0 ± 1.8	96.1 ± 2.3	29.0 ± 1.5	63.1 ± 6.1	38.8 ± 2.1	8.38 ± 0.24	10.1 ± 0.5
		NW	47.0 ± 7.1	80.0 ± 0.1	24.8 ± 2.5	127 ± 2.6	42.2 ± 1.2	7.65 ± 0.38	9.55 ± 0.73
Raw Litter (dry)			16.3 ± 0.5	27.9 ± 1.0	8.24 ± 0.27	42.0 ± 0.6	10.3 ± 0.0	1.11 ± 0.05	7.83 ± 0.01
Raw Cake (dry)			19.6 ± 1.1	30.6 ± 2.4	9.92 ± 0.48	56.8 ± 1.2	13.7 ± 0.4	3.78 ± 0.79	8.52 ± 0.01

¹PFT: post furnace treatment: no-wash, acid wash, rinse only.

Table 2. Elemental Composition in mg/g in Unwashed (NW), Acid Washed (AW) and Rinse-only (RO) Samples for Select Elements (Cu, Cd, Ni, Zn, As) in Litter and Cake and Respective Activated Biochars as Function of Flow Rate (FR) and Post-treatment.

	FR (ml/min)	PFT ¹	Cu	Cd	Ni	Zn	As
Litter Activated Biochar	1	AW	1.35 ± 0.01	0.00 ± 0.00	0.12 ± 0.00	1.40 ± 0.05	0.02 ± 0.00
		RO	1.32 ± 0.03	0.00 ± 0.00	0.09 ± 0.00	1.38 ± 0.07	0.03 ± 0.00
		NW	1.28 ± 0.06	0.00 ± 0.00	0.10 ± 0.01	1.48 ± 0.11	0.03 ± 0.00
	3	AW	1.63 ± 0.07	0.00 ± 0.00	0.11 ± 0.00	1.88 ± 0.08	0.02 ± 0.00
		RO	1.68 ± 0.13	0.00 ± 0.00	0.12 ± 0.03	1.99 ± 0.34	0.04 ± 0.00
		NW	1.38 ± 0.03	0.00 ± 0.00	0.08 ± 0.00	1.60 ± 0.14	0.03 ± 0.01
	5	AW	1.71 ± 0.14	0.00 ± 0.00	0.11 ± 0.01	2.03 ± 0.24	0.05 ± 0.00
		RO	1.75 ± 0.34	0.00 ± 0.00	0.11 ± 0.02	1.96 ± 0.43	0.02 ± 0.04
		NW	1.52 ± 0.22	0.00 ± 0.00	0.10 ± 0.01	1.66 ± 0.34	0.05 ± 0.01
Cake Activated Biochar	1	AW	0.93 ± 0.00	0.00 ± 0.00	0.08 ± 0.00	0.64 ± 0.01	0.02 ± 0.02
		RO	0.92 ± 0.01	0.00 ± 0.00	0.09 ± 0.00	0.64 ± 0.04	0.00 ± 0.00
		NW	0.84 ± 0.02	0.00 ± 0.00	0.08 ± 0.01	0.60 ± 0.03	0.00 ± 0.00
	3	AW	0.96 ± 0.01	0.00 ± 0.00	0.09 ± 0.00	0.64 ± 0.02	0.00 ± 0.00
		RO	1.03 ± 0.08	0.00 ± 0.00	0.08 ± 0.01	0.66 ± 0.04	0.01 ± 0.01
		NW	0.96 ± 0.03	0.00 ± 0.00	0.07 ± 0.01	0.57 ± 0.01	0.02 ± 0.00
	5	AW	1.14 ± 0.03	0.00 ± 0.00	0.08 ± 0.00	0.70 ± 0.02	0.02 ± 0.00
		RO	1.16 ± 0.03	0.00 ± 0.00	0.08 ± 0.00	0.69 ± 0.03	0.02 ± 0.00
		NW	1.02 ± 0.03	0.00 ± 0.00	0.08 ± 0.01	0.57 ± 0.08	0.03 ± 0.01
Raw Litter (dry)			0.374 ± 0.004	0.001 ± 0.000	0.026 ± 0.002	0.530 ± 0.007	0.010 ± 0.001
Raw Cake (dry)			0.395 ± 0.021	0.001 ± 0.000	0.037 ± 0.003	0.675 ± 0.029	0.011 ± 0.002

¹PFT: post furnace treatment: no-wash, acid wash, rinse only.

the atmosphere [22]. Complexity of these interactions is heightened for biochars reported herein due to high concentrations found for various inorganic species.

Acid Wash and Water Rinse Treatments

Acid-washing activated biochars in 0.1 M HCl solution (0.02 w/v ratio) led to partial removal of several elements with an concomitant increase of acid wash pH close to neutral (pH 6.4) at the end of the acid wash cycle. Amount of ash material removed during acid washing or water rinsing ranged from 8–13 % and 2.6–4.4%, respectively, dependent on activation conditions and sample source (litter and cake). During acid washing, aliquots were collected at 1, 5, 10, 30, and 60 min as well as during the two subsequent water rinses and water-only rinsing treatment. Figure 1 displays select elemental removal for litter samples activated at a 1 ml/min flow rate for both treatments (AW and subsequent rinses and RO). Leaching occurred readily for all elements reaching a plateau at around 30 min and highest removal occurred with potassium with up to 80.9 mg/g of sample. Potassium is the dominant alkali source in most biomass fuels [21,23]. Significantly less amounts leached for the remaining elements, with 19.4, 9.4, 5.4, and 2.8 mg/g respectively for sodium, calcium, phosphorous, and magnesium. Furthermore, elements consistently leached in the same order for all

flow rates and feedstock type (litter, cake). Albeit more concentrated in the biochars, solubility of some elements can diminish with pyrolysis. While 19.5% phosphorus from raw poultry litter was extracted in water by Qiu and Guo [24], Szogi and Vanotti [25] extracted up to 80% using organic acids in a treatment process called “quick wash”. Upon conversion into biochars Cantrell *et al.* [26] reported 0.5–31% reductions in the amount of soluble-P in poultry manure biochars from raw feedstock. Amounts leached for cake based activated biochars were consistently lower than those for litter despite higher initial concentrations in raw cake than litter (Table 1). Greater Ca, Mg, K, and Fe in raw cake than in litter samples were also determined by Sistani *et al.* [27]. Apparent disparity between initial concentration and amount removed between litter and cake suggests other factors (e.g. aging, composting, or drying processes) may change the resulting mineral make up [28]. During composting, Tiquia *et al.* [29] found that moisture affected temperature changes as well as cation-exchange capacity and total and water extractable inorganic fractions.

After the acid wash, minor to negligible elemental leaching occurred during two subsequent water rinses which took place eliminating any residual acid (Figure 1, Table 3). Additionally, there were differences across treatments in regards to preferential removal of some elements over others within the same treatment.

Table 3. Amount Removed per Sample (mg/g) for Five Elements (potassium, K; sodium, Na; calcium, Ca; phosphorous, P and magnesium, Mg) during Acid Washing (AW), First Rinse Post Acid Wash (1st WR), Second Rinse Post Acid Wash (2nd WR) and during Water Rinse-only without Acid Wash (RO) in Activated Biochars Made from Cake or Litter and Activated at Three Activation Flow Rates (FR)¹.

FR (ml/min)	Element	Litter Activated Biochar				Cake Activated Biochar			
		AW	1st WR	2nd WR	RO	AW	1st WR	2nd WR	RO
1	K	80.9	1.79		71.9	59.0	1.32		46.8
	Na	19.4	0.45		12.2	15.9	0.37		9.56
	Ca	9.39	0.04	0.02	0.09	8.64	0.07	0.04	0.06
	P	5.38	0.19	0.08	0.43	4.28	0.26	0.18	0.18
	Mg	2.76	0.02	0.01	0.03	3.47	0.16	0.07	0.42
3	K	91.2	1.88		80.7	64.5	1.63		55.4
	Na	21.0	0.55		12.9	11.1	0.42		5.70
	Ca	10.7	0.06	0.00	0.10	10.3	0.03	0.01	0.03
	P	5.81	0.29	0.10	0.51	4.50	0.32	0.14	0.43
	Mg	1.34	0.04	0.01	0.09	2.67	0.07	0.01	0.04
5	K	92.0	2.05		92.3	59.0	1.16		48.6
	Na	19.5	0.49		13.7	15.7	0.40		9.12
	Ca	7.93	0.03	0.02	0.10	10.0	0.08	0.03	0.08
	P	3.77	0.26	0.10	0.65	4.90	0.34	0.19	0.52
	Mg	3.77	0.04	0.02	0.07	0.52	0.14	0.07	0.06

¹Samples were exposed to 60 min each of acid (0.1 M HCl) or DI water in 0.02 w/v ratio.

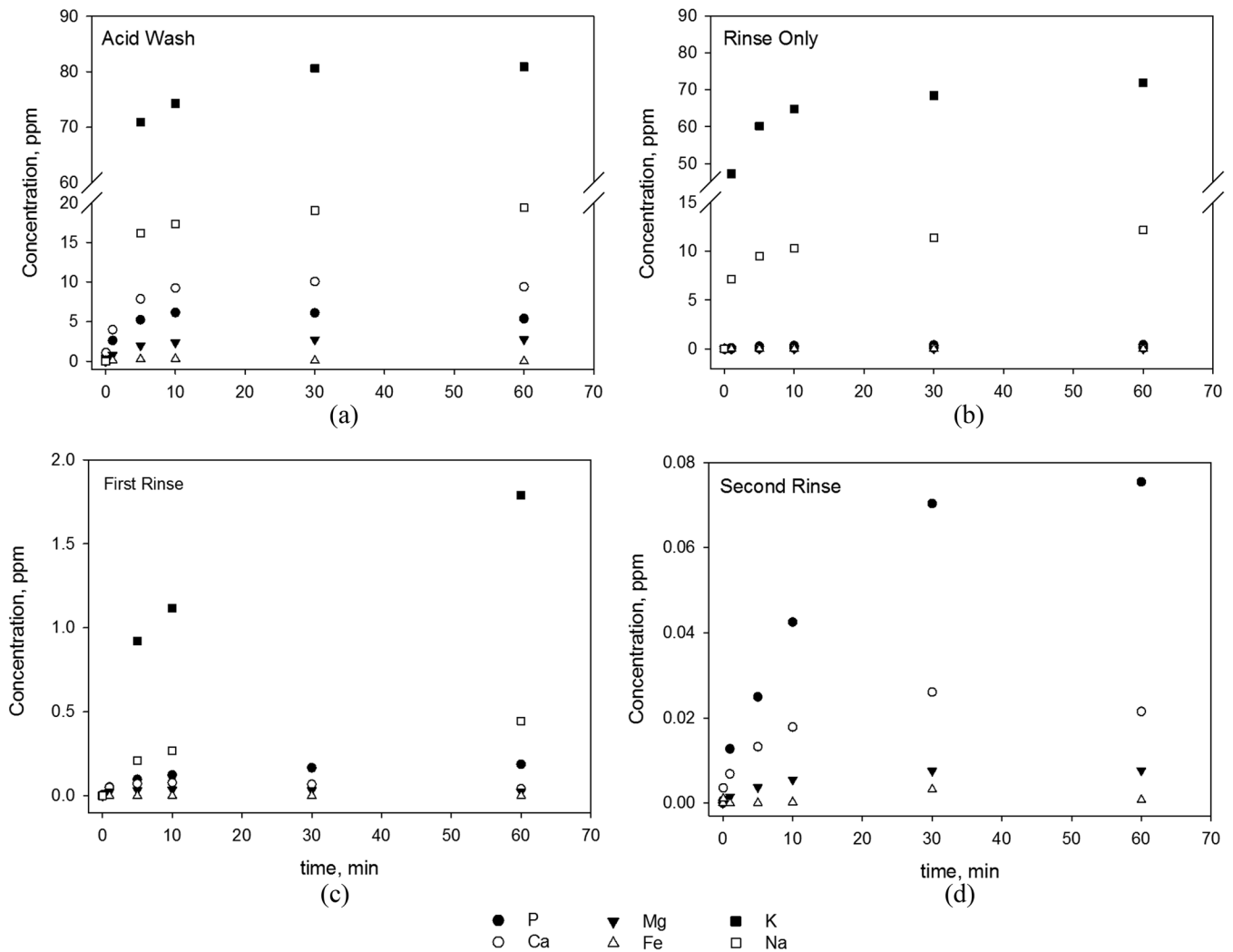


Figure 1. Elemental leach over washing period (acid wash and consecutive first and second water rinses as well as water rinse only treatment) for potassium, calcium, magnesium, iron, phosphorous and sodium for litter samples activated at 1 mL/min flow rate.

Removal was highly element-specific in RO samples that had potassium and sodium leaching in the same order of magnitude as with AW samples (81 and 19 mg/g for AW samples as compared to 72 and 12 mg/g for RO respectively). However, significantly less of the remaining elements were removed in RO with 0.09, 0.43, and 0.03 mg/g for Ca, P, and Mg as compared to AW samples (9.4, 5.4, and 2.8 mg/g of Ca, P, and Mg). Similar general trends were observed for cake and litter samples activated at 3 and 5 ml/min flow rates (Table 3). Using 1:10 w/v ratios for acid wash and water rinse treatments, Guo *et al.* [30] extracted even significantly lower amounts of phosphorus with 1.33 mg/g and 0.074 mg/g, respectively. Reduction of water soluble phosphorus might be the result of intentional additions of iron and aluminum by poultry producers [31]. Cantrell *et al.* [26] linked a very low correlation between percent ash and electrical conductivity of different manure

biochars to the possibility that some elements occurred as insoluble oxides or hydroxides unable to conduct electricity. Also, potassium and sodium concentrations combined and gave the closest relationship (R^2 value of 0.84) to electrical conductivity values. Because of much higher amounts of potassium and sodium removed as compared to remaining elements there was a concentration effect for these which can be seen in Table 1 and clarifies an “apparent” higher concentration in the AW and RO samples as compared to their NW counterparts. This can be exemplified with phosphorus and potassium which represent, respectively 13.4% and 35.3% of the total inorganic content measured with 69% and 4.7% extraction, respectively.

It is of interest to compare the amount removed during treatment to the original amount in the activated biochar to determine readiness of an element to leach when treating activated biochars with either acid or

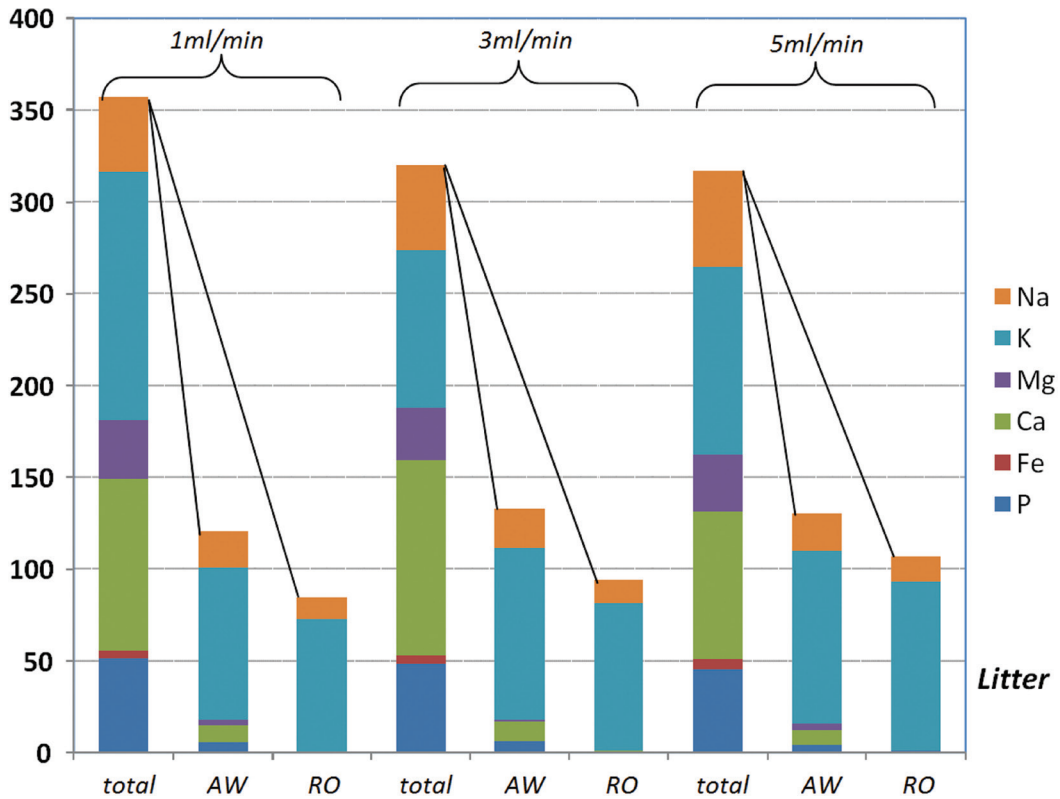


Figure 2. Element distribution (concentrations in mg/g) in activated char from litter (total) as compared to amount leached during AW and RO activation treatments.

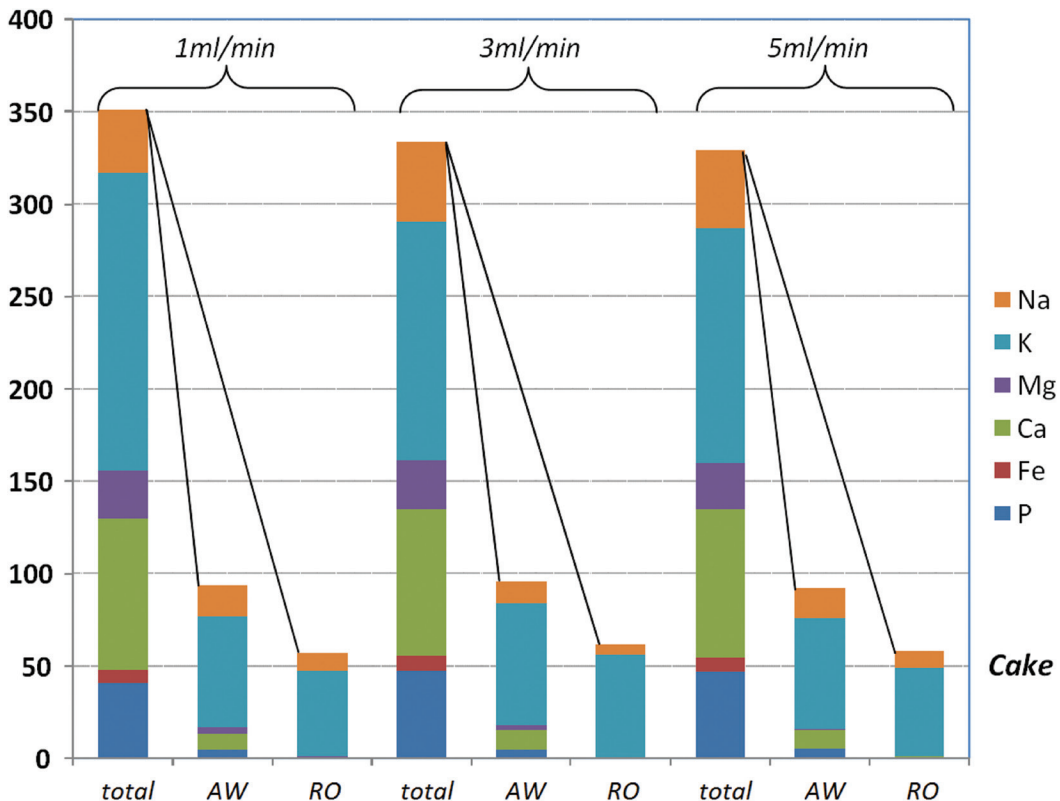


Figure 3. Element distribution (concentrations in mg/g) in activated char from cake (total) as compared to amount leached during AW and RO activation treatments.

Table 4. Percent Leached during Acid-wash (AW) and Rinse-only (RO) in Litter and Cake Activated Biochars in Comparison with Original Total Element Amount in the Unwashed Sample as Function of Flow Rate (FR).

Sample	Flow Rate mL/min	PFT ¹	Element Ratio (leached/original), %					
			P	Fe	Ca	Mg	K	Na
Litter Activated Biochar	1	AW	10.8	0.00	10.1	8.76	61	49
		RO	0.83	0.02	0.10	0.10	53	30
	3	AW	12.6	0.01	10.1	4.86	100	47
		RO	1.06	0.00	0.07	0.30	93	28
	5	AW	8.84	0.00	9.90	12.2	92	39
		RO	1.42	0.02	0.13	0.22	90	27
Cake Activated Biochar	1	AW	11.2	0.01	10.7	13.8	37	47
		RO	0.43	0.01	0.08	1.60	29	28
	3	AW	10.1	0.04	13.0	10.4	51	27
		RO	0.90	0.01	0.03	0.16	43	13
	5	AW	11.1	0.01	12.6	2.67	47	38
		RO	1.10	0.01	0.11	0.24	38	22

¹PFT: post furnace treatment: no-wash, acid wash, rinse only.

water (Figures 2 and 3; y-axis represent the cumulative sum of all measured elements). While potassium and sodium are readily removed during AW and RO treatments, remaining elements are removed in minor amounts in AW and do not readily leach in the RO treatment. Amounts removed as percentage of initial concentration during AW treatment ranged from 37–100% for potassium and 27–49% for sodium reported as percent of initial NW sample composition (Table 4). Jensen *et al.* [32] was able to extract up to 94% potassium from straw biochars using a countercurrent wash method as pretreatment for power production. Significantly less extraction as a percent of initial concentration was observed for the remaining elements ranging from negligible for iron to 2.7–13.8% for Mg, 9.9–13% for Ca, and 10.1–12.6% for P (Table 4). Using a much higher acid concentration than this study (5M HCl at 50°C, 24hr), Yip *et al.* [33] removed the majority of inherent alkali and alkaline earth metallic species in 750°C pyrolyzed wood, mallee leaf, and bark. However, it was determined that there were always some inorganic species not removed despite harsh treatment. Furthermore, it was found that Na, K, and Ca were the most probable species responsible for catalyzing gasification reactions. These observations have implications on solubility of elements in both acidic and neutral conditions.

Scanning electron micrographs of raw litter and respective NW, RO, and AW activated biochars are seen in Figure 4. Different surface structures demonstrated in these figures are representative of heterogeneity associated with manure feedstock. Besides bird drop-

pings, manure can contain different amounts of waste feed, soil, feathers, and bedding material each associated with different individual compositions that upon carbonization and activation processes may result in a wide range of final pore structures. Besides a visible porosity development upon pyrolysis and activation, presence of non-porous ash deposits in the NW sample is particularly noticeable. Removal of surface ash is seen for the RO (C; Figure 4) and particularly for the AW treated samples (D, Figure 4).

Implications on Surface Functionality

It has been postulated in previous studies [15,8] that phosphorus actively participates in the surface functionality of poultry manure biochars as negatively charged phosphate which is able to bind positively charged metal ions such as copper and zinc during adsorption. From FTIR spectra of broiler litter and its biochars, Uchimiya *et al.* [34] revealed a broad band near 1070 cm⁻¹ assigned to phosphorous-containing functional groups. Most importantly is the P–O bond of phosphate, considering the high phosphorous content of broiler manure and biochars. Disparity in element removal specifically retaining phosphorus and dropping potassium and sodium seem to support that view and further demonstrate acid washing serves as a means to remove loosely inorganic material that does not intervene in adsorption while maintaining surface functionality via chemically carbon-bound phosphate groups. Klasson *et al.* [35] have suggested that loose inorganic material negatively affects total surface area

of biochars by blocking pores that otherwise are less accessible for adsorption. Using both low and high ash almond varieties washing led to up to 60% removal of ash and more than a 100% increase in biochar surface areas [35]. By using different HCl concentrations (0.05–0.2 M HCl) to affect release of both anions and cations, Brisolara *et al.* [16] determined release is proportional to acid strength used with highest release and leveling off at 1 M HCl. Amounts released for poultry manure AW in 2 M HCl for calcium, iron, magnesium, phosphorous, and sulfur were 93%, 79%, 100%, 86%, and 49% of initial amounts in activated biochar as compared to 42%, 11%, 55%, 39%, and 38% at 0.05 M HCl. Albeit removing a larger inorganic fraction harsher AW decreased copper ion adsorption from 42–0.32 mg/g indicating concomitant removal of surface functionality. Mild acid treatment (0.1 M HCl) and water treatment of poultry litter and cake based activated biochars did not significantly affect copper

adsorption as reported in Lima *et al.* [8] in addition to extraction of leachable minerals.

Volatility of Inorganic Elements

During pyrolysis and activation, burn-off takes place and carbon, nitrogen, and sulfur readily volatilize to an extent dependent on time, temperature, and activation flow rate [8]. Burn-off is concomitant with concentration of the inorganic fraction (Table 1). Assuming that inorganic constituents are not volatilized during pyrolysis and activation conditions, it is possible to calculate their expected concentration by combining digestion results before and after pyrolysis for each element with yield data. By comparing amounts estimated with those from digestion results it is possible to trace each element during pyrolysis/activation and roughly estimate volatility. Estimated amounts were compared to measured amounts per digestion method and reported

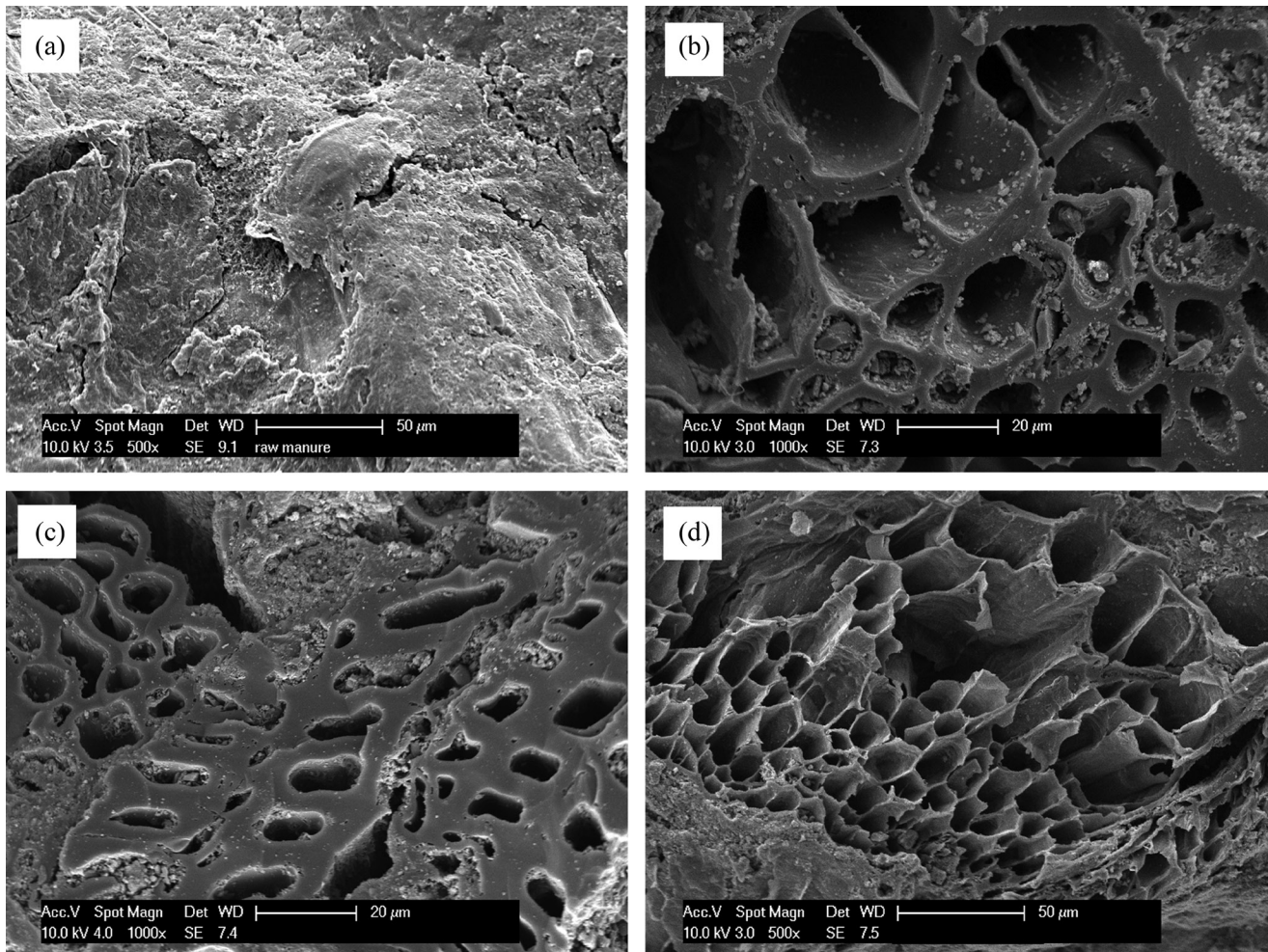


Figure 4. Scanning Electron Micrographs of (a) raw litter, (b) unwashed activated biochars, (c) rinsed activated biochars, and (d) acid-washed activated biochar.

in Table 5. It can be clearly seen that actual element amounts measured in activated biochars fall behind those predicted from concentration (raw and activated biochars) and yield data and discrepancies are element specific and related to the volatility of the element. Release of atomically dispersed inorganic material from biomass undergoing pyrolysis is likely influenced both by its inherent volatility and reactions of organic portions of the biomass. Material inherently volatile at combustion temperatures includes derivatives of some of the alkali and alkaline earth metals most notably potassium and sodium whereas other non-volatile material (Ca, Mg etc.) can be released by convective transport during rapid pyrolysis [36]. For pyrolysis temperatures below 700°C, Jensen *et al.* [37,38] reported no significant potassium release via volatilization with a progressive increase in release with temperature and presence of chlorine [39]. Yet, Sheth and Bagchi [40] reported that all phosphorus remained in biochar residue upon gasification of poultry litter regardless of temperature. Pyrolysis and activation were carried out respectively at 700°C and 800°C indicating that it is reasonable to assume that lower than expected numbers calculated for element composition in biochars are in part due to partial volatilization. Reviewing Table 5 it is apparent that volatilization was likely compounded with activation flow rate and higher for litter than for cake. Sodium was the only element for which measured amounts were close to those estimated. Potassium in litter samples activated with 3 and 5 ml/min

water flow rates displayed the highest differences with up to less than half the amount expected. Mentioned prior, higher activation flow rates may lead to higher vapor pressures and perhaps enhanced volatilization rates by convective transportation via steam as the carrier. The apparent increase in volatilization rates with activation flow rate might help explain earlier trends on leaching as a function of flow rate. It had been discovered that higher activation flow rates led to higher carbon burn-off with concomitant higher ash. Therefore, it seems more likely for higher activation flow rates to also lead to higher leaching. However, this was not observed and Tables 1 and 2 show no obvious trend in respect to amount leached and activation flow rate. Rather, higher volatilization rates observed at higher activation flow rates result in less than expected (based on yield alone) inorganic content which in proportion translates to lower or equal apparent leaching amounts for all activation flow rates.

Heavy Metals

Reusing poultry litter is of economic and environmental importance to sustainable agriculture. Therefore, measuring the amount of these elements in litter and their fate through the process of pyrolysis and post-treatment technologies becomes fundamental. Heavy metals can be present in poultry manure as waste feed as well as excess feed micronutrients that are excreted. Arsenic as 3-nitro-4-hydroxy-phenylarsonic acid [41]

Table 5. Comparison of Select Element Composition Measured per Digestion Method with Estimated Amount based on Pyrolysis/activation Yield and Element Composition in Raw Amount, as Function of Flow Rate (FR).

Sample	Flow Rate mL/min	Method	Yield %	Composition, mg/g					
				P	Fe	Ca	Mg	K	Na
Litter Activated Biochar	1	digested		51.5	4.02	93.5	31.8	136	40.4
		calculated	25.1	65.0	4.41	111	32.8	167	40.9
	3	digested		48.5	4.31	106	28.4	86.7	45.8
		calculated	22.5	72.4	4.92	124	36.6	186	45.6
	5	digested		45.5	5.06	80.4	31.4	103	51.7
		calculated	20.0	81.8	5.55	140	41.3	211	51.5
Cake Activated Biochar	1	digested		40.6	7.57	81.2	26.4	161	34.4
		calculated	37.7	51.9	10.0	81.2	26.3	151	36.3
	3	digested		47.6	7.80	79.4	26.4	129	43.5
		calculated	32.3	60.8	11.7	95.0	30.7	176	42.4
	5	digested		47.0	7.65	80.0	24.8	127	42.2
		calculated	30.8	63.7	12.3	99.6	32.2	185	44.5
Raw cake		digested		19.6	3.78	30.6	9.92	56.8	13.7
Raw litter		digested		16.3	1.11	27.9	8.24	42.0	10.3

is added as a coccidiostat or growth promoter, Copper sulfate (CuSO_4) is added as a fungistat, and Zn is added as a mineral supplement [28]. Table 2 displays amounts of copper, cadmium, zinc, and arsenic measured both in raw litter and cake as well as in respective activated biochars. All trace elements were present in negligent amounts except for copper and zinc. Nonetheless, these trace elements did not readily leach during acid washing and water rinsing (data not shown). Similar results were reported by Guo *et al.* [30] and Qiu and Guo [24]. However, because arsenic is highly water-extractable it is important that final concentrations of this element in water extracts do not exceed limits determined by the Environmental Protection Agency's National Pollutant Discharge Elimination System (NPDES) for surface water discharge limits (0.01 mg/L maximum contaminant level). Very low leaching of heavy metals concentrated in biochars from pyrolysis has been reported by Caballero *et al.* [42]. Naturally, because ashes from thermo-chemical conversion of biomass contain valuable plant nutrient elements (e.g., Ca, Mg, K, and P) they could be used directly as fertilizer or as raw materials to manufacture fertilizers and returned back to soil in a sustainable fashion. Additionally, many kinds of biomass ashes may be added to concrete as mineral admixtures because of the pozzolanic properties [43].

CONCLUSIONS

This study was conducted to determine effectiveness of AW and RO treatments for removing leachable elements and implications on resulting properties of poultry manure-based activated biochar. Reductions in ash content were observed with both treatments and more importantly both were able to remove loose inorganic material that can negatively affect surface properties and usability of activated biochar. Due to significant amounts of inorganic material in biochar and activated biochar, final ash content was still high even after treatment. Selective removal of elements was observed in both treatments resulting from both initial element concentrations in raw sample as well as their solubility in acid and/or water and effect of pyrolysis and activation processes. Highest rates of extraction as percentage of original amounts were observed for potassium and sodium for which acid washing and rinsing were equally efficient removal methods. By tracing the fate of individual elements through the pyrolysis/activation/post treatment processes it was found that some elements volatilized to a certain extent during pyrolysis/activation with higher volatility measured for

potassium and lowest for sodium. More importantly, besides negligent leaching of heavy metals, mild acid treatment also seemed to allow for retention of other inorganic species, particularly phosphorus, which are likely key participants in activated biochar surface functionality which is an important characteristic of these activated biochars. When additional reduction in inorganic content is necessary, care must be taken to ensure treatment for minerals removal is not too harsh and at the expense of decreased surface functionality.

ACKNOWLEDGMENTS

The authors would like to thank Renee Bigner for various analyses and technical assistance in this study and Dana Miles for supplying broiler litter and broiler cake samples. Mention of trade names or commercial products in this publication is solely for the purpose of providing specific information and does not imply recommendation or endorsement by the U.S. Department of Agriculture. USDA is an equal opportunity provider and employer.

REFERENCES

- Laird, D.A., The charcoal vision: a win-win scenario for simultaneously producing bioenergy, permanently sequestering carbon, while improving soil and water quality, *Agron. J.*, Vol. 100, 2008, pp. 178–181. <http://dx.doi.org/10.2134/agrojn2007.0161>
- Lehman, J., Bio-energy in the black, *Front. Ecol. Environ.*, Vol. 5, 2007, pp. 381–387.
- U.S.D.A. National Agricultural Statistics Service, Agricultural Statistics Data Base, Dairy and Poultry statistics, 2011.
- S. Koutcheiko, S., Monreal, C.M., Kodama, H., McCracken, T., Kotlyar, L., Preparation and characterization of activated carbon derived from the thermo-chemical conversion of chicken manure, *Bior. Technol.*, Vol. 98, 2007, pp. 2459–2464.
- Bailey, S.E., Olini, T.J., Bricka, R.M., Adrian, D.D., A review of potentially low cost sorbents for heavy metals, *Water Res.*, Vol. 33, 1999, pp. 2469–2479. [http://dx.doi.org/10.1016/S0043-1354\(98\)00475-8](http://dx.doi.org/10.1016/S0043-1354(98)00475-8)
- Ioannidou, O., Zabaniotou, A., Agricultural residues as precursors for activated carbon production—A review, *Renew. Sustain. Energy Rev.*, Vol. 11, 2007, pp. 1966–2005. <http://dx.doi.org/10.1016/j.rser.2006.03.013>
- Fan, X.D., Zhang, X.K., Adsorption of Heavy Metals by Adsorbents from Food Waste Residue, *J. Res. Sci. & Technol.*, Vol. 12, 2015, pp. S155–S158. <http://dx.doi.org/10.12783/issn.1544-8053/12/s1/22>
- Lima, I.M., Boykin, D.L., Klasson, K.T., Uchimiya, M., Influence of post-treatment strategies on the properties of activated chars from broiler manure, *Chemosphere*, Vol. 95, 2014, pp. 96–104. <http://dx.doi.org/10.1016/j.chemosphere.2013.08.027>
- Roskill, S., *The Economics of Activated Carbon*, eighth Ed., Roskill Information Services, London, UK 2008.
- Freedonia Group, *World Activated Carbon to 2012*. The Freedonia Group Inc., Cleveland, OH 2009.
- Lima, I.M., McAloon, A., Boateng, A.A., Activated carbon from broiler litter: process description and cost of production, *J. Biom. and Bioener.*, Vol. 32, 2008, pp. 568–572. <http://dx.doi.org/10.1016/j.biombioe.2007.11.008>

12. NRC. *Nutrient Requirements of Poultry: ninth revised Ed*, The National Academies Press, Washington DC, 1994.
13. Raveendran, K., Ganesh, A., Khilar K.C., Influence of mineral matter on biomass pyrolysis characteristics, *Fuel*, Vol. 74, 1995, pp. 1812–1822. [http://dx.doi.org/10.1016/0016-2361\(95\)80013-8](http://dx.doi.org/10.1016/0016-2361(95)80013-8)
14. Day, D.L., Funk, T.L., Processing Manure: Physical, Chemical and Biological Treatment, in: J.L. Hatfield, B.A. Stewart, Eds. *Animal Waste Utilization: Effective Use of Manure as a Soil Resource*, Ann Arbor Press, 1998, pp. 320.
15. Lima, I.M., Marshall, W.E., Adsorption of select environmentally important metals by poultry manure-based granular activated carbons, *J. Chem. Technol. Biotechnol.*, Vol. 80, 2005, pp. 1054–1061. <http://dx.doi.org/10.1002/jctb.1283>
16. Brisolará, K.F., Lima, I.M., Marshall, W.E., Cation and Anion Release from Broiler Litter and Cake Activated Carbons and the Role of Released Anions in Copper Ion Uptake, *Waste Biomass Valor.*, 2013, DOI 10.1007/s12649-013-9258-3. <http://dx.doi.org/10.1007/s12649-013-9258-3>
17. Pendyal, B., Johns, M.M., Marshall, W.E., Ahmedna, M., Rao, R.M., The effect of binders and agricultural by-products on physical and chemical properties of granular activated carbons, *Bior. Technol.* Vol. 68, 1999, pp. 247–254.
18. Ng, C., Losso, J.N., Marshall, W.E., Rao, R.M., Physical and chemical properties of selected agricultural byproduct-based activated carbons and their ability to adsorb geosmin, *Bior. Technol.*, Vol. 84, 2002, pp. 177–185.
19. Fitzmorris, K.B., Lima, I.M., Marshall, W.E., Reimers, R.S., Anion and Cation Removal from Solution using Activated Carbons from Municipal Sludge and Poultry Manure, *J. Resid. Sci. & Technol.*, Vol. 3, 2006, pp. 161–167.
20. Rodríguez-Mirasol, J., Cordero, T., Rodríguez J.J., Preparation and characterization of activated carbons from eucalyptus kraft lignin, *Carbon*, Vol. 31, 1993, pp. 87–95. [http://dx.doi.org/10.1016/0008-6223\(93\)90160-C](http://dx.doi.org/10.1016/0008-6223(93)90160-C)
21. Jenkins, B.M., Baxter, L.L., Miles Jr., T.M., Miles, T.R., Combustion properties of biomass, *Fuel Proc. Technol.*, Vol. 54, 1998, pp. 17–46. [http://dx.doi.org/10.1016/S0378-3820\(97\)00059-3](http://dx.doi.org/10.1016/S0378-3820(97)00059-3)
22. Zawadzki, J., *Chemistry and Physics of Carbon*, Vol. 21, Marcel Dekker Inc., New York, 1989.
23. Demirbas A., Fuel and combustion properties of bio-wastes, *Ener. Sourc.*, Vol. 27, 2005, pp. 451–462. <http://dx.doi.org/10.1080/00908310490441863>
24. Qiu, G., Guo, M., Quality of poultry litter-derived granular activated carbon, *Bior. Technol.*, Vol. 101, 2010, pp. 379–386.
25. Szogi, A.A., Vanotti, M.B., Prospects for phosphorus recovery from poultry litter, *Bior. Technol.*, Vol. 100, 2009, pp. 5461–5465.
26. Cantrell, K.B., Hunt, P.G., Uchimiya, M.S., Novak, J.M., Ro, K.S., Impact of Pyrolysis temperature and manure source on physicochemical characteristics of biochar, *Biores. Technol.*, Vol. 107, 2012, pp. 419–428. <http://dx.doi.org/10.1016/j.biortech.2011.11.084>
27. Sistani, K.R., Brink, G.E., McGowen, S.L., Rowe, D.E., Oldham, J., Characterization of broiler cake and broiler litter, the by-products of two management practices, *Bior. Technol.*, Vol. 90, 2003, pp. 27–32.
28. Kelley, T.R., Pancorbo, O.C., Merka, W.C., Thompson, S.A., Cabrera, M.L., Barnhart, H.M., Elemental concentrations of stored whole and fractionated broiler litter, *J. Appl. Poultry Sci.*, Vol. 5, 1996, pp. 276–281. <http://dx.doi.org/10.1093/japr/5.3.276>
29. Tiquia, S.M., Tam, N.F.Y., Hodgkiss, I.J., Changes in chemical properties during composting of spent pig litter at different moisture contents, *Agric. Ecosyst. and Environm.*, Vol. 67, 1998, pp. 79–89. [http://dx.doi.org/10.1016/S0167-8809\(97\)00132-1](http://dx.doi.org/10.1016/S0167-8809(97)00132-1)
30. Guo, M., Qiu, G., Song, W., Poultry litter-based activated carbon for removing heavy metal ions in water, *Waste Managem.*, Vol. 30, 2010, pp. 308–315. <http://dx.doi.org/10.1016/j.wasman.2009.08.010>
31. Codling, E.E., Chaney, R.L., Mulchi, C.L., Use of aluminum and iron rich residue to immobilize phosphorus in poultry litter and litter amended soils, *J. Environm. Qual.*, Vol. 29, 2000, pp. 1924–1931. <http://dx.doi.org/10.2134/jeq2000.00472425002900060027x>
32. Jensen, P.A., Sander, B., Dam-Johansen, K., Pretreatment of straw for power production by pyrolysis and char wash, *Biom. and Bioener.*, Vol. 20, 2001, pp. 431–446. [http://dx.doi.org/10.1016/S0961-9534\(01\)00005-8](http://dx.doi.org/10.1016/S0961-9534(01)00005-8)
33. Yip, K., Tian, F., Hayashi, J., Wu, H., Effect of Alkali and alkaline earth metallic species on biochars reactivity and syngas compositions during steam gasification, *Energy & Fuels*, Vol. 24, 2010, pp. 173–181. <http://dx.doi.org/10.1021/ef900534n>
34. Uchimiya, M., Lima, I.M., Klasson, K., Chang, S., Wartelle, L.H., Rodgers, J.E., Immobilization of heavy metal ions, CuII, CdII, NiII, and PbII, by broiler litter derived biochars in water and soil, *J. Agric. Food Chem.*, Vol. 58, 2010, pp. 5538–5544. <http://dx.doi.org/10.1021/jf9044217>
35. Klasson, K.T., Uchimiya, M., Lima, I.M., Uncovering surface area and micropores in almond shell biochars by rainwater wash, *Chemosphere*, Vol. 111, 2014, pp. 129–134. <http://dx.doi.org/10.1016/j.chemosphere.2014.03.065>
36. Khan, A.A., de Jong, W., Jansens, P.J., Spliethoff, H., Biomass combustion in fluidized bed boilers: Potential problems and remedies, *Fuel Proc. Technol.*, Vol. 90, 2009, pp. 21–50. <http://dx.doi.org/10.1016/j.fuproc.2008.07.012>
37. Jensen, P.A., Frandsen, F.J., Dam-Johansen, K., Sander, B., Experimental investigation of the transformation and release to gas phase of potassium and chlorine during straw pyrolysis, *Energy & Fuels*, Vol. 14, 2000, pp. 1280–1285. <http://dx.doi.org/10.1021/ef000104v>
38. Jensen, P.A., Sander, B., Dam-Johansen, K., Removal of K and Cl by leaching of straw char, *Biom. and Bioener.*, Vol. 20, 2001, pp. 447–457. [http://dx.doi.org/10.1016/S0961-9534\(01\)00006-X](http://dx.doi.org/10.1016/S0961-9534(01)00006-X)
39. Olsson, J.G., Jäglid, U., Pettersson, J.B.C., Alkali metal emission during pyrolysis of biomass, *Energy & Fuels*, Vol. 11, 1997, pp. 779–784. <http://dx.doi.org/10.1021/ef960096b>
40. Sheth, A.C., Bagchi, B., Investigation of Nitrogen-Bearing Species in *Catalytic Steam Gasification of Poultry Litter, Air and Waste Managem. Assoc.*, Vol. 55, 2005, pp. 619–628. <http://dx.doi.org/10.1080/10473289.2005.10464653>
41. Kunkle, W.E., Carr, L.E., Carter, T.A., Bossard, E.H., Effect of Flock and Floor Type on the Levels of Nutrients and Heavy Metals in Broiler Litter, *Poultry Sci.*, Vol. 60, 1981, pp. 1160–1164. <http://dx.doi.org/10.3382/ps.0601160>
42. Caballero, J.A., Front, R., Marcilla, A., Conesa, J.A., Characterization of sewage sludges by primary and secondary pyrolysis, *J. Anal. Applied Pyrol.*, Vol. 40–41, 1997, pp. 433–450. [http://dx.doi.org/10.1016/S0165-2370\(97\)00045-4](http://dx.doi.org/10.1016/S0165-2370(97)00045-4)
43. Wang, G., Shenk, S., Sheng, C., Characterization of Biomass Ashes from Power Plants Firing Agricultural Residues, *Energy & Fuels*, Vol. 26, 2012, pp. 102–111. <http://dx.doi.org/10.1021/ef201134m>

Improvements to Manufactured Tiles using Sewage Sludge Ash Based on Kiln Temperature and Nano-SiO₂ Additive

DENG-FONG LIN¹, HUAN-LIN LUO^{1,*}, LISA Y. CHEN² and SHU-WEN ZHANG¹

¹Department of Civil and Ecological Engineering, I-Shou University, No.1, Sec. 1, Syuecheng Rd., Dashu District, Kaohsiung City 84001, Taiwan, R.O.C.

²Department of Information Management, I-Shou University, No.1, Sec. 1, Syuecheng Rd., Dashu District, Kaohsiung City 84001, Taiwan, R.O.C.

ABSTRACT: Effects of kiln temperature and nanomaterial quantity on properties of incinerated sewage sludge ash clay tiles was evaluated. Observing crystalline and mineralogical changes in the internal structure of the tiles, microstructural development of tiles was observed using X-ray diffraction and scanning electron microscopy. Results indicated for kiln temperatures lower than 1,100°C, the bending strength of tile specimens increased with increasing temperature. However, when fired at temperatures greater than 1,150°C, both bending strength and firing shrinkage decreased. Moreover, swollen specimens were observed at 1,200°C.

INTRODUCTION

SEWAGE sludge has been widely investigated for use in applications for resource recovery and for different disposal methods. After comparing different strategies for disposal of sewage sludge (conventional disposal/reuse and waste to energy), Asirai [1] reported that application of a full cycle of waste to energy can balance out considerable electricity usage for sewage treatment processes. A similar observation was reported by Hu *et al.* [2] and Zsabokorszky [3]. Anaerobic digestion is another answer for sludge management. Organic matter was converted into methane as a renewable energy. Rashed *et al.* [4] used this energy with application of rice straw and effective microorganisms (EM1) for improvement of performance on co-digestion of sewage sludge. They suggested that 20% rice straw and a 1:250 EM1 mixing rate was the most appropriate ratio according to chemical oxygen demand and a total volatile suspended solids destruction percentage. Hashimoto *et al.* [5] studied thermophilic and aerobic digestion (TAD) of sewage sludge efficiency by applying different wood chips. They observed approximately 60% of digestion efficiency was attained by the *Chamaecyparis obtusa* and *Cryptomeria japonica* wood chips while the *Pinus densiflora*

wood chip was only 40%. However, reclamation of sludge is still an important issue. Commonly, sewage sludge is incinerated into ash and then manufactured into products with higher commercial value like eco-cement, construction bricks, or tiles. They are used in other engineering applications such as pavement engineering [6,7]. Eliche-Quesada *et al.* [8] applied urban sewage sludge, bagasse, and sludge mixed with clay to manufacture bricks. Prior to producing bricks, all of the ingredients including clay and wastes were analyzed using X-ray diffraction, X-ray fluorescence, thermogravimetric analysis, and differential thermal and elemental chemical analyses. They found that water absorption and thermal insulation for bricks containing wastes were increased to 35% and 8%, respectively. However, compressive strength decreased by a maximum of 19%. Donatello and Cheeseman [9] reviewed the possibility of recycling or reusing incinerated sewage sludge ash (SSA) as an ingredient for construction materials. They suggested that incinerated SSA can be used as a clay substitute to produce calcined bricks, tiles, and pavers. Moreover, incinerated SSA can be applied as a raw material for producing lightweight aggregate. Zhou *et al.* [10] directly used as much as 60 wt% sewage sludge to manufacture split tiles. Water absorption and bending strength of split tile samples with 60 wt% sewage sludge fired at 1,210°C were 1.14% and 25.5 MPa, respectively. They suggested that use of this sludge to manufacture split tiles may help to consider-

*Author to whom correspondence should be addressed.
Tel. +886 7 6577711 ext. 3318, Fax. +886 7 6577461, E-mail: hlluo@isu.edu.tw

ably reduce environmental impacts. Incinerated SSA can be used as a renewable green resource and provides incinerated SSA to manufacture tiles. Jordan *et al.* [11] mixed clay with different ratios of incinerated SSA to produce ceramic tiles and showed that incinerated SSA is beneficial for resource recycling. However, due to the porous nature of incinerated SSA tiles manufactured by adding incinerated SSA are characterized by better water absorption, higher abrasion, and larger shrinkage in the tile body compared to pure clay tile. Although, the bending strength of the incinerated SSA tile does meet required specifications [12]. During a study of application of waste residues in the manufacturing of ceramic tiles Vidal and Migue [13] reported that using sewage sludge as a partial replacement for clayey raw materials for production of traditional ceramics may be cost effective. Their results suggested that addition of sewage sludge to ceramics resulted in an increase in water absorption and a decrease in bending strength. Therefore, they proposed that a suitable percentage of sludge to be selected and added to the ceramic tile body will be determined by standards applied to specific construction materials. Kayaci *et al.* [14] investigated potential for reusing sewage sludge as a replacement for raw clay material for manufacturing commercial walls, floors, and porcelain tile formulations. First, complete characteristics for all applied ingredients were obtained. Then, the thermal behavior and physical and technological properties of specimens containing various quantities of wastes (up to 10 wt. %) were acquired from different tests. They suggested it was possible to recycle wastes in tile manufacturing without deteriorating relevant technological properties of dried and fired ceramic bodies. Regarding another study, Liew *et al.* [15] substituted 10–40% of sewage sludge for clay in brick. They found the surface appearance of the sludge clay brick noticeably degraded and particularly for bricks in which 30% or greater sludge was added. However, kiln temperature plays an important role in the manufacturing of sludge bricks. Regarding some cases, compressive strength of bricks with 30% waterworks sludge added may reach 200 kg/cm² or more when fired at a kiln temperature of 1,050°C (Huang *et al.*, [16]). Furthermore, another study on influence of different types of clay on the amount of sludge ash replacement has shown that a kiln temperature of 1,100°C had a positive effect on brick made using potter's clay (Weng *et al.*, [17]). Different glazes were sintered onto surfaces of sludge ash tile overcoming aforementioned issues and results indicated some basic properties of sludge ash tile were improved when

a glaze concentration of 0.02 g/cm² was applied (Lin *et al.*, [18]). Furthermore, Lin *et al.* [19] studied influences of glazes with different colorants on properties of sludge ash tiles. Their findings revealed that red glazed tiles exhibited the most stable performance followed by blue, yellow, and purple glazed tiles. During their review of the possible application of SSA in the construction industry as a way towards a circular economy Smol *et al.* [20] provided detailed descriptions for possible uses of SSA for manufacturing of building materials and for bases, subbases, and embankments used in road constructions. Determining potential hazardous metals that leached out from bricks containing sewage sludge Geric *et al.* [21] simulated precipitation exposure of such bricks to observe quantity of heavy metals that may leach out of bricks. They reported leachates from bricks containing sewage sludge may result in adverse effects on exposed human populations and that a lower percentage of sludge may be an option for decreasing toxicity of final sewage sludge-produced bricks. Cusidó *et al.* [22] studied leachability and toxicity of clay bricks containing sewage sludge on the environment. They determined that sludge may be successfully incorporated into bricks and that content of sludge additions ranged from 5–25% by weight. Moreover, their test results suggested that clay bricks containing different levels of sludge had no effect on the environment. Results obtained from leaching tests following the standards NEN 7345, ESA PSS-01-702 and ESA PSS-01-729 suggested there were no environmental restrictions on use of clay bricks produced using sewage sludge acquired from different treatments.

Amirkhanian *et al.* [23] mentioned that nanotechnology has been applied to many engineering applications. Nano-sized particles are used to improve or enhance physical and chemical properties of various materials such as asphalt binders. Moreover, the same nanotechnology has recently been applied in the field of resource recycling and has shown promising results. During a previous study to improve properties of incinerated SSA clay tile the authors focused only on improving the surface by applying a glaze onto the tile. However, changes in tile structure caused by addition of incinerated SSA were neither studied nor improved. Nano-SiO₂ was added to improve and enhance liquid-phase sintering in an incinerated SSA clay tile body with the expectation that the nano-SiO₂ additive would not only increase the strength of the tile but also would improve other tile properties extending reuse of sewage sludge in the future.

Table 1. Physical Properties of Clay, Incinerated Sewage Sludge Ash, and Nano-SiO₂.

	Averaged Particle Size (nm)	Specific Surface Area (m ² /g)	Specific Weight
Clay	–	17.72	2.55
Sewage Sludge Ash	–	0.44	2.23
Nano-SiO ₂	10	670	–

MATERIALS AND METHODS

Materials

Three main components used to create tile specimens are listed below and their physical properties are presented in Table 1. They are as follows. First, brownish-yellow clay samples were obtained from a local tile factory. Results from energy-dispersive spectroscopic (EDS) analysis indicated that silicon with a concentration of 43.73%, is the main component of the clay (See Table 2). Second, dewatered sewage sludge samples were obtained from a local wastewater treatment plant in Kaohsiung City, Taiwan. Incinerated SSA, reddish-brown in color, is the residue of the sludge samples after they have been incinerated at 800°C. Again, as shown in Table 2, Al, with a concentration of 22.38%, is the main component in the incinerated SSA, followed by Fe and Si. Third, nano-SiO₂ was purchased from a local material company in Kaohsiung City. It is a white powder that contains 99.9% SiO₂ and 0.028% Cl. Concentrations of other chemical components like Cu, Al, Ca, Fe, Mg, and Sn are less than 0.002%.

Methods

Tile specimens were manufactured using different mix designs with assigned mix ratios. Amount of clay replaced by incinerated SSA was 0, 20, 30, 40, or 50% by weight. Nano-SiO₂ additives at 0 or 2% of the combined weight of the incinerated SSA and clay were added to each ash substitution in the mix. Different optimum amounts of water for each incinerated SSA replacement were uniformly mixed with clay, incinerat-

ed SSA, and nano-SiO₂. Prior to producing greenware specimens with dimensions of 12 × 6 × 1 cm the air in the mixture was expelled using a de-airing vacuum pugmill to knead the mixture. Next, the mixture was pressed by a pressing machine to produce 1-cm-thick strips. Strips were then left in a 27°C room for a few days. Subsequently, greenware specimens were oven-dried at 105°C. Finally, biscuit tile specimens were manufactured by firing specimens at different kiln temperatures from 1,000–1,200°C. Microstructures and properties of tile specimens were then studied at each kiln temperature in increments of 50°C.

Shrinkage, weight loss on ignition, water absorption, bending strength, and abrasion tests were performed on biscuit tile specimens according to CNS 3299 R3071 (Methods of Test for Ceramic Tiles, [24]) standards. To investigate effects of different kiln temperatures on biscuit tile specimens with added nanomaterial, scanning electron microscopy (SEM) was used allowing observation of the microstructures of specimens. X-ray diffraction (XRD) was also used to perform mineralogical analysis of the specimens.

RESULTS AND DISCUSSION

Shrinkage Test

Figures 1(a) and 1(b) suggest that firing shrinkages in length for the incinerated SSA clay tile specimens with 0% and 2% nano-SiO₂ were 8–10% and 12–13%, respectively, at a temperature of 1,100°C. This result implies 2% nano-SiO₂ additive may increase the firing shrinkage of tile specimens. However, the nano-SiO₂ additive had a relatively small influence on firing shrinkage at other temperatures. Moreover, firing shrinkages of less than 8% and 6% were observed at temperatures of 1,000°C and 1,150°C, respectively. This result indicates that firing shrinkage decreased as kiln temperature increased between 1,000°C and 1,150°C. Seen in Figure 1(b) the firing shrinkage for specimens containing 2% nano-SiO₂ decreased as amounts of clay replaced by incinerated SSA increased. The amount that decreased ranged from 0.2–1%. Furthermore, swelling of tile specimens was observed at 1,200°C where

Table 2. Results of EDS for incinerated sewage sludge ash, incinerated SSA, and clay (weight percent).

Element	O	Al	Ca	Fe	K	Na	Mg	Si	Total
Incinerated SSA	30.02	22.38	7.22	21.26	2.47	1.12	3.29	14.24	100
Clay	18.88	17.74	1.80	9.51	4.24	1.39	2.7	43.73	100

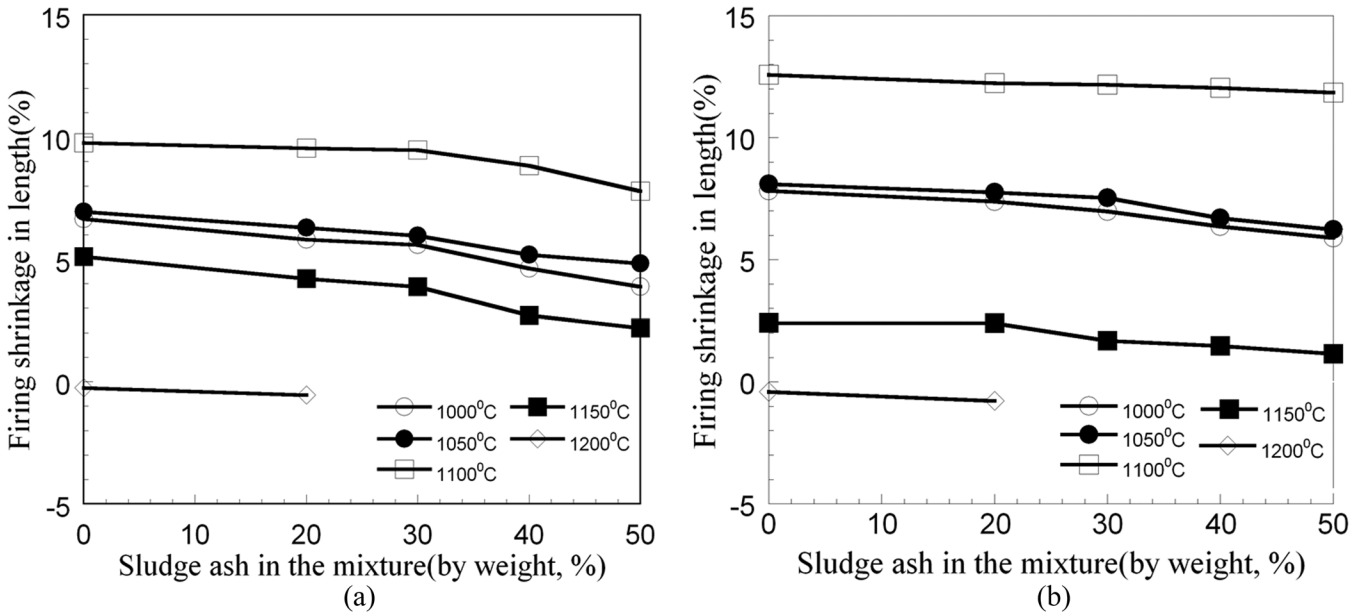


Figure 1. Firing shrinkages in length for the incinerated SSA clay tile specimens with (a) 0% and (b) 2% nano-SiO₂ added.

observed shrinkage was negative. Amount of swelling was between 0.2–1.6%. Hence, the tile body shrank slowly at lower temperatures, shrank severely at higher temperatures, and finally swelled at 1,200°C. This implies that kiln temperatures played an important role regarding shrinkage of the tile specimens.

Weight Loss on Ignition

Weight loss on ignition decreased as amount of in-

cinerated SSA added increased during different kiln temperatures (See Figures 2(a) and 2(b)). Figure 2(a) shows that weight loss on ignition for specimens with 0% nano-SiO₂ additive increased with increasing kiln temperature. Amount of increase was approximately 1.2–1.9%. Furthermore, when 2% nano-SiO₂ was added to the specimens weight loss on ignition was higher than for specimens with no added nano-SiO₂. Amount of increase was approximately 0.7–1.2% as displayed in Figure 2(b). Because different mineral compositions

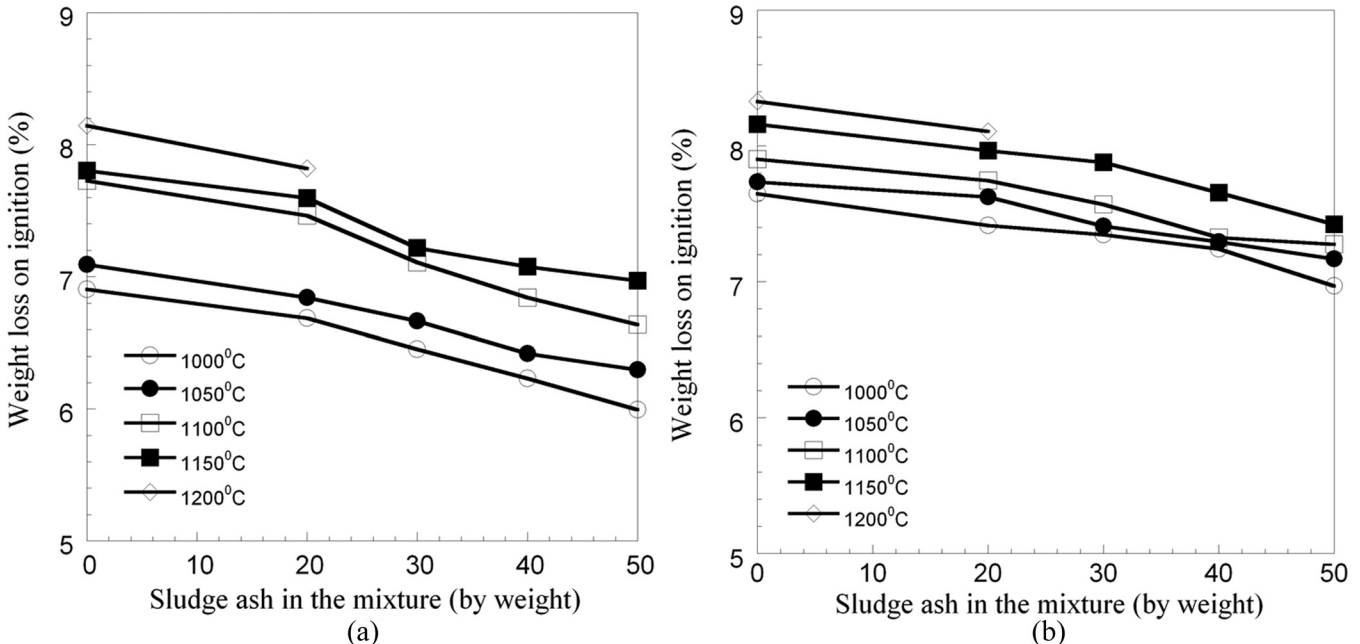


Figure 2. Weight losses on ignition for the incinerated SSA clay tile specimens with (a) 0% and (b) 2% nano-SiO₂ added.

in the tile body were decomposed and then gaseous carbonic acid was produced and evaporated, the implication is that weight loss on ignition increased as kiln temperature increased.

Water Absorption

Seen in Figures 3(a) and 3(b) 1,100°C is a temperature of demarcation for water absorption. Water absorption of the tile specimens slightly decreased with increasing temperature when the temperature was less than 1,100°C. Additionally, water absorption of the tile specimens increased with increasing amounts of incinerated SSA additions. During kiln temperatures over 1,100°C water absorption slightly increased with increasing temperature. Specimens with nano-SiO₂ added exhibited less water absorption than those without nano-SiO₂ when the kiln temperature was less than 1,100°C. Quartz melted at 1,100°C and solubility increased as temperature increased. This melting process led to development of glassy gangue crystals which have a dense structure and help resist invasion of water into the tile body. Furthermore, nano-SiO₂ may improve foam formation in the tile body. Hence, water absorption slightly increased with addition of nano-SiO₂ for temperatures over 1,100°C.

Bending Strength

Relationships between bending strength of tile specimens and different amounts of incinerated SSA replace-

ment and nano-SiO₂ additive are seen in Figures 4(a) and 4(b) for various kiln temperatures. Generally speaking bending strength decreased as amount of incinerated SSA replacement increased. However, bending strength increased when nano-SiO₂ was added. When the kiln temperature was lower than 1,100°C bending strength increased with increasing temperature. This result implies that a denser structure was produced during this temperature range. However, when the kiln temperature reached 1,150°C bending strength decreased due to foam formation in the tile body. Numerous weak micro-structural spots which are caused by bubbles in the foam were formed. This led to a considerable reduction in bending strength. Similar results were demonstrated during the shrinkage test and SEM analysis.

Abrasion

Relationships between abrasion of tile specimens and different amounts of incinerated SSA replacement and nano-SiO₂ additive are seen in Figures 5(a) and 5(b) for various kiln temperatures. The impact abrasion was measured according to CNS regulation 3299 R3071 [24]. Abrasion of the tile specimens was proportional to quantities of clay replaced by incinerated SSA as seen in Figures 5(a) and (b). Results indicate that abrasion decreased by approximately 0.036–0.09 g with increasing kiln temperature. Moreover, when the temperature was lower than 1,100°C the abrasion of the tile specimens increased with increasing quantities of clay replaced by incinerated SSA as seen in Figures

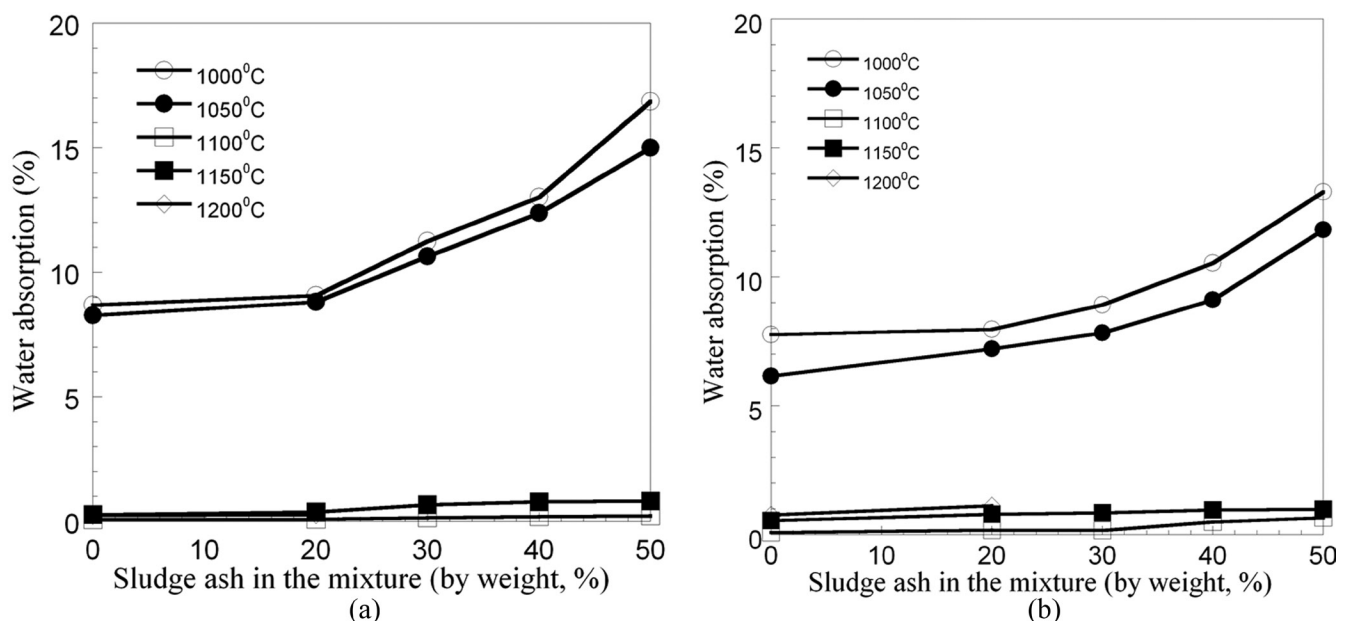


Figure 3. Water absorptions for the incinerated SSA clay tile specimens with (a) 0% and (b) 2% nano-SiO₂ added.

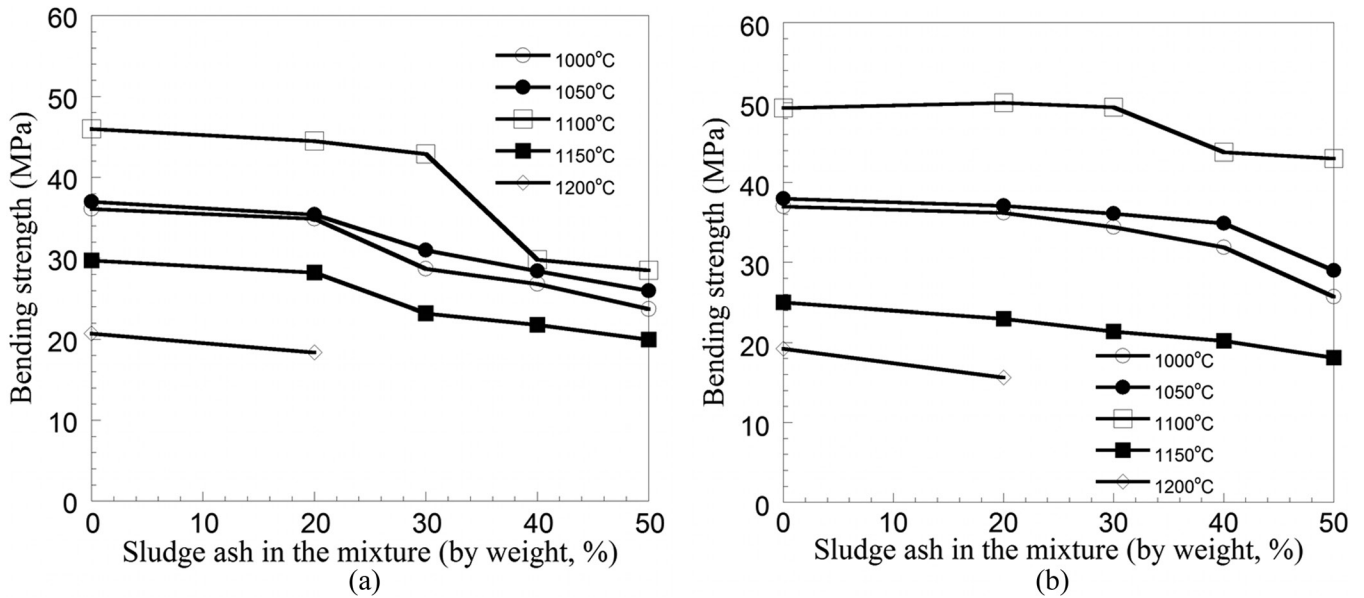


Figure 4. Bending strengths for the incinerated SSA clay tile specimens with (a) 0% and (b) 2% nano-SiO₂ added.

5(a) and 5(b). Incinerated SSA replacement has a slight effect on abrasion for kiln temperatures of 1,150°C and 1,200°C. These figures also show that abrasion of the specimens was greater than 0.01 g for temperatures of 1,000°C and 1,050°C but less than 0.01 g for temperatures of 1,100°C, 1,150°C, and 1,200°C. This implies that vitrification of the tile body became more mature as kiln temperature increased and impact resistance improved. Furthermore, amount of abrasion slightly decreased with an increase in nano-SiO₂. It was more than 0.02 g for temperatures lower than 1,100°C and

less than 0.02 g for temperatures higher than 1,100°C. Because nano-SiO₂ helps develop foam formations at higher temperatures numerous very fine holes were produced. Hence, impact resistance of the tile surface was slightly reduced.

SEM Analysis

SEM analysis was performed to better understand effects of kiln temperature on variation of crystalline states. Crystalline structures of tile specimens with 0%

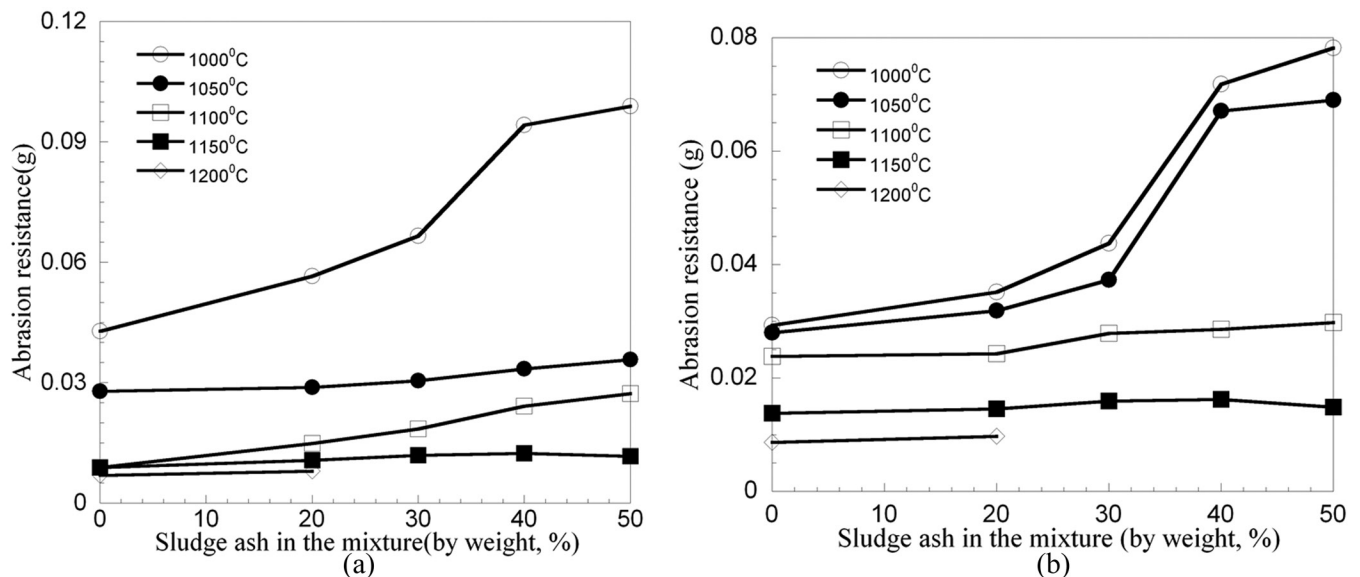


Figure 5. Abrasion resistances for the incinerated SSA clay tile specimens with (a) 0% and (b) 2% nano-SiO₂ added.

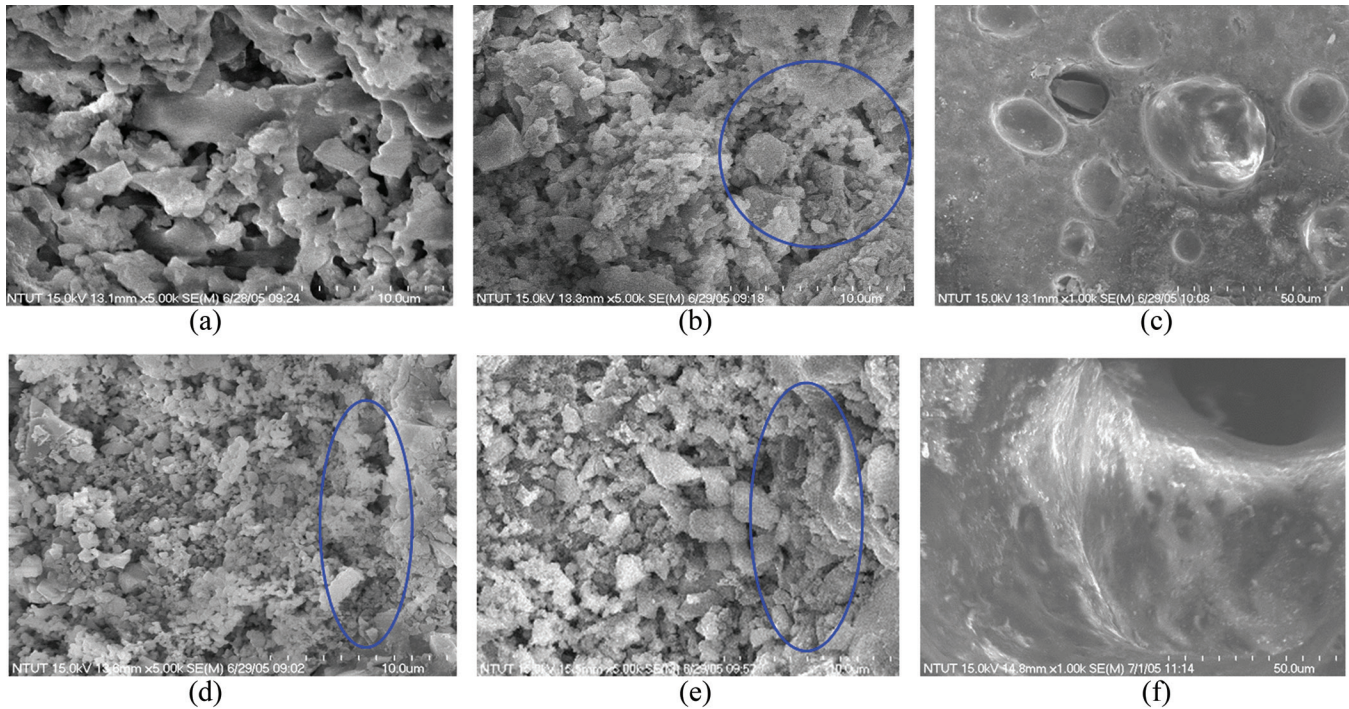


Figure 6. SEM pictures for tile specimens (a) pure clay at 1,000°C (b) pure clay at 1,100°C (c) pure clay at 1,200°C (d) 20% incinerated SSA clay at 1,000°C (e) 20% incinerated SSA clay at 1,100°C (f) 20% incinerated SSA clay at 1,200°C (crystal production is circled).

and 20% incinerated SSA replacement are displayed in Figures 6(a) to 6(f). Seen in Figure 6 the microstructure of the tile body became denser as kiln temperature increased. When temperature increased from 1,000–1,200°C, the shape of the crystal changed from granulated to flaky. The glassy phenomenon was observed at 1,200°C. Furthermore, tile specimens with 20% incinerated SSA replacement had more flake crystals and fewer pores than those with no incinerated SSA replacement. This result implies incinerated SSA was beneficial to crystallization and melting of tile bodies.

XRD Analysis

Albite was observed in crystal products of specimens fired at 1,200°C with 2% nano-SiO₂ added and 20% incinerated SSA replacing clay (See Figure 7). Crystallization of the tile body became denser as a result of increasing temperature. Furthermore, due to influence of nano-SiO₂ additive crystal products tended to be siliconized often including quartz and calcium silicate.

CONCLUSIONS

Effects of different kiln temperatures on incinerated

SSA clay tile specimens with 2% nano-SiO₂ added indicate that kiln temperature greatly affects properties of incinerated SSA clay tile. The critical kiln temperature falling between 1,100–1,150°C was obtained from tests of firing shrinkage, abrasion, and compressive strength. When temperature was less than or equal to 1,100°C, firing shrinkage, abrasion, and compressive strength increased with increasing kiln temperature.

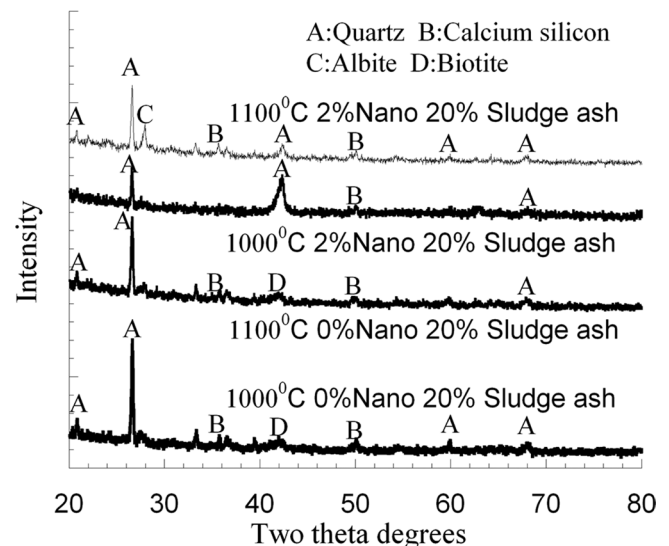


Figure 7. XRD analyses for the 20% incinerated SSA clay tile specimens with 0% and 2% nano-SiO₂ added at 1,000°C and 1,100°C.

However, firing shrinkage and abrasion decreased for temperatures higher than 1,150°C. Moreover, swollen tile bodies were observed at 1,200°C which implies that extra caution should be used when producing incinerated SSA clay tile at such a high temperature. Furthermore, addition of nano-SiO₂ may reduce water absorption and increase the bending strength of incinerated SSA clay tile specimens. This effect became more noticeable when larger amounts of clay were replaced by incinerated SSA. However, because nano-SiO₂ may improve foam formation which leads to an increase of pores in the tile body the water absorption slightly increased and bending strength decreased for firing temperatures over 1,100°C. Again, extra caution should be used when applying nano-SiO₂ additives to incinerated SSA clay tile.

ACKNOWLEDGEMENTS

This study was partly supported by the National Science Council of the Republic of China (Grant No. NSC 101-2221-E-214 -063 -MY3-1).

REFERENCES

- Zsirai, I., "Sewage sludge as renewable energy", *J. Residuals Sci. Technol.*, Vol. 8, No. 4, 2011, pp. 165–179.
- Hu, X. Y., L. N. Wu, C. Q. Dong, "Thermodynamic analysis of a sludge drying and incinerating process system", *J. Residuals Sci. Technol.*, Vol. 12, 2015, pp. S61–S66. <http://dx.doi.org/10.12783/issn.1544-8053/12/S1/9>
- Zsabokorszky, F., "Present and future sewage sludge treatment in Hungary and its energetic utilisation", *J. Residuals Sci. Technol.*, Vol. 10, No. 4, 2013, pp. 161–164.
- Rashed, E., A. Hassan, L. Ahmed, "Co-digesting sewage sludge using rice straw and effective microorganisms (EM1)", *J. Residuals Sci. Technol.*, Vol. 11, No. 3, 2014, pp. 77–82.
- Hashimoto, K., T. Doi, T. Okuda, W. Nishijima, S. Nakai, K. Nishimura, "Function of wood chips for composting of sewage sludge by thermophilic and aerobic digestion", *J. Residuals Sci. Technol.*, Vol. 12, No. 2, 2015, pp. 53–59. <http://dx.doi.org/10.12783/issn.1544-8053/12/2/3>
- Chen, L. and D. F. Lin. "Stabilization treatment of soft subgrade soil by sewage sludge ash and cement", *J. Hazard. Mater.*, Vol. 162, No. 1, 2009, pp. 321–327. <http://dx.doi.org/10.1016/j.jhazmat.2008.05.060>
- Lin, D. F., K. L. Lin, M. J. Hung, H. L. Luo. "Sludge ash/hydrated lime on the geotechnical properties of soft soil", *J. Hazard. Mater.*, Vol. 145, No. 1–2, 2007, pp. 58–64. <http://dx.doi.org/10.1016/j.jhazmat.2006.10.087>
- Eliche-Quesada, D., C. Martínez-García, M. L. Martínez-Cartas, M. T. Cotes-Palomino, L. Pérez-Villarejo, N. Cruz-Pérez, F. A. Corpas-Iglesias. "The use of different forms of waste in the manufacture of ceramic brick", *Appl. Clay Sci.*, Vol. 52, No. 3, 2011, pp. 270–276. <http://dx.doi.org/10.1016/j.clay.2011.03.003>
- Donatello, S. and C. Cheeseman. "Recycling and recovery routes for incinerated sewage sludge ash (ISSA): A review", *Waste Manage.*, Vol. 33, No. 11, 2013, pp. 2328–2340. <http://dx.doi.org/10.1016/j.wasman.2013.05.024>
- Zhou, J., T. T. Li, Q. Y. Zhang, Y. X. Wang. "Direct-utilization of sewage sludge to prepare split tiles", *Ceram. Int.*, Vol. 39, No. 8, 2013, pp. 9179–9186. <http://dx.doi.org/10.1016/j.ceramint.2013.05.019>
- Jordan, M. M., M. B. Almendro-Candel, M. Romero, J. M. Rincon. "Application of sewage sludge in the manufacturing of ceramic tile bodies", *Appl. Clay Sci.*, Vol. 30, No. 3–4, 2005, pp. 219–224. <http://dx.doi.org/10.1016/j.clay.2005.05.001>
- Tay, J. H. and K. Y. Show. "Utilization of municipal wastewater sludge as building and construction materials", *Resour. Conserv. Recycl.*, Vol. 6, No. 3, 1992, pp. 191–204. [http://dx.doi.org/10.1016/0921-3449\(92\)90030-6](http://dx.doi.org/10.1016/0921-3449(92)90030-6)
- Vidal, J. and M. Miguel. "The use of residues in the manufacture of ceramic tile bodies", *InterCeram: Int. Ceram. Rev.*, Vol. 59, No. 2, 2010, pp. 115–118.
- Kayaci, B., A. Kara, K. Kayaci, A. Samet Küçüker. "Re-use of mud from process waste water purification plant in ceramic tile production", *Ind. Ceram.*, Vol. 30, No. 3, 2010, pp. 195–207.
- Liew, A. G., A. Idris, C. H. K. Wong, A. A. Samad, M. J. M. M. Noor, A. M. Baki. "Incorporation of sewage sludge in clay brick and its characterization", *Waste Manage. Res.*, Vol. 22, No. 4, 2004, pp. 226–233. <http://dx.doi.org/10.1177/0734242X04044989>
- Huang, C. P., R. X. Yuan, Y. R. Liu, M. R. Wang. "Resource recycling by sintering waterworks sludge—a study of manufacture of brick and construction aggregates", In: *Proceeding of the 16th Conference on the Waste Treatment Technology, Taipei, Taiwan, s-c-006*, CD-ROM (2002).
- Weng, C. H., D. F. Lin, P. C. Chiang. "Utilization of Sludge as Brick Materials", *Adv. Environ. Res.*, Vol. 7, No. 3, 2003, pp. 679–685. [http://dx.doi.org/10.1016/S1093-0191\(02\)00037-0](http://dx.doi.org/10.1016/S1093-0191(02)00037-0)
- Lin, D. F., H. L. Luo, Y. N. Sheen. "Glazed tiles manufactured from incinerated sewage sludge ash and clay", *J. Air Waste Manage. Assoc.*, Vol. 55, No. 2, 2005, pp. 163–172. <http://dx.doi.org/10.1080/10473289.2005.10464614>
- Lin, D. F., W. C. Chang, C. Yuan, H. L. Luo. "Production and characterization of glazed tiles containing incinerated sewage sludge", *Waste Manage.*, Vol. 28, No. 3, 2007, pp. 502–508. <http://dx.doi.org/10.1016/j.wasman.2007.01.018>
- Smol, M., J. Kulczycka, A. Henclik, K. Gorazda, Z. Wzorek. "The possible use of sewage sludge ash (SSA) in the construction industry as a way towards a circular economy", *J. Clean Prod.*, Vol. 95, 2015, pp. 45–54. <http://dx.doi.org/10.1016/j.jclepro.2015.02.051>
- Geric, M., G. Gajski, V. Orešcanin, R. Kollar, V. Garaj-Vrhovac. "Chemical and toxicological characterization of the bricks produced from clay/sewage sludge mixture", *J. Environ. Sci. Health Part A—Toxic/Hazard. Subst. Environ. Eng.*, Vol. 47, No. 11, 2012, pp. 1521–1527. <http://dx.doi.org/10.1080/10934529.2012.680360>
- Cusidó, J. A. and L. V. Cremades. "Environmental effects of using clay bricks produced with sewage sludge: Leachability and toxicity studies", *Waste Manage.*, Vol. 32, 2012, pp. 1202–1208. <http://dx.doi.org/10.1016/j.wasman.2011.12.024>
- Amirkhanian, A. N., F. P. Xiao, S. N. Amirkhanian. "Characterization of unaged asphalt binder modified with carbon nano particles", *Int. J. Pav. Res. Technol.*, Vol. 4, No. 5, 2011, pp. 281–286.
- CNS Catalog. Method of test for ceramic tiles, CNS 3299 R3071; Ministry of Economic Affairs, Taiwan, Republic of China, 2011.

Comparison of Energy Efficiencies for Advanced Anaerobic Digestion, Incineration, and Gasification Processes in Municipal Sludge Management

A. GEZER GORGEÇ¹, G. INSEL^{2,*}, N. YAĞCI¹, M. DOĞRU³, A. ERDİNÇLER³, D. SANIN⁴, A. FILİBELİ⁵,
B. KESKİNLER² and E.U. ÇOKGÖR¹

¹Environmental Engineering Department, Gebze Technical University

²Environmental Engineering Department, Istanbul Technical University

³Environmental Engineering Department, Bogazici University

⁴Environmental Engineering Department, Middle East Technical University

⁵Environmental Engineering Department, Dokuz Eylul University

ABSTRACT: Municipal sludge has energy content in the range of (9,000–23,000 kJ/kg) depending upon the organic content. This entrapped energy can be transformed into heat and electrical energies by different technologies combining biological and thermal processes. Recently, the combination of advanced digestion and incineration or gasification was found to be advantageous for energy recovery. The energy balance was based upon a full-scale wastewater treatment plant (WWTP) using conventional and advanced treatment configurations. In this respect, the unit electricity production from sludge was calculated to be in the range of 675–1,240 kWhE per tones of dry solids.

INTRODUCTION

FINDING a sustainable solution for management of biosolids has become a major problem faced by many large cities. Corresponding with inexorable population increase considerable amounts of municipal sludge have been generated as an energy rich by-product from wastewater treatment processes. Additionally, land limitations in dense agglomerations requires rapid and energy efficient solutions to utilize energy by complying with environmental issues. Excess sludge is an inevitable drawback inherent to the activated sludge process. Generally, municipal sludge has energy content in the range of 2,149–5,492 cal/g dry sludge (9,000–23,000 kJ/kg) depending upon its organic content [1]. Energy production from wastewater sludge through anaerobic digestion is a common way of reevaluating biosolids. Energy production depends on biodegradability of organic content of sludge, organic loading rate, sludge retention time, temperature, pressure, and more. [2]. Hydrolysis is a rate-limiting step of anaerobic digestion of wastewater sludge. During this step both solubilization of particulate matter

and biological decomposition of organic polymers to monomers or dimers takes place [3].

Considering today's increasing pressures for energy efficiency and for sustainable biosolids disposal, the promise of benefits from pretreatment systems that break up cell structures in sludge became now more valuable than ever before. Thermal, chemical, biological, and mechanical processes as well as combinations of these have been studied as possible pre-treatments to accelerate sludge hydrolysis. These pre-treatment methods cause lysis or disintegration of sludge cells permitting release of intracellular matter that becomes more accessible to anaerobic microorganisms. This fact improves overall digestion process velocity and degree of sludge degradation and thus reducing anaerobic digester retention time and increasing methane production rates [4]. Thermal hydrolysis allows degradation of the sludge gel structure and a release of linked water. Optimal temperatures for thermal hydrolysis are in the range of 160–180°C and treatment times from 30–60 min. Pressure associated with these temperatures may vary from 600–2,500 kPa. By de-coupling long-chain polymers and hydrolyzing proteins it makes sludge more readily available for anaerobic digestion [5]. Thermal hydrolysis is able to split and decompose a significant part of the sludge solid fraction into soluble and less complex

*Author to whom correspondence should be addressed.
E-mail of the corresponding author: aragezer@yahoo.com

molecules [6,7]. It has been demonstrated that anaerobic digestion can consistently achieve 55–60% volatile solids destruction after thermal hydrolysis [8]. Porteous, Zimpro, and Cambi are some of the commercial illustrations for thermal pre-treatment processes [9]. Studies on the effect of thermal pretreatment on characteristics of degradation of waste activated sludge (WAS) in anaerobic digestion reveal that anaerobic digestion with thermal hydrolysis as pre-treatment has produced effective results such as a 25–30% increase of VS removal and 23–33% more biogas generation [2]. However, all options for pretreatment have substantial capital cost with thermal hydrolysis being more capitally intensive than mechanical options. Often, the cost of ancillary items such as odor control and sludge receivables in a centralized facility substantially exceed the cost of pretreatment equipment [10].

Another viable option could be gasification of municipal sludge that can offer a sustainable solution to biosolids disposal by using renewable fuel already available on-site. Gasification is defined as thermal decomposition of coal, biomass, or carbon containing organic solid material into synthetic gas (syngas) with a limited (sub-stoichiometric) amount of oxygen at high temperatures. Heating value of the syngas from waste sludge is around 4 MJ/m³ and efficient performance is taken from 90% DS content of sludge [11]. Gasification has advantages over incineration in terms of size and cost of exhaust gas control equipment for air emissions and by yielding a combustible gaseous product that can be used for energy generation from highly efficient prime movers (e.g. internal combustion gas engines and turbines) and as a revenue against operational costs for treatment plants [12,13]. Therefore, gasification has a potential to produce more energy with lower emissions. Due to this technology holding promise of energy savings as well as lower emissions compared to incineration it can be utilized as an alternative to the sewage sludge incineration system.

In this study; digestions, advanced anaerobic digestions and thermal sludge treatment process alternatives were compared on the basis of gross energy production from a large scale wastewater treatment plant.

MATERIALS AND METHODS

Wastewater Treatment Plant

The wastewater treatment plant under study is composed of a coarse screen, an inlet pumping station, a fine screen, grit/grease removal, primary sedimentation

tanks, and an activated sludge system together with an effluent pumping station. Average influent flowrate was measured at 120,000 m³/day (31 MGD) under dry weather conditions. The WWTP is located in the Hurma region of the Antalya province. Hydraulic retention time for the primary sedimentation tank is approximately 1 hr providing that TSS removal efficiency is around 40–50%. The activated sludge system was designed as an oxidation ditch system and Bio-P tanks in order to meet discharge limits for total $N < 10$ mgN/L and $TP < 1$ mgP/L. Treated wastewater is discharged into the Mediterranean Sea with an outfall system. The outfall system includes 5 km discharge pipeline with a 1,600 mm diameter. Oxygen transfer is provided by 3 turbo blowers with 25,000 m³/hour capacity each. The total solids retention time (SRT) of activated sludge system is 8 days. During actual operations, primary sludge is blended with 50% thickened secondary sludge and directly fed into a mesophilic (35°C) anaerobic digester. The digester VSS destruction is around approximately 35–40% yielding and SRT is 23 days with 4,000–5,000 m³/day biogas potential. Methane content of biogas is measured as 65%. Digested sludge is dewatered using decanter centrifuges prior to the belt drying system. After belt drying, the TSS content is increased up to 95% and is suitable for utilization in cement factories. Biogas is burned in gas engines just after H₂S treatment for energy and heat production. The flow scheme of the WWTP is illustrated in Figure 1.

Energy Content of Sludge

Sewage sludge has a calorific (heating) value close to that of brown coal at approximately 25,600 kJ/kg in dry basis due to substantial organic carbon and is finally converted into energy [14]. Therefore, when dried it is considered as a biomass or an alternative to primary fuels to be used in combustion processes.

However, the calorific value of sludge depends on the treatment processes that it has gone through. Digestion and composting processes for example reduce the calorific value since they reduce the organic content of sludge. Table 1 displays heating values of sludge at different stages of treatment. Figure 2 summarizes the energy contents of stabilized and un-stabilized sludge subjected to different processes for selected large scale WWTPs in Turkey.

Mass Balance and Energy Calculations

Energy flows based on process configurations were

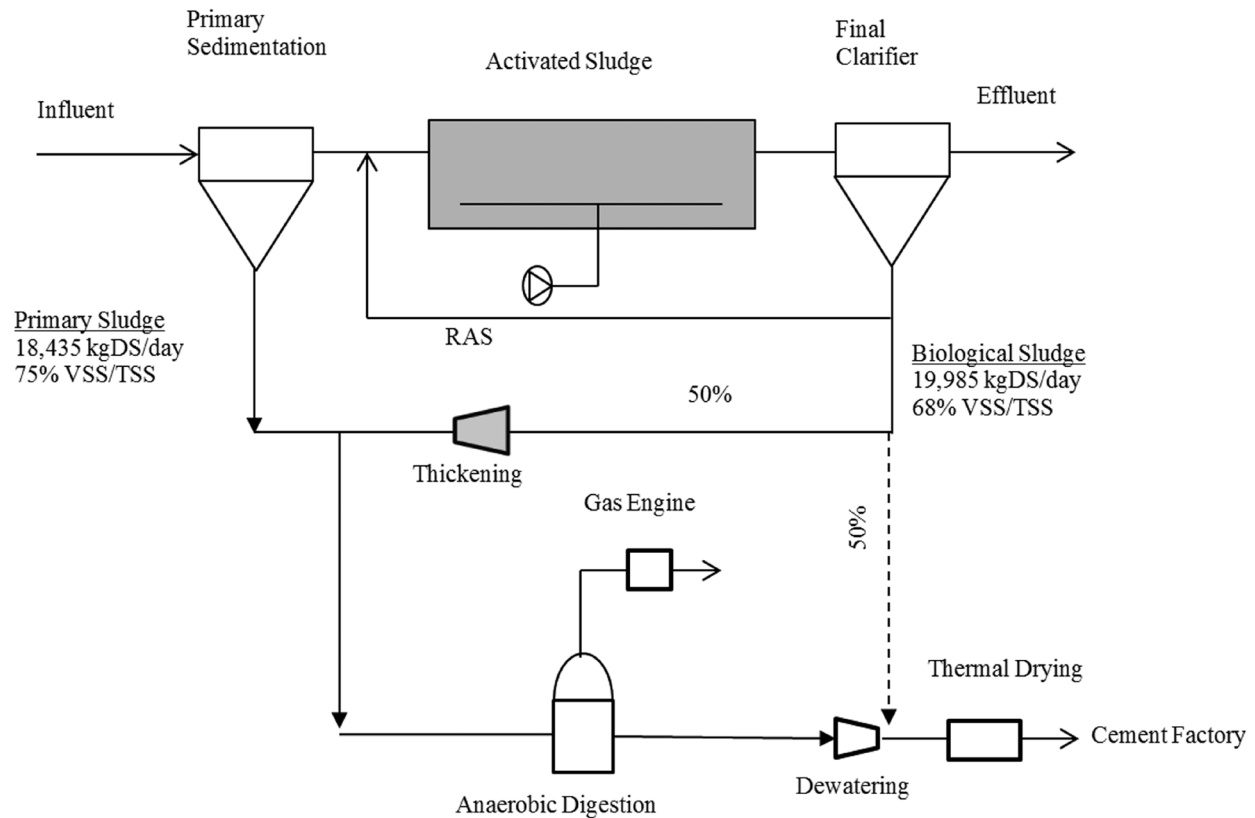


Figure 1. Flow scheme for a wastewater treatment plant.

performed based on VSS content of the sludge. Potential of sludge was converted into electrical and heat energy based on selected technology. Recently, sludge disintegration methods are widely used before anaerobic digestion. Disintegration methods of thermal, pressure, ultrasound, mechanical, and more are used before digestion of sludge in order to enhance anaerobic degradation. This increases biodegradability of biological sludge. By using primary and secondary sludge production capacity of the WWTP, (1) incineration, (2) digestion with incineration, (3) advanced digestion with incineration, and (4) gasification technologies were compared by using the heating value relationship between VSS content of the sludge as seen in Figure 2.

Table 1. Calorific Value of Various Types of Sewage Sludge [1].

Type of Sludge	VSS Content (VSS %)	Calorific Value (kJ/kg)
Raw primary sludge	84	23,000
Activated sludge	69	19,000
Anaerobic digested sludge	59	17,000
Anaerobic digested sludge	47	12,300
Anaerobic digested sludge	38	8,900

Electrical energy yields for biogas engines and ORC turbines (for gasification) were accepted as 40% and 24% respectively. Moreover, it is accepted that 15% of total gross energy may be recovered as an electrical energy from incineration with the aid of steam turbines. All heat losses were neglected in energy calculations.

RESULTS AND DISCUSSIONS

Plant Mass Balance and Energy Utilization

The wastewater treatment plant of interest in this study receives daily nearly 72 tons of COD and nearly 40 tons of TSS load under dry weather conditions. During steady state operation the daily primary and biological sludge (undigested) productions were calculated as 18,435 and 19,985 kg/day, respectively, which are in agreement with pump capacities. Additionally, the VSS/TSS ratios of primary and excess biological sludge were measured as 75% and 68%. Treated water quality complies with EU discharge limits enforced by the Urban Wastewater Directive (EEC1991/271). Daily biogas production varies in the range of 3,000–5,000 m³. Daily electrical energy consumption from the wastewater treatment plant is 65,500 kWh/day

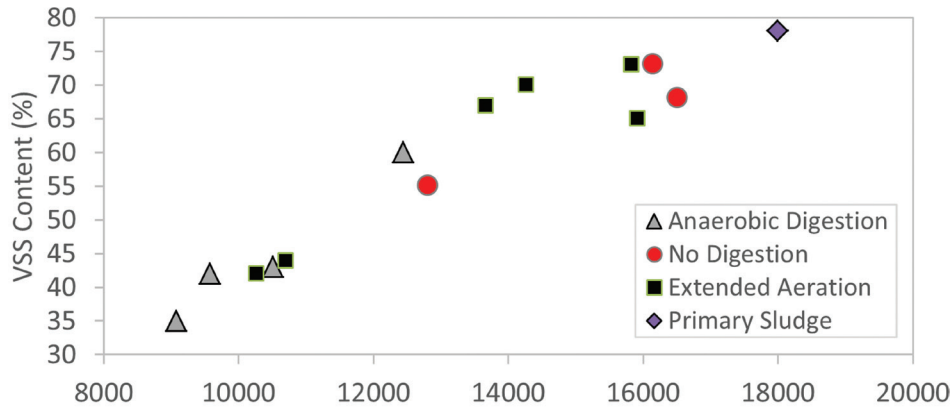


Figure 2. Energy content of sludge from different wastewater treatment plants in Turkey (Adapted from TUBİTAK-KAMAG; 2003) [16].

based on yearly averaged data. This corresponds to the unit electricity consumption of 30 kWh/year per population equivalence. However, the WWTP requires heat energy for the thermal belt sludge drying system and to keep digesters at 35°C. The thermal belt dryer and heat exchanger of digesters daily consume 100,000 kWh and 9,200 kWh heat energy, respectively. The pie-chart displayed in Figure 3 illustrates distribution of electrical energy consumptions within different units of the system. As seen in Figure 3, discharge pumping, aeration, and primary treatment units have the highest energy consumption rate at 29%, 28%, and 23%, respectively.

Energy Production Using Sludge Treatment Configurations

Energy content of sludge is important for calculating electrical and heat energy potentials derived from

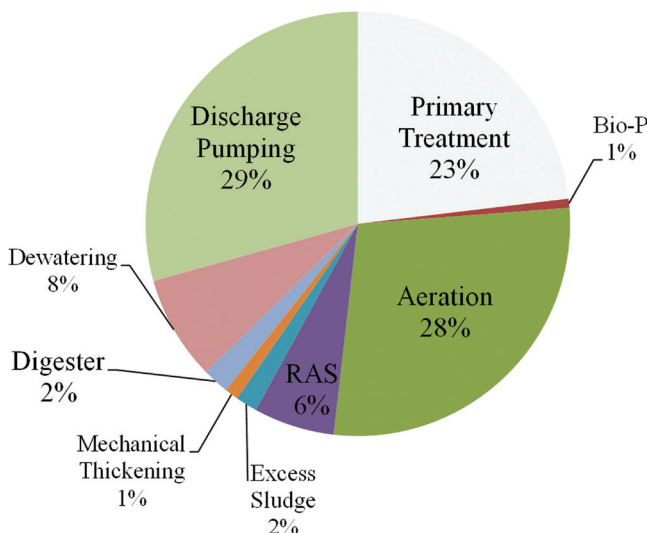


Figure 3. Distribution of electrical energy utilization in WWTP.

sludge using different technologies. Based on the information obtained from different treatment plants (Figure 2), energy contents of WWTP sludges were found to be dependent upon organic content (VSS%) of the sludge. According to the data collected from different WWTPs, no correlation was observed between the sludge digestion method and the calorific value. The data on the right edge of the graphic in Figure 2 reflects energy content of primary sludge measured to be 19,730 kJ/kg in a bomb calorimeter. Additionally, the energy content of biological undigested sludge was measured around 15,000 kJ/kg. Table 1 displays energy contents of sludge sampled from different points of the WWTP. Compared to literature values provided in Table 2, calorific values of sludge are relatively lower than that of their counterparts in the literature. It is important to note that overall investment costs, treatment costs for environmental compliances (stack-gas treatment, residual treatment, and disposal), and energy requirement for return of pollutant loads to the main treatment are not considered in the evaluation.

Alternative 1: Direct Incineration of Sludge

First alternative, calculations were made for direct combustion of sludge in incineration systems. Regard-

Table 2. Calorific Values from WWTP (LHV).

Type of Sludge	Solids Content %DS	Energy Content kJ/kgDS
Primary sludge	3.5	19,750
Undigested blended (P+S) sludge	5.0	13,450
Sludge after digestion	3.3	12,400
After thermal drying*	95	13,600

*50% biological sludge digested.

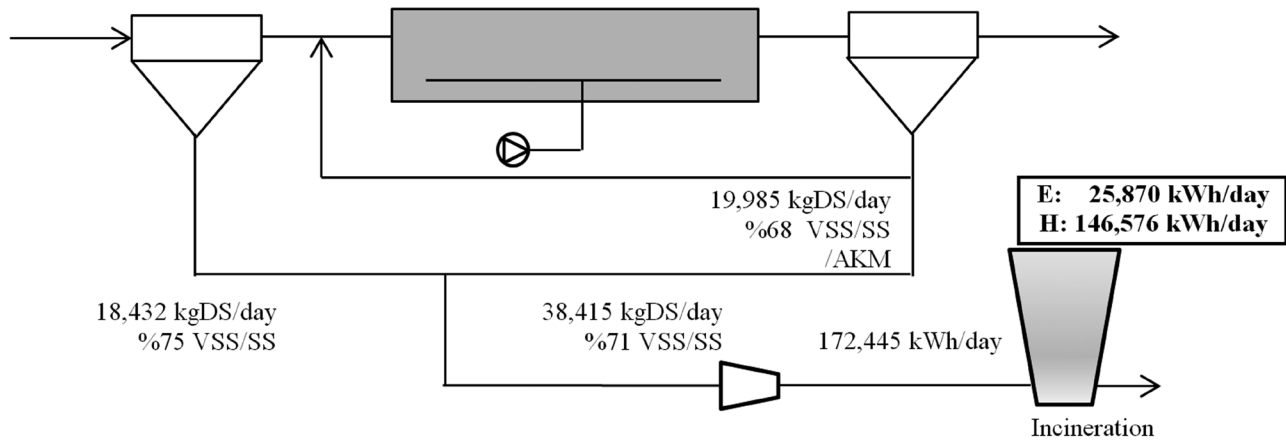


Figure 4. Direct incineration of primary and secondary sludge.

less of the technology selected, it was accepted that 15% of total sludge energy was converted into electrical energy by recovery via steam turbines. In cases of generating electricity by direct incineration of sludge with steam turbine the electrical energy (E) of 25,870 kWh/day could be recovered with direct incineration of primary and biological sludge from the WWTP. Calculations suggested that recovered electrical energy is able to cover approximately 40% of total electrical energy demand for the system. This alternative is illustrated in Figure 4. Aside from electrical energy the total amount of 146,576 kWh/day energy was obtained as heat energy. It is important to note energy loss by entropy was not included in calculations.

terms of energy recovery (Figure 5). Basically, energy may be recovered from (1) biogas obtained from anaerobic digestion and (2) heat energy from the incineration plant. As mentioned above, biogas is burned in gas engines to produce electrical and heat energy. VSS destruction was accepted as 35% based on the historical data from the WWTP. The result, total daily electrical energy of 39,758 kWh/day can be recovered from a combination of biogas and incineration technologies. The remaining sludge is directed to a sludge incineration system. Energy obtained during this alternative has the potential of 60% of total electrical energy demand for the WWTP. 58% of electrical energy produced is recovered with gas engines with biogas utilization.

Alternative 2: Anaerobic Digestion and Incineration

Regarding this alternative, the combination of anaerobic digestion and incineration was evaluated in

Alternative 3: Advanced Anaerobic Digestion and Incineration

During this alternative, a high pressure-thermal hy-

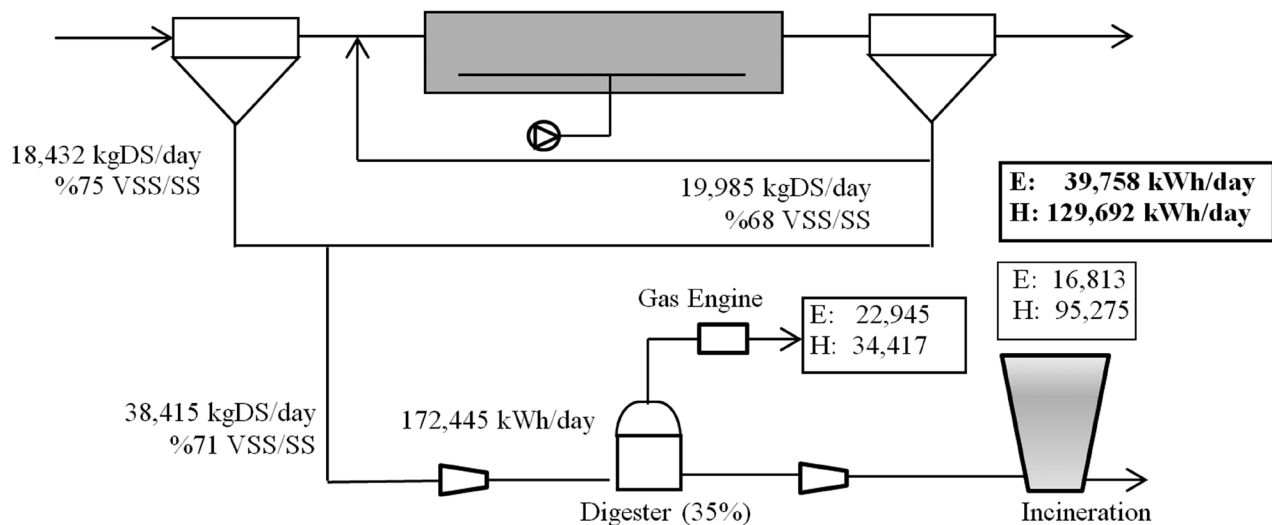


Figure 5. Incineration after primary and secondary sludge digestion.

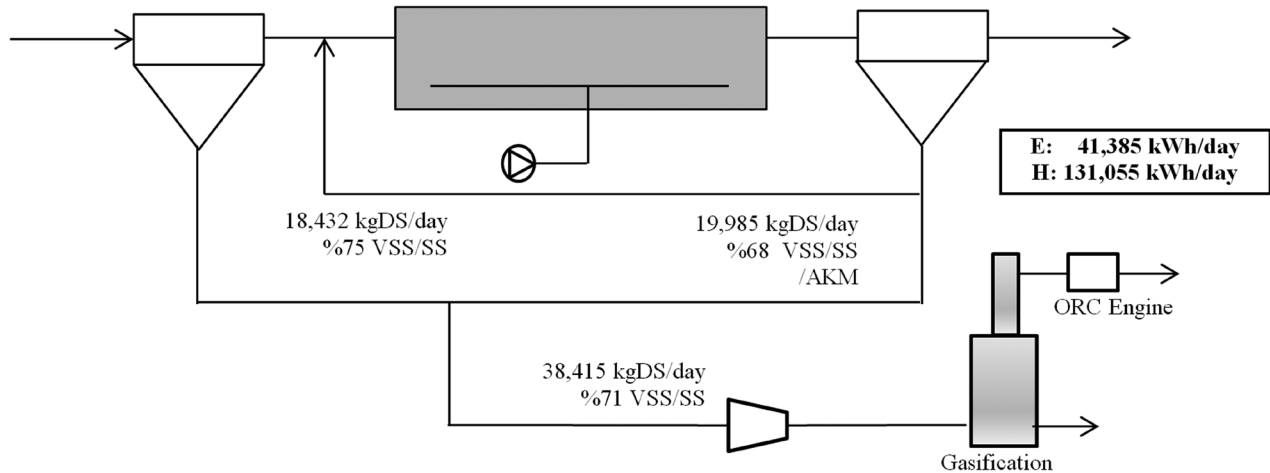


Figure 6. Sludge disintegration (THP) and anaerobic digestion prior to incineration.

drolysis process (THP) was selected as a pretreatment of biological sludge before entering anaerobic digesters. Calculations were made by assuming an anaerobic digester performance of 55% with respect to VSS destruction. Similar to the previous alternative, gas engines are to be fueled with biogas from the digester. Again, remaining sludge is completely oxidized in the sludge incinerator together with electrical energy production by combined steam turbines. The process flow scheme is illustrated in Figure 6.

Electrical power to be derived from the digester and incinerator is estimated to be 47,696 kWh/day. Approximately 70% of total electrical energy of the plant as a result can be recovered by implementing this alternative. Electrical energy generated by biogas is 76% of total electrical energy produced by this alternative. However, incineration is able to generate 73% of the heat (thermal) energy produced.

Alternative 4: Gasification of Sludge

Gasification is considered a novel process for producing syngas that has a high calorific value due to its CO and H₂ contents [16]. During this study a simplified example of energy recovery from the gasification process was evaluated for comparison of other applied sludge reduction technologies. Primary and secondary sludge is pre-dried and subjected to the gasification reactor. Efficiency of the gasification reactor and thermal oil unit was accepted as 100% by assuming no energy lost in the process. Efficiency of electrical energy production of the ORC engine was accepted as 24% for syngas utilization from the gasifier. Finally, electrical and heat energy produced by gasification are calculated to be 41,385 and 131,055 kWh/day, respectively. Table 3 provided below summarizes 4 alternatives for sludge reduction and energy production.

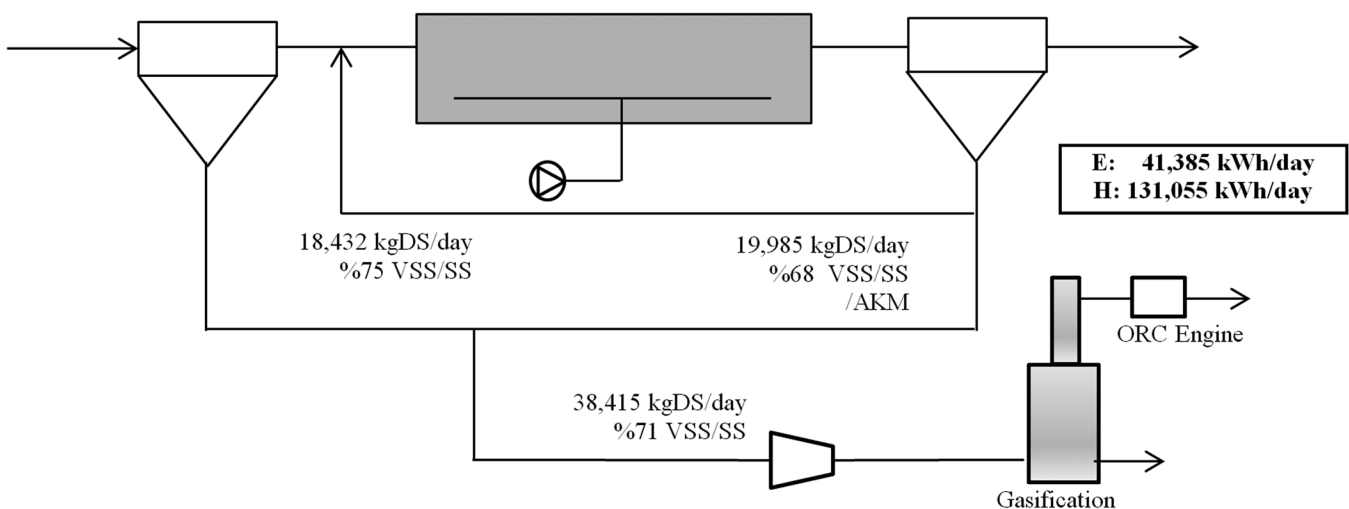


Figure 7. Gasification of primary and secondary sludge.

Table 3. Comparison of Gross Energy Yields from Sludge using Different Sludge Treatment Strains.

Treatment Method	Electricity kWh/day			Heat kWh/day			Unit Energy kWh/ton DS	
	Biogas	Thermal	E_{TOTAL}	Biogas	Thermal	H_{TOTAL}	Electricity	Heat
1 IN	–	25,870	25,870	–	146,576	146,576	675	3,815
2 AD+IN	22,945	16,813	39,758	34,417	95,275	129,692	1,035	3,375
3 AAD+IN	36,056	11,640	47,696	54,085	65,950	120,045	1,240	3,125
4 GS	–	41,385	41,385	–	131,055	131,055	1,075	3,340

IN: Incineration, AD: Anaerobic Digestion, AAD: Advanced Anaerobic Digestion, GS: Gasification.

CONCLUSIONS

Depending upon plant size, energy recovery is important that utilizes sludge that can be processed by different energy recovery technologies. Four alternative WWTP operation alternatives have been studied through mass and energy balance. From an energy production point of view processes such as advanced digestion coupled with incineration and gasification were found to be more effective for producing electricity from sludge. Based on the assumptions and calculations, the lowest electrical energy production is from direct incineration of the sludge (25,870 kWh/day). The highest electrical energy production can be achieved by advanced digestion (THP) and incineration of sludge that yields 47,670 kWh/day energy. The gasification process seems to be more advantageous compared to conventional anaerobic digestion and incineration of sludge with respect to more electrical energy outputs per ton of dry sludge. Gasification can yield up to 41,385 kWh/day electrical energy via syn-gas utilization. Alternatively, the unit energy (electrical) production varies in the range of 675–1,240 kWh/ton dry solids. Total heat requirement of the WWTP was calculated to be nearly 85,000 kWh/day including digester heating, steam production, and evaporation purposes. Incineration and gasification processes as a result should be used to generate heat energy to completely meet the heat requirement of units in the WWTP. Approximately 85% of energy in biosolids is converted to heat and electrical energy for the WWTP's operational requirements.

Thermal (heat) energy requirements necessitate implementation of terminal oxidation processes such as incineration and gasification. Further efforts should be dedicated towards answering the challenging questions and needs for more information in regards to technologies used in this study. Detailed calculations must take into account all heat energy and electrical power requirements and losses of the plant units. Moreover,

CAPEX and OPEX together with impact on wastewater treatment plant performance, stack-gas treatment, other recovery technologies, and carbon footprint of the system should also be investigated. Solutions for energy recovery may be different from theoretical approximation based upon local environmental factors and the operational strategy of treatment system.

SYMBOLS

WWTP = Waste Water Treatment Plant
 LHV = Lower Heating Value
 DS = Dry Sludge
 WAS = Waste Activated Sludge
 VS = Volatile Solids
 COD = Chemical Oxygen Demand
 MGD = Million Gallons per Day
 TSS = Total Suspended Solids
 N = Nitrogen
 TP = Total Phosphorous
 SRT = Solid Retention Time
 VSS = Volatile Suspended Solids
 RAS = Return Activated Sludge
 ORC = Organic Rankine Cycle
 SS = Suspended Solids
 THP = Thermal Hydrolysis Process
 IN = Incineration
 AD = Anaerobic Digestion
 ADD = Advanced Anaerobic Digestion
 GS = Gasification
 CAPEX = Capital Investment Cost
 OPEX = Operational Cost
 H = Heating
 E = Energy

ACKNOWLEDGMENTS

National Research Council of Turkey, TUBITAK (Project: 108G167) and Antalya Water and Wastewater Administration (ASAT) are kindly acknowledged.

REFERENCES

1. Cao, Y., Pawlowski, A., “Sewage sludge-to-energy approaches based on anaerobic digestion and pyrolysis: Brief overview and energy efficiency assessment”, *Renewable and Sustainable Energy Reviews*, 16, 2012, pp. 1657–1665. <http://dx.doi.org/10.1016/j.rser.2011.12.014>
2. Ferrer, I., Vazquez, F., Font, X., “Comparison of the Mesophilic and Thermophilic Anaerobic Digestion from an Energy Perspective”, *Journal of Residual Science & Technology*, Vol. 8, No.2, 2011, pp. 81–87.
3. Pérez-Elvira, S.I., Polanco, F.F., “Continuous thermal hydrolysis and anaerobic digestion of sludge. Energy integration study”, *Water Science & Technology*, Vol. 65, No. 10, 2012, pp. 1839–1846. <http://dx.doi.org/10.2166/wst.2012.863>
4. Müller, J. A., “Pre-treatment processes for recycling and reuse of sewage sludge”, *Water Science and Technology*, Vol. 42 No. 9, 2000, pp. 167–174.
5. Carrère, H., Dumas, C., Battimelli, A., Batstone, D.J., Delgenes, J.P., Steyer, J.P., Ferrer, I., “Pretreatment methods to improve sludge anaerobic degradability: A review”, *Journal of Hazardous Materials*, 183, 2010, pp. 1–15. <http://dx.doi.org/10.1016/j.jhazmat.2010.06.129>
6. McCarty, P. L., Smith, D. P., “Anaerobic wastewater treatment”, *Environ. Sci. Technol.*, Vol. 20, No. 12, 1986, pp. 1200–1206. <http://dx.doi.org/10.1021/es00154a002>
7. Haug R. T., Stuckey D. C., Gosset J. M., McCarty P.L., “Effect of thermal pretreatment on digestibility and dewaterability of organic sludges”, *J. Water Pollut. Control Fed. (JWPCF)*, 1978, pp. 5073–5085.
8. Jolis, D., “High-Solids anaerobic digestion of municipal sludge pretreated by thermal hydrolysis”, *Water Environment Research*, Vol. 80, No.7, 2008, pp. 654–662. <http://dx.doi.org/10.2175/193864708X267414>
9. Kepp, U., Machenbach, I., Weisz, N., and Solheim, O. E., “Enhanced stabilization of sewage through thermal hydrolysis—three years of experience with full scale plant”, *Water Science and Technology*, Vol. 42, No. 9, 2000, pp. 89–96.
10. Müller, J. A., “Prospects and problems of sludge pre-treatment processes”, *Water Science and Technology*, Vol. 44, No. 10, 2001, pp. 121–128.
11. Spinosa, L., Akyol, A., Baundez, J.C., Canziani, R., Jenicek, P., Leonard, A., Rulkens, W., Xu, G. and Dijk, L.V., “Sustainable and innovative solutions for sewage sludge management”, *Water Journal*, 3, 2011, pp. 702–717. <http://dx.doi.org/10.3390/w3020702>
12. Dogru, M., Fixed-bed gasification of biomass, PhD Thesis, University of Newcastle, 2000, UK.
13. Fericelli, P.D. “Comparison of Sludge Treatment by Gasification vs. Incineration”. Ninth LACCEI Latin American and Caribbean Conference (LACCEI'2011), Engineering for a Smart Planet, Innovation, Information Technology and Computational Tools for Sustainable Development, August 3–5, 2011, Medellín, Columbia.
14. Gerhardt, Th., Cenni, R., Siegle, H., “Fuel characteristic of sewage sludge and other supplemental fuels regarding their effect on the co-combustion process with coal”, University of Stuttgart, 2008, pp. 197–202.
15. WEF, Solids Process Design and Management, Editors: Timothy G. Shea and Michael D. Moore, 2012, ISBN: 978-0-07-178095-7, Water Environment Federation, Alexandria, USA.
16. TUBITAK-KAMAG 108G167 Project, “Management of Domestic/Urban Wastewater Sludges in Turkey, Final Report”, 2013.

Effect of Cadmium Stress on Enzyme Activity and Concentration of Mineral Nitrogen in Soil when Growing *Quercus acutissima* Seedlings

FEI HE^{1,2,**}, XIURONG GAO^{1,**}, NA CHEN¹, BAOSHAN YANG^{1,2}, HUI WANG^{1,3,*} and YIBING MA^{1,2}

¹School of Resources and Environment, University of Jinan, Jinan 250022, China

²Shandong Provincial Engineering Technology Research Center for Ecological Carbon Sink and Capture Utilization, Jinan 250022, China

³State Key Laboratory of Forest and Soil Ecology, Qingyuan Forest CERN, Institute of Applied Ecology, Chinese Academy of Sciences, Shenyang 110016, China

ABSTRACT: *Quercus acutissima*, soil enzymes peroxidase and invertase activities, and mineral nitrogen ($\text{NH}_4^+\text{-N}$, $\text{NO}_3^-\text{-N}$) concentrations were measured on the 50th and 100th day under treatments of Cd (0, 15, 30 mg kg^{-1}) with or without addition of benomyl. Results suggested enzyme activities increased with growth. A lower concentration of Cd (15 mg kg^{-1}) stimulated peroxidase and invertase activities while a higher concentration of Cd (30 mg kg^{-1}) produced a negative effect on invertase. Cd increased the soil $\text{NH}_4^+\text{-N}$ concentration. Therefore, a lower concentration of Cd increased the $\text{NO}_3^-\text{-N}$ concentration while a higher concentration of Cd reduced the $\text{NO}_3^-\text{-N}$ concentration. Addition of benomyl had no significant effect on the two enzymes of interest and mineral nitrogen ($\text{NH}_4^+\text{-N}$ and $\text{NO}_3^-\text{-N}$) concentrations at the control check treatment (0 mg Cd kg^{-1}).

INTRODUCTION

CADMIUM (Cd) poses a serious threat to the environment and human health. Its cumulative properties together with its ability to disrupt many biological systems makes it a very toxic element [1]. Cd is widely produced due to increases in anthropogenic activities and industrial development [2]. It is easily taken up by plants and its hazardous effects are well documented [3]. Thus, phytoremediation has been considered an effective technology to remedy Cd-polluted soil and much attention has been paid to related environmental remediation. *Quercus acutissima* is a keystone and widespread species across Asia, Europe, North America, and Africa [4]. It has received much attention because of its importance in producing timber, fuel wood or bioenergy, and acorns [5]. Oak can endure heavy metal pollution. However, research on effects of heavy metals on soil biochemical processes are few [6].

Mycorrhizal fungi in heavy metal polluted soils can

help plants absorb mineral nutrients to promote growth. However, mycorrhizal fungi have mycelium which absorb and fix metals and thus reducing efficacy and toxicity of soil heavy metals on plants. This results increasing tolerance of plants to heavy metal pollution [1]. Benomyl is a widely applied systemic fungicide used to kill soil fungi and basically has no direct effect on plants [7]. Therefore, addition of benomyl may be regarded as a sterilization treatment of soil fungi.

Soil enzymes are widely used for evaluation of biological indicators of soil health [8]. There are lots of reports about influence of heavy metals on soil enzymes [9] but there are no studies about soil enzyme activity when *Q. acutissima* is grown in soil polluted by Cd. $\text{NH}_4^+\text{-N}$ and $\text{NO}_3^-\text{-N}$ are sole sources of plant nitrogen absorption. Presently, the study of nitrogen mineralization mainly focuses on different ways of land use, fertilizer, temperature and humidity, hydrothermal factor, influence of climate change, and other factors [10]. However, information on changes of $\text{NH}_4^+\text{-N}$ and $\text{NO}_3^-\text{-N}$ concentrations in Cd-polluted soil with the growth of *Q. acutissima* seedlings has not been obtained. Present pot experiments studied soil enzyme (peroxidase and invertase) activities and changes of the $\text{NH}_4^+\text{-N}$ and $\text{NO}_3^-\text{-N}$ under Cd stress with or without addition of benomyl.

*Author to whom correspondence should be addressed.
E-mail: hwang_118@163.com, 86-531-82767237, University of Jinan, No. 336,
West Road of Nan Xinzhuang, Jinan, Shandong Province, China, 250022.

**Both authors contributed equally to this work.

Results will provide the theoretical basis for phytoremediation of Cd pollution and protection of oak seedlings.

MATERIALS AND METHODS

Experimental Design

Soil samples were collected from the Research Station of the Taishan Forest Ecosystem, Shandong Province (N117.10276, E36.350497). Prior to soil collection the litter layer and organic layer were removed. 0–20 cm surface soil was collected and then sieved through a 2 mm sieve. The soil is a sandy loam (sand 73.49%, silt 17.12%, and clay 9.39%) and the main soil physical and chemical properties were: pH of 4.27, water content at 9%, NH_4^+ -N at 11.09 mg kg^{-1} , NO_3^- -N 4.66 at mg kg^{-1} , soil organic carbon at 41.74 g kg^{-1} , total P at 1.70%, available P at 8.51 mg kg^{-1} , and concentration of Cd in soil was below a detection limit.

A wet separation method was applied for selecting high quality seeds. Oak seeds (Jinqiu Seed Company, Jinan, China) were washed in demineralized water, surface sterilized in 30% H_2O_2 for 30 minutes, washed in demineralized water three times, and then placed on moist filter paper for pre-germination. The developing seedlings were transferred to 8 cm diameter and 9 cm high pots which contained 200 g of dry soil and cultured in a Plant Growth Chamber. Artificial climate box culture conditions were as follows: 450 $\mu\text{mol m}^{-2} \text{s}^{-1}$ light intensity, a cycle of 14 h of light at 30°C and 10 h of dark at 18°C, and 70% humidity. Cd was added in the form of a $\text{CdCl}_2 \cdot 2.5\text{H}_2\text{O}$ solution and a modified 30 ml Hoagland's nutrient solution was added every two days. This experiment had six treatments: (1) 0 mg Cd kg^{-1} , (2) 15 mg Cd kg^{-1} , (3) 30 mg Cd kg^{-1} , (4) 0 mg Cd kg^{-1} + benomyl, (5) 15 mg Cd kg^{-1} + benomyl, and (6) 30 mg Cd kg^{-1} + benomyl. There were 36 pot seedlings for the experiment and each treatment was repeated six times. Again, benomyl was added on the 51th day to adequately kill the fungi. The pattern of adding benomyl was according to previous research. 50 mg benomyl was dissolved in 100 ml of distilled water and then add to 1 kg soil [11]. Half of the seedlings were taken out on the 50th day and all seedlings were taken out on the 100th day to measure soil enzyme activity and NH_4^+ -N and NO_3^- -N concentrations.

Determination Methods

Basic soil physical and chemical properties were

measured using conventional analytic methods [12]. Invertase activity was determined using a 3, 5—two nitro salicylic acid colorimetric method and peroxidase activity was measured using the colorimetric method [13]. Ammonium and nitrate concentrations were determined using an indophenol blue colorimetric method and a phenol disulfonic acid method, respectively [14].

Data Analysis

Effects of treatments on soil enzyme activity and NH_4^+ -N and NO_3^- -N concentrations were carried out using a one-way analysis of variance (ANOVA) at $P < 0.05$. All experimental data were means of three replications. All figures were produced by SigmaPlot 11.0. Statistical analyses were performed using SPSS Software (PASW Statistics 18.0). If the P value was < 0.05 in the ANOVA, a least significant difference (LSD) method was used between the two treatments. Differences between values at $P < 0.05$ were considered statistically significant.

RESULTS

Responses of Soil Enzyme Activities

Soil peroxidase activity on the 100th day was generally higher than on the 50th day (See Figure 1). Lower Cd concentration (15 mg kg^{-1}) had a greater positive effect on soil peroxidase activity and higher Cd concentration (30 mg kg^{-1}) had a slight positive effect on the 50th day. Both lower and higher concentrations of Cd caused no significant effect on the soil peroxidase

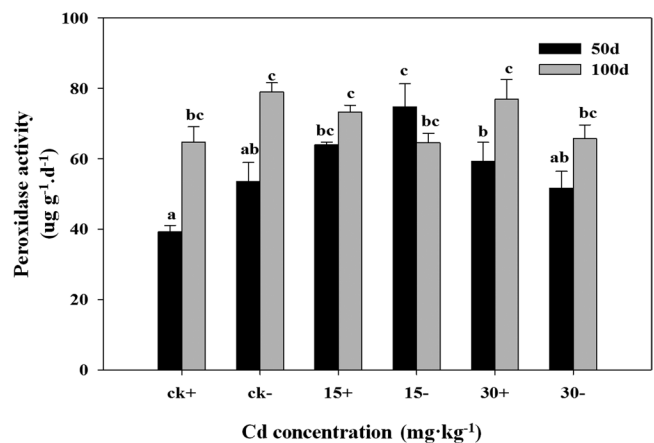


Figure 1. Peroxidase activity in different treatments. Values (means \pm SE, $n = 3$) followed by different letters indicate significant differences between treatments or time at $P < 0.05$. “+” and “-” present treatments with or without benomyl.

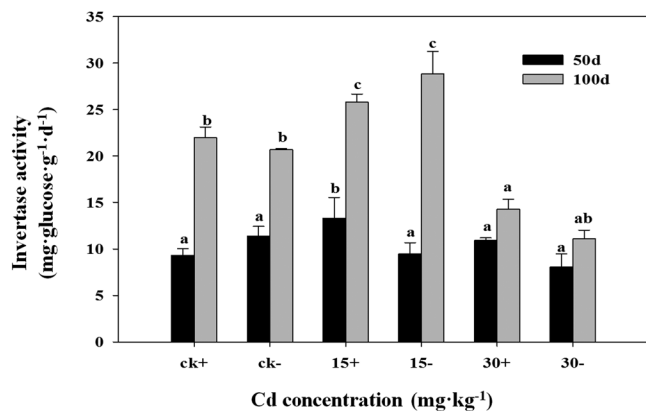


Figure 2. Invertase activity in different treatments. Values (means \pm SE, $n = 3$) followed by different letters indicate significant differences between treatments or time at $P < 0.05$. "+" and "-" present treatments with or without benomyl.

activity on the 100th day. Invertase activity changes are seen in Figure 2. Invertase activity on the 100th day was generally higher than it was on the 50th day. Regarding both the 50th and 100th day, invertase activity increased at 15 mg Cd kg⁻¹ and decreased at 30 mg Cd kg⁻¹. Effects of adding benomyl on invertase and peroxidase activities were not significant.

Responses of NH₄⁺-N and NO₃⁻-N Concentration

NH₄⁺-N increased with increasing Cd concentrations in oak rhizosphere soil under laboratory conditions (Table 1). During the 0 mg Cd kg⁻¹ treatment there was no significant NH₄⁺-N difference between the benomyl treatment and without-benomyl treatment. However, for the Cd treatment NH₄⁺-N of pot rhizosphere soil with benomyl was significantly higher than without benomyl for both the 50th day and 100th day. NO₃⁻-N concentrations under different treatments are displayed in Table 2. On the 50th day and 100th day, NO₃⁻-N values first increased with an increase of Cd concentration and then decreased at higher Cd

Table 1. Ammonium Nitrogen Concentration in Different Treatments (mg kg⁻¹).

Time (d)	Cd Concentration (mg kg ⁻¹)	NH ₄ ⁺ -N Concentration with Benomyl	NH ₄ ⁺ -N Concentration without Benomyl
50	0	0.3147 ab	0.3116 a
	15	0.3594 c	0.3252 b
	30	0.5120 d	0.3865 e
100	0	0.4681 a	0.4625 a
	15	0.6033 b	0.5137 d
	30	0.7758 c	0.5238 d

Table 2. Nitrate Nitrogen Concentration in Different Treatments (mg kg⁻¹).

Time (d)	Cd Concentration (mg kg ⁻¹)	NH ₃ ⁻ -N Concentration with Benomyl	NH ₃ ⁻ -N Concentration without Benomyl
50	0	0.3428 a	0.3370 a
	15	1.6966 b	0.4149 d
	30	1.2075 c	0.6361 e
100	0	39.65 a	40.18 a
	15	62.63 b	43.58 c
	30	58.95 d	40.50 a

concentration. The NO₃⁻-N concentration reached its maximum at 15 mg Cd kg⁻¹. During the 0 mg Cd kg⁻¹ treatment addition of benomyl had no obvious effect on the NO₃⁻-N concentration. However, for the Cd treatment the NO₃⁻-N concentration with benomyl was significantly higher than without benomyl.

DISCUSSION

Peroxidase and invertase activity demonstrated a decreasing trend after the first increase with an increase of Cd concentration on the 50th day. This is consistent with Li *et al.* [15] who carried out a pot experiment to evaluate effects of heavy metals including Cd on enzyme activities of eight vegetables grown in a saline soil. They also found that peroxidase activity increased at a low heavy metal concentration and decreased at a high concentration. This may be that a low concentration of Cd stimulated soil microbial activities [16], but the adaptability of soil to a certain Cd concentration is limited [17]. When the Cd concentration reached 30 mg kg⁻¹ over its limit invertase and peroxidase activities were reduced. Heavy metals may reduce enzymes activities interacting with the enzyme-substrate complex denaturing the enzyme protein or interacting with the protein-active group [18–19]. They can also affect synthesis of enzymes by microbial cells. Yang *et al.* [20] observed that activity of invertase was significantly decreased with an increase of Cd concentration in the soil. However, Sun *et al.* [21] observed no significant effect on soil invertase activity. This is inconsistent with the present study.

With an increase of seedling incubation time the adaptability and bioremediation function of oak seedlings were reinforced under Cd stress thus weakening the inhibition effect of the higher Cd concentration on enzyme activity [17]. Additionally, with the growth of plant roots soil microbial activities gradually increased

and may be the reason why peroxidase activity did not significantly change with an increase of Cd concentration on the 100th day [18].

Benomyl had no significant effects on peroxidase and invertase activities. The reason may be the plant root secretions increase microbial biomass [18] thereby offsetting the benomyl inhibitory effect. Presence of Cd in the soil stimulated the soil microorganism and it may decrease the effect of benomyl on invertase and peroxidase activities. Another possible reason may be the combined effects of seedlings, Cd, and benomyl. Further investigations are needed to explore the relationship between soil enzyme activity and soil microorganisms.

Heavy metals may reduce soil ammonification and nitrification potentials but in the present study the soil NH_4^+ -N concentration on the 50th and 100th days increased with an increase of Cd concentration. It may be that Cd stimulated soil microbial activities [16] and thus promoted the soil nitrogen mineralization process [22]. NO_3^- -N on the 50th and 100th day increased at lower concentration (15 mg Cd kg^{-1}) and decreased at higher concentration (30 mg Cd kg^{-1}). This is consistent with Xue *et al.* [23] who found there was a higher soil NO_3^- -N concentration in a polluted-soil with lower metal concentration. When NH_4^+ -N content was inhibited by Cd NO_3^- -N was still in the stage of increase due to Cd stimulation under the same Cd concentration stress. It may be that Cd concentrations stimulation scope is different for different types of nitrogen transformation microorganisms.

It was reported that application of benomyl may kill or inhibit some fungi and lower microbial respiration and biomass. However, benomyl may also provide a substrate and energy for live microorganisms resulting in microorganism activity enhancement. An increase of quantity and activity of microorganisms may increase nitrogen mineralization rate and available nitrogen content as well as influencing the soil nitrogen transformation process [24]. Therefore, NH_4^+ -N and NO_3^- -N contents with benomyl were generally higher than without benomyl. However, influences of adding benomyl on NH_4^+ -N and NO_3^- -N contents were not obvious for the without-Cd treatment. It may be that the Cd stimulated the effect of benomyl on nitrogen transformation microorganisms. Further research on effects of the combination effect of Cd and benomyl on soil microbial communities is necessary to ascertain the mechanism of biological processing. Additionally, it is possible to study accumulation and transfer of Cd to assess accumulation and transferability of heavy

metals in the *Q. acutissima* just as Yu *et al.* [25] and Akinci *et al.* [26] did.

CONCLUSIONS

Rhizosphere soil peroxidase and invertase activities generally increased with an increase of incubation time. Lower concentration of Cd stimulated peroxidase and invertase activities while higher concentration of Cd had an inhibitory effect on invertase. Effect of adding benomyl to soil enzymes activities of peroxidase and invertase was not obvious. Cd promoted an increasing of soil NH_4^+ -N concentration. Lower concentration of Cd promoted an increasing of soil NO_3^- -N concentration. Benomyl promoted the increasing of soil mineral concentration under Cd pollution treatments. Results from the *Quercus acutissima* pot growing experiment under Cd and/or benomyl stress improves understanding of soil enzyme activity and mineral nitrogen concentration and could provide insights into other *Q. acutissima* pot experiments. Also, the methods presented here may provide a biological tool in reforestation processes of heavy metal contaminated areas. Although, further investigations are needed to identify linkages between soil fungal functions and soil enzyme activity and mineral nitrogen concentration.

ACKNOWLEDGMENTS

The study was supported by National Natural Science Foundation of China (31270586), Science and Technology Development Plan of Shandong Province (2014GSF117029), State Key Laboratory of Forest and Soil Ecology (Grant No.LFSE2014-07), and China Scholarship Council Foundation (201402000002). Thanks to Dr. Edward C. Mignot, Shandong University, for linguistic advice.

REFERENCES

1. N. R. Sousa, M. A. Ramos, Ana P.G.C. Marques, P. M. L. Castro. A genotype dependent-response to cadmium contamination in soil is displayed by *Pinus pinaster* in symbiosis with different mycorrhizal fungi. *Appl Soil Ecol*, 2014, 76, 7–13. <http://dx.doi.org/10.1016/j.apsoil.2013.12.005>
2. C.G. Kim, S.A. Power, J.N.B. Bell. Effects of host plant exposure to cadmium on mycorrhizal infection and soluble carbohydrate levels of *Pinus sylvestris* seedlings. *Environ Pollut*, 2004, 131, 287–94. <http://dx.doi.org/10.1016/j.envpol.2004.02.015>
3. N. R. Sousa, M. A. Ramos, Ana P. G. C. Marques, P. M. L. Castro. The effect of ectomycorrhizal fungi forming symbiosis with *Pinus pinaster* seedlings exposed to cadmium. *Sci Total Environ* 2012, 414, 63–67. <http://dx.doi.org/10.1016/j.scitotenv.2011.10.053>
4. C. Sasaki, Y. Kushiki, C. Asada, Y. Nakamura. Acetone–butanol–ethanol production by separate hydrolysis and fermentation (SHF) and

- simultaneous saccharification and fermentation (SSF) methods using acorns and wood chips of *Quercus acutissima* as a carbon source. *Ind Crop Prod* 2014, 62, 286–292. <http://dx.doi.org/10.1016/j.indcrop.2014.08.049>
5. T. Wu, G. G. Wang, Q.T. Wu, X.R. Cheng, M. K. Yu, W. Wang, X. B. Yu. Patterns of leaf nitrogen and phosphorus stoichiometry among *Quercus acutissima* provenances across China. *Ecol Complex*, 2014, 17, 32–39. <http://dx.doi.org/10.1016/j.ecocom.2013.07.003>
 6. J. Opydo, K. Ufnalski, W. Opydo. Heavy Metals in Polish Forest Stands of *Quercus Robur* and *Q. Petraea*. *Water, Air, Soil Poll*, 2005, 161, 175–192. <http://dx.doi.org/10.1007/s11270-005-3522-5>
 7. B. D. Chen, Y. Q. Sun, S. Zhang. The research progress of mycorrhizal fungi heavy metal tolerance mechanism. *J Environ Sci*, 2015, 36(3), 1123–1132.
 8. O. N. Belyaeva, R. J. Haynes, O. A. Birukova. Barley yield and soil microbial and enzyme activities as affected by contamination of two soils with lead, zinc or copper. *Biol Fert Soils*, 2005, 41, 85–94. <http://dx.doi.org/10.1007/s00374-004-0820-9>
 9. B. A. Caldwell. Enzyme activities as a component of soil biodiversity: A Review. *Pedobiologia*, 2005, 49, 637–644. <http://dx.doi.org/10.1016/j.pedobi.2005.06.003>
 10. M. Zaman and S. X. Chang. Substrate type, temperature, and moisture content affect gross and net N mineralization and nitrification rates in agroforestry systems. *Biol Fert Soils*, 2004, 39, 269–279. <http://dx.doi.org/10.1007/s00374-003-0716-0>
 11. R. M. Callaway, B.E. Mahall, C. Wicks, J. Pankey, C. Zabinski. Soil fungi and the effects of an invasive forb on grasses: Neighbor identity matters. *Ecology*, 2003, 84, 129–135. [http://dx.doi.org/10.1890/0012-9658\(2003\)084\[0129:SFATEO\]2.0.CO;2](http://dx.doi.org/10.1890/0012-9658(2003)084[0129:SFATEO]2.0.CO;2)
 12. R. K. Lu. *Soil agricultural chemical analysis method*. Beijing: China Agricultural Science and Technology Press, 2000.
 13. S. Y. Guan. *Soil enzyme and its method*. Beijing: Agriculture Press, 1986.
 14. S. Bao. *Soil agricultural chemical analysis*, China Agriculture Press, Beijing, 2005, pp. 47–57.
 15. Q. S. Li, S. S. Cai, C. H. Mo, B. Chu, L. H. Peng, F.B. Yang. Toxic effects of heavy metals and their accumulation in vegetables grown in a saline soil. *Ecotox Environ Safe*, 2010, 73, 84–88. <http://dx.doi.org/10.1016/j.ecoenv.2009.09.002>
 16. B. Wang. *Ecological effect and mechanism of heavy metal Cd, Zn, Cu and Pb on soil microbes and enzymes*. Chongqing: Southwest University, 2008.
 17. G. R. Wu and J. C. Liu. Effects of Cd on the soil enzyme activity of *Aegiceras corniculatum* seedlings. *Journal of Xiamen University*, 2008, 47 (2), 118–122.
 18. P. Nannipieri. The potential use of soil enzymes as indicators of productivity, sustainability and pollution // C. E. Pankhurst, B. M. Doube, V. V. S. R Gupta. *Soil biota management in sustainable farming systems*. Melbourne: CSIRO, 1994, 238–244.
 19. X. F. Hu, Y. Jiang, Y. Shu, X. Hu, L. Liu, F. Luo. Effects of mining wastewater discharges on heavy metal pollution and soil enzyme activity of the paddy fields. *J Geochem Explor*, 2014, 139–150. <http://dx.doi.org/10.1016/j.gexplo.2014.08.001>
 20. Z. X. Yang, S.Q. Liu, D. W. Zheng, S. D. Feng. Effects of cadmium, zinc and lead on soil enzyme activities. *J Environ Sci*, 2006, 18, 1135–1141. [http://dx.doi.org/10.1016/S1001-0742\(06\)60051-X](http://dx.doi.org/10.1016/S1001-0742(06)60051-X)
 21. Y. Sun, G. Sun, Y. Xu, L. Wang, X. Liang, D. Lin, F. Hu. Assessment of natural sepiolite on cadmium stabilization, microbial communities, and enzyme activities in acidic soil. *Environ Sci Pollut Res*, 2013, 20, 3290–3299. <http://dx.doi.org/10.1007/s11356-012-1261-x>
 22. H. D. Tian. *Characteristics of soil nitrogen mineralization of different urban forests in karst areas*. Changsha: Central South University of Forestry and Technology, 2013.
 23. K. Xue, J.D. van Nostrand, J. Vangronsveld, N. Witters, J.O. Janssen, J. Kumpiene, G. Siebielec, R. Galazka, L. Giagnoni, M. Arenella, J.-Z. Zhou, G. Renella. Management with willow short rotation coppice increase the functional gene diversity and functional activity of a heavy metal polluted soil. *Chemosphere*, 2015, 138, 469–477. <http://dx.doi.org/10.1016/j.chemosphere.2015.06.062>
 24. M. Lang, P. Li, Z. C. Cai. Degradation of carbendazim in soil and its eco-environment effect. *Agrochemicals*, 2012, 51 (1), 8–11.
 25. R. L. Yu, G. R. Hu, W. F. Zhang, B. X. Liu. Accumulation and Transfer of Heavy Metals in the Mangroves from Quanzhou Bay Wetland, SE Coast of China. *J Residuals Sci Tech*, 2015, 12, 79–83.
 26. G. Akinci, D. Güven, G. Gök, T. Şentürk. Heavy Metals Transfer from Soil to Grass Types in Tannery Sludge Compost Amended Soil. *J Residuals Sci Tech*, 2014, 11(1), 3–7.

Trace Metals Risk Evaluation and Pollution Identification in Surficial Sediment from the Haikou Bay, South China Sea

PING SHI^{1,**}, JUN SHI^{2,**}, LINGLONG CAO^{1,3,*}, JIAN XIE^{1,*}, HAITAO TIAN¹ and YANHUI ZHAI¹

¹South China Sea Institute of Planning and Environmental Research, State Oceanic Administration People's Republic of China, Guangzhou 510300, PR China

²Haikou Marine Environment Monitoring Center, State Oceanic Administration People's Republic of China, Haikou 570310, PR China

³School of Earth Sciences and Engineering Geology, SunYat-sen University, Guangzhou 510275, PR China

ABSTRACT: Potential contamination risks and relevance of source identification for five trace metals (As, Cd, Cr, Cu, and Pb) from surficial sediments obtained in Haikou Bay were investigated by applying a set of multivariate analysis methods for the first time. It was demonstrated that metal concentrations reflecting distribution features for the metals of interest were slightly higher on the east side than those on the west side. A risk assessment conclusion revealed potential contamination areas were present in the vicinity of highly intense human development activities. Speciation obtained by an optimized BCR sequential extraction technique demonstrated that As and Cr were dominated by residual fraction. However, Pb, Cu, and Cd were mainly composed with non-residual fractions and of high bioavailability indicating these trace metals had significant anthropogenic sources. The relationship between content characteristics and trace metal fractions was revealed by Pearsons' correlation analysis. Hierarchical cluster analysis suggested that Pb, Cu, and Cd had similar sources relevant to anthropogenic sources and confirmed by chemical speciation analysis. Results provide a base for the local authority in the area of interest to monitor long term contribution of trace metals in coastal sediments and then apply strategies to address the polluted sediments.

INTRODUCTION

MARINE sediment forms a dynamic system and functions as reservoirs of metals originating from weathering of parent rocks [1–3]. Marine sediment is subjected to various pollutants of natural and artificial origin (mining, industrial, and urban effluents). Metals are concentrated gradually in sediments and are toxic at high concentrations for marine biota and humans. Since toxic metals may drastically increase in concentrations in a short time due to catastrophic events and resulting in significant effects on human health it is of considerable interest to investigate toxic metals in marine environments [4]. Toxic impact and coastal biogeochemical cycles of metals may be investigated based on measurements of these fractions. Earlier research has proven that using only total concentrations is insufficient as a standard to appraise environmental

impact of contaminated sediments since these methods are critically dependent upon particular chemical species and the binding forms of contaminants in sediments [5–6]. Measurement of the geochemical fraction of trace metals in sediment is as essential as the measurement of their total concentrations for assessment of biotoxicity and harm to organisms.

Haikou Bay located in the north of Hainan Island and with a size of approximately 43.7 km² is an important bay in south China for maritime transport and tourism. During recent years the rapid boom of the local economy and urban development have dramatically increased emissions from industrial and municipal sewage and exhaust emissions to a critical level of pollution in Haikou Bay. However, there has been little research on the temporal-spatial distribution and potential eco-toxicological risks of metals in Haikou Bay thus far.

Purposes of this research were to determine: (1) spatial patterns and chemical forms of selected metals; (2) trace metal occurrence and potential toxic pollution by Sediment Quality Guidelines (SQGs); and (3) possible sources of individual metals using multivariate statisti-

*Author to whom correspondence should be addressed.

E-mail: cllsoa@163.com (L.C.). Tel./Fax: +86-20-8421-2787

E-mail: scsmeci@163.com (J.X.). Tel./Fax: +86-20-8428-4359

**These authors contributed equally to this work

cal analyses. Results herein provide insight on levels of contamination of metals and contributes to prevention and control of metal contamination in Haikou Bay.

MATERIALS AND METHODS

Sediment Stations

During the April of 2013 14 surficial sediment (0–8 cm) samples were collected in triplicate using a vanveen grab sampler with a small vessel and then sealed in polyethylene bags for further experiments. Figure 1 displays a map of sampling locations.

Metal Analysis

Sequential extraction was employed according to an optimized BCR four step procedure [7]. Table 1 displays brief steps for sequential extraction of samples. General recovery rates of all the metals ranged from 88% to 110%.

Regarding total digestion about 200 mg of sediment samples were placed in a 10 ml aqua regia and hydrofluoric acid solution in a Polytetrafluoroethylene digestion vessel.

Metal contents were determined by ICP-MS and quality control was guaranteed with standard samples

(GBW 07314). Duplicate determinations were performed for all samples. Control determinations were conducted for given analysis under the same conditions as true determination but with omission of the samples results also deemed reliable.

Data Analysis

Pearson correlation (PC) and Hierarchical cluster analysis (HCA) were conducted using SPSS where a $P < 0.05$ was considered statistically significant. PC was used to analyze relationships among different metal fractions. HCA was conducted for evaluation of similarities and differences in metal behaviors for each fraction as well as analysis and characterization of possible sources of metal pollution and assessment of the level of relationship among variables.

RESULTS AND DISCUSSION

Levels of Metals

Table 2 summarizes statistical results of metal concentration collected from Haikou Bay. The large spatial distribution variation of metals in Haikou Bay was presented in Figure 2 and suggested that Cd content was slightly higher in the east side versus the west side.

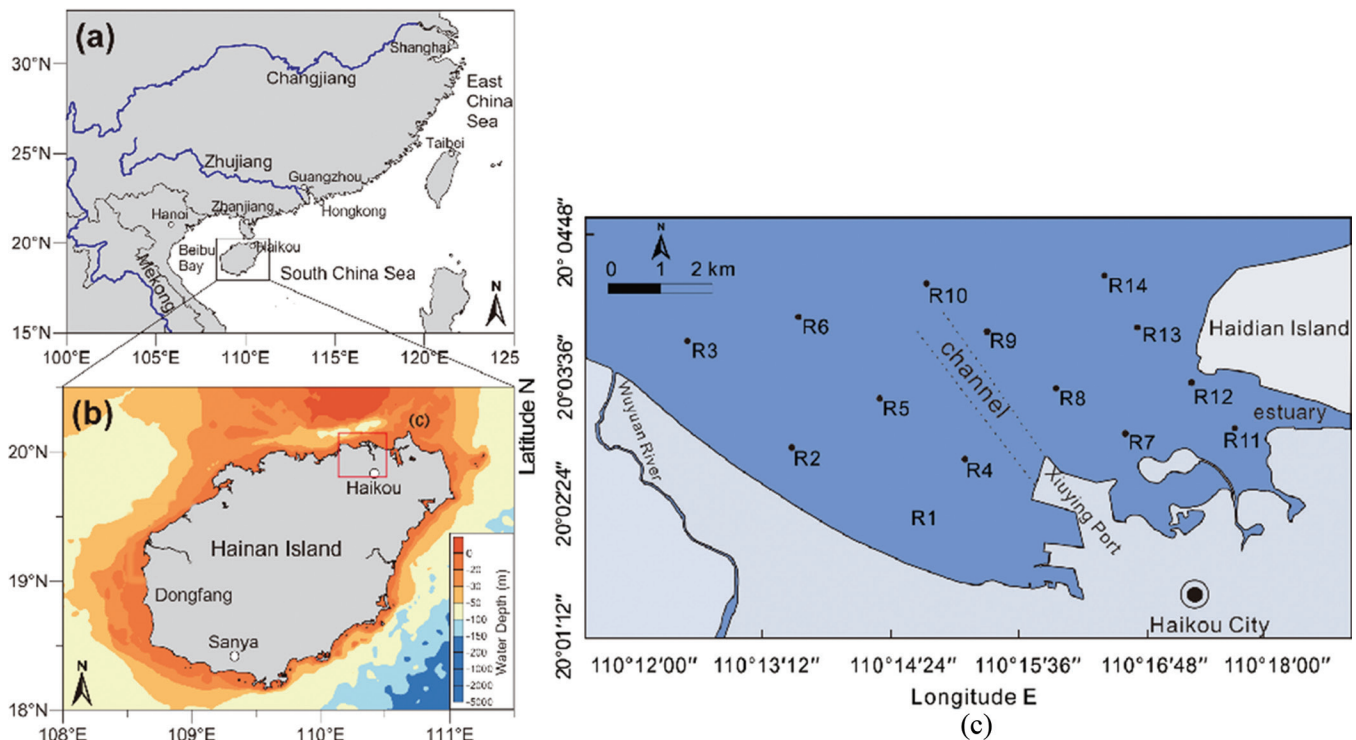


Figure 1. Locations of Haikou Bay and sampling sites.

Table 1. Speciation Analysis Scheme for Fractionation of Trace Metals.

Step	Phases	Procedure
1	Fraction 1 (F1, Acid soluble fraction)	Acetic acid (30 mL) was added to 0.5 g of dry sample and shaken at room temperature for 20 h.
2	Fraction 2 (F2, Reducible fraction)	0.5 M hydroxylamine hydrochloride (20 mL, pH = 1.5) was added to the residues in the tube obtained during Step 1, shaken for 15h at 20 ± 2°C.
3	Fraction 3 (F3, Oxidizable fraction)	Incubated at 85°C for 1 h with occasional shaking; 8.8 M H ₂ O ₂ (20 mL, pH = 2.0) were added and incubated for 2 h, followed by addition of 1 M MNH ₄ C ₂ H ₃ O ₂ (25 mL, pH = 2.0), and shaking at room temperature for 15 h.
4	Fraction 4 (R, Residual fraction)	The residue from the last step was performed using the same method as described above.

Distribution features for most selected metals concentrations displayed a ring shape and descended from the shore to the bay by different levels except for Pb. The highest concentrations of Pb occurred at locations Z4, Z5, and Z6 located in the sea channel of the Xiuying Port.

Among typical coastal and estuary bays selected for comparative analysis (Table 2), average contents of As and Cr in the Haikou Bay were higher than for those in Sanya Bay, Daya Bay, and Zhelin Bay but less than those in Quanzhou Bay and Bohai Bay. Mean value of Cd (0.11 mg kg⁻¹) in the Haikou Bay was lower than that in Sanya Bay, Quanzhou Bay, and Bohai Bay and nearly 2 times higher than that in Zhelin Bay and Daya Bay. Seen in Table 2, mean content of Pb and Cu in study areas were less than those in other national coastal bays except Sanya Bay, a tropical tourist destination in south China's Hainan Province. Furthermore, concentrations of the five metals in Haikou Bay were much less than for those in the bigger coastal bays around the world including Masan Bay in the South Gyeongsang Province, South Korea. It should be pointed out that

sediments were severely polluted by Cu, Cr, and Pb in Haikou Bay as compared with corresponding continental shelves of the South China Sea (BMSC) background levels.

Metal Enrichment and Potential Risk

SQGs are useful for analysis of sediment pollution by comparing metal concentration in sediment with quality guidelines [8]. Two levels of sediment quality guidelines (TEL and PEL) were adopted in this study even though different SQGs have been developed. TEL and PEL designate three scopes of chemical contents and each with a different level of association with adverse biological effects: rare (minimal effect scope; C (content) ≤ TEL), occasional (possible effect scope; TEL ≤ C (content) ≤ PEL), and frequent (probable effect scope; C (content) ≥ PEL) [14].

Table 2 suggests that PEL as a limit was never exceeded within the study areas and even Cd and Cu never exceeded TEL. This indicates that these metallic elements would likely not cause negative impact in

Table 2. Summary of Metal Contents in Different Bay Areas (ug g⁻¹).

Location		As	Cd	Cr	Cu	Pb	References	Anthropogenic Activities
Haikou Bay	range	2.24–21.60	0.015–0.25	9.70–81.20	1.30–22.30	13.3–41.7	this study	Tourism, transportation and marine reclamation land
	average	9.11	0.11	41.04	11.21	28.43		
Sanya Bay		7.1	0.13	12.4	9.5	17.5	[3]	Tourism
Daya Bay		7.01	0.04	30.03	11.40	44.18	[1]	Fish, tourism, industrial and transportation
Zhelin Bay		5.47	0.051	20.20	11.90	41.7	[8]	Fish
Quanzhou Bay	average	21.70	0.69	82.00	71.40	67.70	[9]	Fish and transportation
Bohai Bay		—	0.22	101.00	38.50	34.70	[10]	Fish, industrial and transportation
Masan Bay, Korea		—	1.24	67.10	43.40	44.00	[11]	Industrial activities
BMSC	—	9.71	0.18	39.30	7.43	15.60	[12]	
SQGs	TEL	7.90	0.60	42	3537	35.0	[13]	
	PEL	17.0	3.53	90	197	91.3		
% samples exceeded TEL		57	0	43	0	28	—	
% samples exceeded PEL		0	0	0	0	0	—	

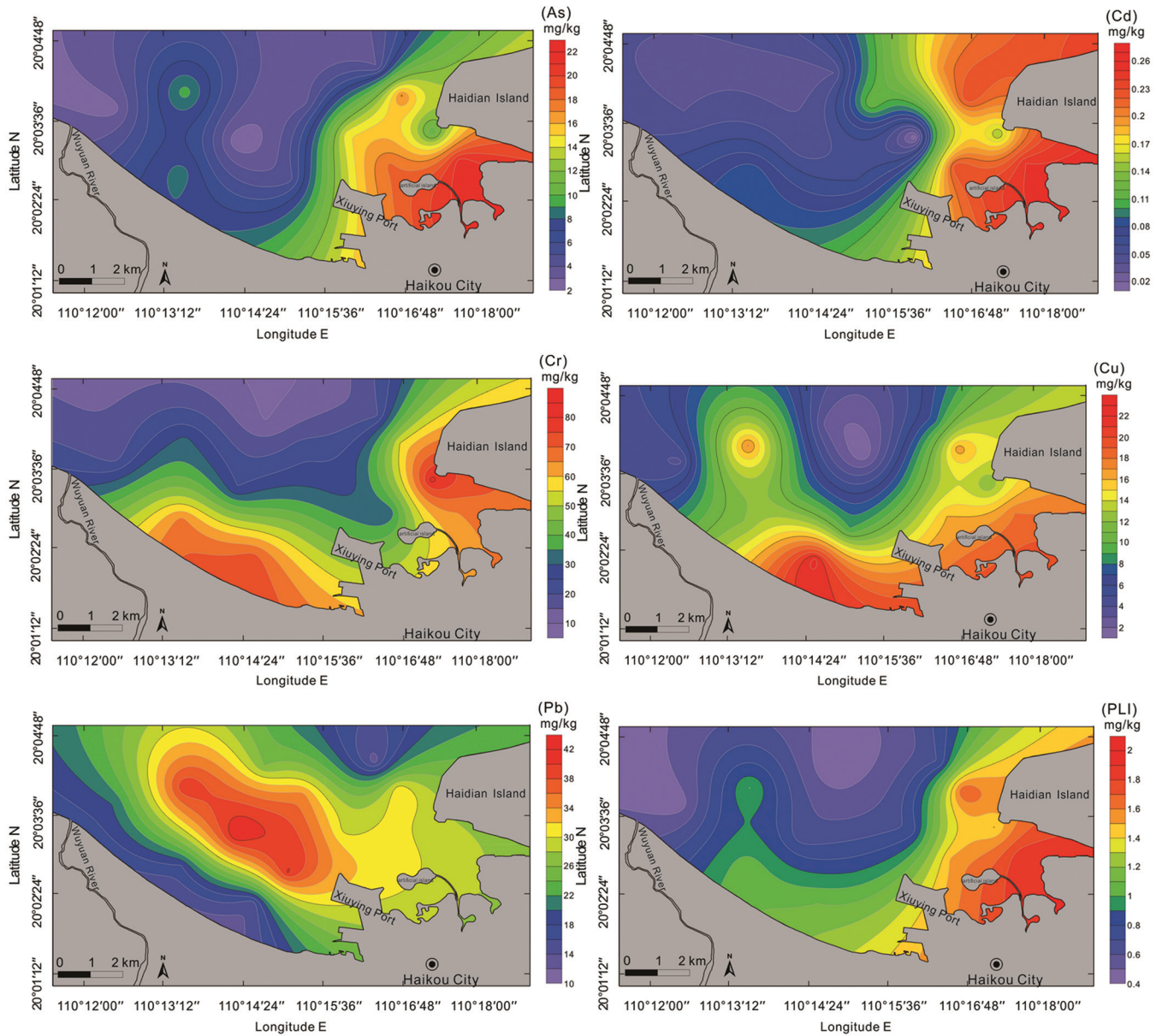


Figure 2. *PLI and spatial distribution of metal concentrations.*

the study areas. Percentages of samples exceeding the TEL for As, Cr, and Pb were 21%, 7%, and 14%, separately, indicating that adverse effects on benthic organisms were occasionally observed in the sea area. These findings suggested that more attention should be paid to As, Cr, and Pb on the shore side of Haikou Bay due to potential environmental risks. However, concentrations of As and Pb in about 30% and 25% of sediment samples were higher than their respective regional background levels. Thus, it should be more reliable to evaluate contamination of As and Pb in sediments by comparison to regional background levels.

Pollution load index (*PLI*) is the other well documented and frequently used norm for evaluation of

metal contamination. *PLI* could be acquired as a concentration factor (*CF*) for each individual metallic element using a corresponding background value [13] with the following equation:

$$CF = C_{\text{metal}}/C_{\text{background}} \quad (1)$$

$$PLI = (CF_1x, CF_2x, CF_4x, \dots CF_n) 1/n \quad (2)$$

where *n* is number of metals examined.

PLI was employed to evaluate integrated contamination of combined poisonous groups at sample sites. *PLI* > 1 demonstrates contamination of trace metals and *PLI* < 1 indicates no metal contamination. Distribution of *PLI* in Figure 2 and Figure 3 demonstrated

that pollution characteristics were generally in line with content distribution. *PLI* values were clearly lower than 1 in Z3 (0.45), Z4 (0.90), Z5 (0.64), Z8 (0.73), Z9 (0.56), Z10 (0.42), and Z14 (0.72). *PLI* values for rest stations varied from 1.06 to 1.87. A maximum *PLI* value of 1.87 was at station Z11 making it the most contaminated site and followed in order by Z13, Z7, Z12, Z1, Z2, and Z6 with respective *PLI* values of 1.71, 1.53, 1.40, 1.10, and 1.06. This suggests that contamination areas were in the vicinity of human development activities with high intensity.

Application of Metal Speciation

It has been documented that trace metal speciation and solubility primarily depend on physiochemical form and influence migration, biological availability, and virulence of metals [7]. Therefore, sediments collected from the study areas were processed with optimized BCR sequential extraction protocols and behavior of metals in sediments is presented in Figure 4. Selected metals exhibited various speciation patterns and some showed dramatic spatial variations. During each fraction the descending orders of metals were as follows:

F1 (Acid soluble): Cd > Pb > Cu > As > Cr

F2 (Reducible) : Pb > Cu > Cd > As > Cr

F3 (Oxidizable): Cd > Cu > Pb > Cr > As

F4 (Residual): As > Cr > Cu > Cd > Pb

Seen in Figure 2, fractionation patterns of As and Cr were somewhat similar in different sediment samples. Dominance of the residual fraction (R) for As and Cr in the sediment samples was 73% and 69%, respectively. These results suggested that metallic fractions were closely correlated with aluminosilicate minerals. Most of the residual metals fraction bind to silicate lat-

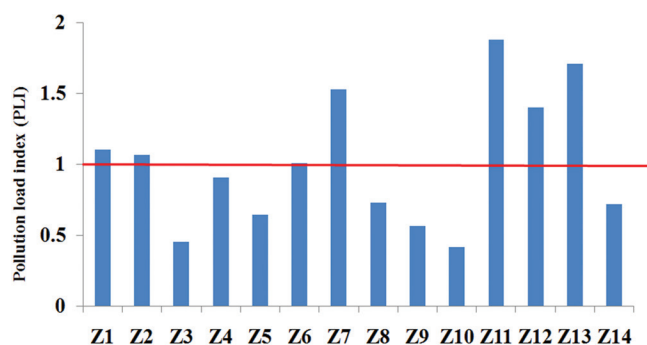


Figure 3. Pollution load index (PLI) of selected metals from Haikou Bay.

tices and can hardly be released unless a weathering process is present. Thus, in this fraction metals are in the most stable state. However, the least contributions were found to be the acid soluble phase with 4% for As and 3% for Cr. Because content of the acid soluble phase is entirely negligible it may be concluded that As and Cr in Haikou Bay are irrelevant contaminants mainly derived from weathering, soil formation, and other natural processes.

Cu was bound to non-residual phases and account for 52%. Further, 28%, 19%, and 5% of Cu was bound to reducible, oxidizable, and acid soluble phases. Even though percentage of Cu in acid soluble fraction was only 5%, with a mean value of total Cu (41.04 mg/kg) Cu may also be released from the reducible fraction into water with constant changes in environmental conditions. Cu is an environmental hormone and may significantly impact procreation capability of a biological system [11]. Thus, if Cu is released to the water from the sediment it is of a relatively higher ecological risk and potential risk of Cu contamination in the river should be monitored.

Pb was primarily related to the reducible fraction (48%) and then the residual (22%), oxidizable (17%), and acid soluble (13%) phases. The change of Pb in different phases of samples was the most significant among the metals investigated. Non-residual are regarded as mobile fractions and trace metals in these fractions are extractable. Order of extractability of metals in mobile fractions was as follows: Pb (78%) > Cd (76%) > Cu (52%) > Cr (31%) > As (27%). More attention should be given to the potential Pb pollution in Haikou Bay.

According to the content of Cd in each fraction the descending order was as follows: acid soluble (37%) > residual (24%) > oxidizable (20%) > reducible (19%). The acid-soluble fraction (F1) obtained from the initial step of successive extraction includes water soluble, ion exchangeable, and carbonate binding forms of trace metals. Since these metals are primarily associated with clay and soil humus and are relatively vulnerable to changing environments, transformation and migration of these metals occur readily in acidic environments. Therefore, trace metals in the acid soluble fraction are of great concern for aquatic organisms because their bioavailability and mobility are relatively high and potential toxicity cannot be ignored. It has been reported that alterations in salinity level and increase of pH value increase the mobility of trace metals in aquatic ecosystems [15]. Cd was the most predominant one among the selected metals in the acid soluble phase. It has long been recognized that Cd is an important metal for environmental

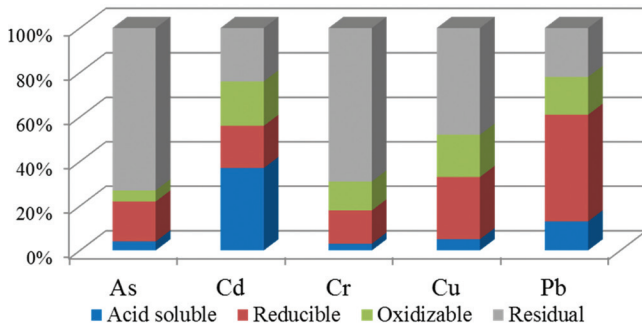


Figure 4. Distribution of studied metals in different chemical fractionation from Haikou Bay.

behavior. Furthermore, Cd concentration in study areas was high from 0.015 to 0.25 mg/kg. It could be inferred that possible Cd contamination in Haikou Bay should be monitored regularly.

Identification of Pollution Sources

The acid-soluble phase and reducible phase constitute more available phases where trace metals have high bio-availability, mobility, and potential toxicity [6–7]. Based on extractable amounts of metals in reducible and acid soluble fractions the descending order of trace metals in these fractions was as follows: Pb > Cd > Cu > As > Cr.

Displayed in Figure 3, Pb, Cd, and Cu were among the top three of the most mobile metals while As and Cr were the least two mobile metals. Metals in contaminated sediments are mobile while in uncontaminated sediments they are mainly immobile since metals are primarily bound to extractable fractions in contaminated sediments but bound to silicate in uncontaminated sediments. Since As and Cr are primarily in immobile fractions instead of mobile fractions they are thought to be from lithosphere.

Human-induced effects are considered primary reasons that contents of Pb, Cd, and Cu are higher in mobile fractions than for those in immobile fractions. Results that Cd, Pb, and Cu had higher mobility rates in more available fractions F1 and F2 indicated that there were

Table 3. Pearson's Correlation for Geochemical Phases and Trace Metal Concentration.

	Cr	Cu	Pb	Cd	As
F1	0.314	0.510*	0.396	0.622*	0.211
F2	0.510*	0.649*	0.458*	0.689**	0.691**
F3	0.071	0.810**	0.748**	0.764**	0.566*
R	0.904**	0.753**	0.965**	0.315	0.899**

Notes: ** $p < 0.01$, * $p < 0.05$.

environmental pollutions and probable toxic effects of these trace metals largely due to anthropogenic activity.

Statistical tools were used to further analyze level of metal pollution and identify its sources. Factor analysis and cluster analysis together with the correlation matrix provided critical information for identification of contamination sources and dynamics of the pollutants.

It is crucial to understand trace metal pollution and improve management of coastal sediments for the purpose of integrating risk evaluation and geochemical fractionation as well as total amounts of metals. The correlation matrix between the fraction and concentration of trace metals was summarized in Table 3. It was seen that except As-F1, Cr-F1, Cd-R Cr-F3, and Pb-F1 the contents of all the selected trace metals were highly and positively correlated with their corresponding metals speciation. This suggests that total content of metals could be used to assess level of pollution.

Demonstrated in Table 4 many trace metals were significantly associated with each other ($p < 0.05$) based on values for Pearson correlation coefficients. The Pearson matrix for example indicated a close association among metals Pb, Cd, and Cu. Significant positive correlations between Pb and Cu or Cd ($p = 0.831$ and $p = 0.869$) and those between Cu and Cd ($p = 0.712$) indicated these three metals might have identical sources most probably related to anthropogenic activities like discharges of wastewater from urban and industrial areas. It was a significant associated between As and Cr ($p = 0.665$) suggesting these two metals were originated from lithogenic sources.

Hierarchical Cluster Analysis for Metals in Fractions

Based on similarities/dissimilarities, the trace metals could be classified into two clusters by HCA which was performed using the Ward method and squared Euclidean distance.

Dendrograms are presented in Figure 5(a). While the

Table 4. Correlation Analysis of Trace Metals of Sediment Samples.

	Cr	Cu	Pb	Cd	As
Cr	1				
Cu	0.310	1			
Pb	0.351	0.831**	1		
Cd	0.433*	0.712**	0.869**	1	
As	0.665**	0.228	0.398	0.451*	1

Notes: * $p < 0.05$ and ** $p < 0.01$.

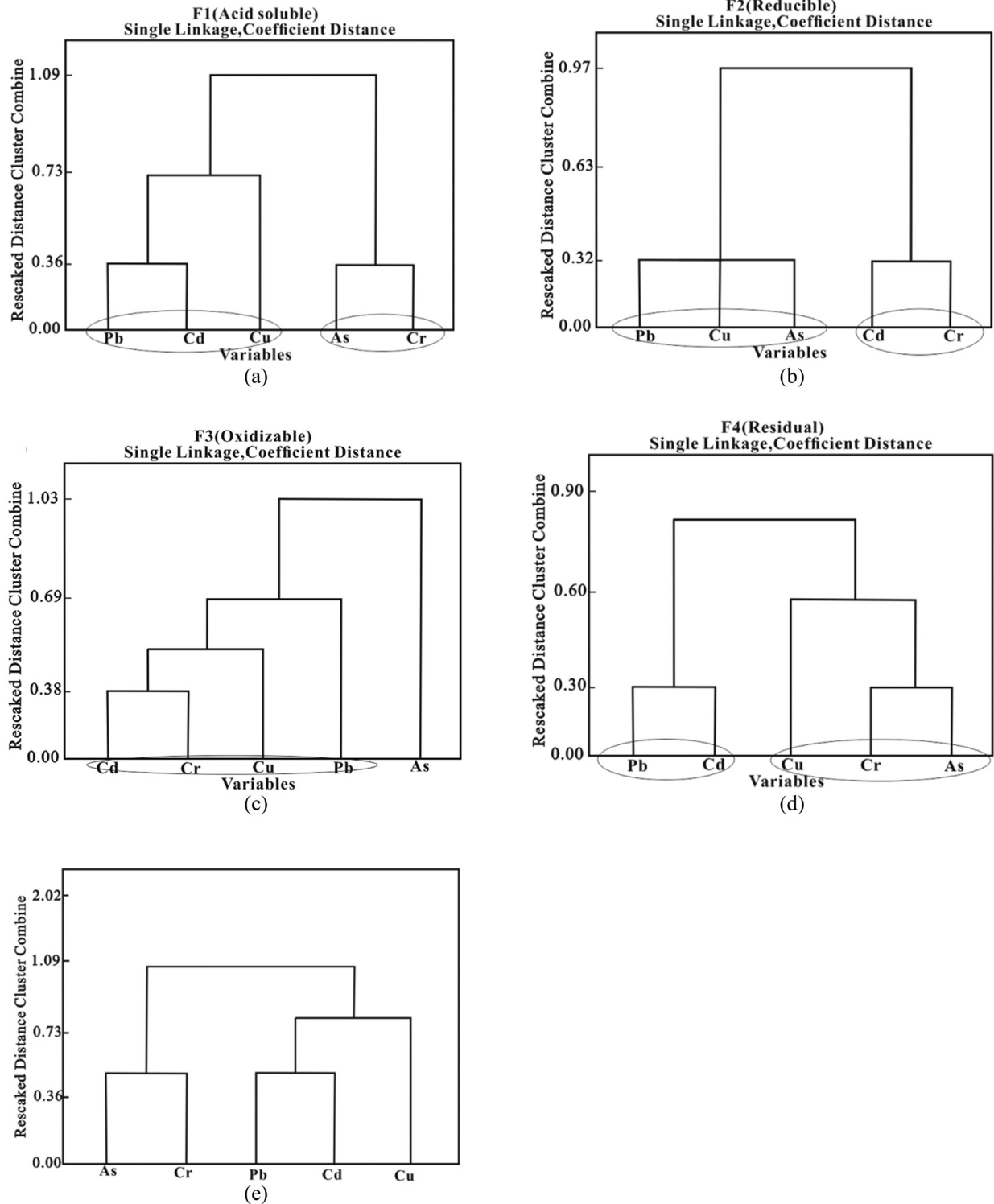


Figure 5. Dendrogram of trace metal of each fraction and concentrations.

first group of Pb, Cu, and Cd in F1 fraction exhibited subjective behaviors, As and Cr were classified into the second group. Similar behaviors were exhibited in Figure 5e. Seen in Table 3, correlations could be seen between clustering metals and total metals. Such a case

may be related to sensitive environmental changes for acid-soluble fractions [16].

Regarding HCA results for the F2, Cr and Cd showed various behaviors as compared with the other three metals. There were two sub-groups for the other three met-

als of which Pb and As were categorized into the first group due to their similarities in behavior. Cu was classified into the second group [Figure 5(b)]. These clusters reflected metal concentration in the reducible fraction.

Metals in the F3 fraction were divided into two subgroups as seen in Figure 5(c). Cd, Cr, Cu, and Pb were classified into the first group and As was classified into the second group. F3 is associated with the organic and sulfide fraction [1]. Therefore, these similarities and dissimilarities are essentially caused by binding affinities of metals to organic matter.

Figure 5(d) displays the results of the residual fraction obtained with HCA. It was discovered that behaviors of Pb and Cd were relatively different from the other three metals. Trace metals are associated with aluminosilicate minerals in the residual fraction (R). This may be the reason that Pb and Cd produced by human activities are in the sediment rather than in the soil parent materials.

The dendrogram generated with HCA is seen in Figure 5(e). Pb, Cd, and Cu were in cluster 1 and all of which were identified as pollutants originated from anthropogenic sources (i.e., urban/industrial areas). A correlation matrix and HCA were performed to determine main differences among the studied metals. A statistically significant positive correlation was observed among Pb, Cd, and Cu suggesting these three trace metals were originated from similar sources and moved together. The two groups of spatial similarities identified by HCA were formed by either anthropogenic sources or natural origin. Taken together, different evaluation techniques and different assessment indices ought to be deliberately chosen and utilized for distinctive purposes and scales and extensive comparison of different methods could lessen errors and increase accuracy.

CONCLUSION

Significantly high content of metals was found in sediment samples from the west side of Haikou Bay and especially the estuary area suggesting that contamination areas were in the vicinity of human development activities and with high intensity. Results suggest that trace metals Cd, Pb, and Cu are expected to cause toxic effects which are likely to occur frequently.

Speciation results obtained by an optimized BCR sequential extraction technique demonstrated that Pb, Cu, and Cd were abundant in the non-residual phases with high bioavailability. However, As and Cr were dominant in the residual phase with relatively low bioavailability. Based on contents of trace metals in extractable fractions, order of trace metals in descending rank in acid

soluble and reducible phases (the more available fractions) was as follows: Pb > Cd > Cu > As > Cr. PCA suggested that total content of metals could be used reliably for determination of pollution level. HCA suggested that Pb, Cu, and Cd had similar origins related to anthropogenic sources which was confirmed by chemical speciation analysis. The study suggests that it is essential for the local authority to have a base to monitor long term access of trace metals into coastal sediments for better understanding and preventing trace metals contamination in the target area.

ACKNOWLEDGEMENTS

This work was supported by the Ocean Public Welfare Scientific Research Project, State Oceanic Administration People's Republic of China (Grant No.201105024).

REFERENCES

1. Cao L.L., Huang C.G., Wang J.H., Xie J. 2014. "Pollution status of selected metals in surface sediments of the Pearl River Estuary and Daya Bay, South China Sea," *Journal of Residuals Science & Technology*. 11(4), 119–130.
2. Delgado J., Barba-Brioso C., Nieto J.M., Boski T. 2011. "Speciation and ecological risk of toxic elements in estuarine sediments affected by multiple anthropogenic contributions (Guadiana saltmarshes, SW Iberian Peninsula): I. Surficial sediments," *Science of the Total Environment*. 409, 3666–3679. <http://dx.doi.org/10.1016/j.scitotenv.2011.06.013>
3. Hu B.Q., Cui R.Y. 2013. "Occurrence and distribution of trace metals in surface sediments of the Changhua River Estuary and adjacent shelf (Hainan Island)," *Marine Pollution Bulletin*. 76, 400–405. <http://dx.doi.org/10.1016/j.marpolbul.2013.08.020>
4. Cao L.L., Tian H.T. 2015. "Multivariate Analyses and Evaluation of Trace metals by Chemometric BCR Sequential Extraction Method in Surface Sediments from Lingdingyang Bay, South China," *Sustainability*. 7, 4938–4951. <http://dx.doi.org/10.3390/su7054938>
5. Wu Q.Q., Liu G.Q. 2015. "Screening of Heavy Metal Tolerant Microbes in Sludge and Removal Capability of Lead," *Journal of Residuals Science & Technology*. 12, (2), 85–91. <http://dx.doi.org/10.12783/issn.1544-8053/12/2/7>
6. Cao L.L., Zhao M.L. 2014. "Spatial risk assessment and sources of trace metals in surface sediments from Yangpu Port in the western Hainan Island," *BioTechnology: An Indian Journal*. 10(12):828–835.
7. Huang L.L., Pu X.M., Pan J.F., Wang B. 2013. "Heavy metal pollution status in surface sediments of Swan Lake lagoon and Rongcheng Bay in the northern Yellow Sea," *Chemosphere*. 93, 1957–1964. <http://dx.doi.org/10.1016/j.chemosphere.2013.06.080>
8. Gu Y.G., Lin Q. 2014. "Metal pollution status in Zhelin Bay surface sediments inferred from a sequential extraction technique, South China Sea," *Marine Pollution Bulletin*. 64, 712–720. <http://dx.doi.org/10.1016/j.marpolbul.2014.01.030>
9. Yu R.L., Yuan X. 2008. "Trace metal pollution in intertidal sediments from Quanzhou Bay, China," *Journal of Environmental Sciences*. 20, 664–669. [http://dx.doi.org/10.1016/S1001-0742\(08\)62110-5](http://dx.doi.org/10.1016/S1001-0742(08)62110-5)
10. Gao X.L., Li P.M. 2012. "Concentration and fractionation of trace metals in surface sediments of intertidal Bohai Bay, China," *Marine Pollution Bulletin*. 2012, 64, 1529–1536. <http://dx.doi.org/10.1016/j.marpolbul.2012.04.026>
11. Hyun S., Lee C.H., Lee T., Choi J.W. 2007. "Anthropogenic contributions to trace metal distributions in the surface sediments of Masan Bay, Korea," *Marine Pollution Bulletin*. 54, 1059–1068. <http://dx.doi.org/10.1016/j.marpolbul.2007.02.013>

12. Zhang Y.H., Du J. M. 2005. "Background values of pollutants in sediments of the South China," *Acta Oceanologica Sinica*. 27,161–166.
13. ISQG, 1995. *Interim Sediment Quality Guidelines*, Environment Canada, Ottawa. p.9.
14. Qiu Y.W., Yu K.F. 2011. "Accumulation of trace metals in sediment of mangrove wetland from Hainan Island," *Journal of Hazardous Materials*. 30, 102–108.
15. Ozbas E.E., Ozcan H.K., Balkaya N., Demir G., Bayat C. 2007. "Trace metal amounts in soil and sediments of surface water sources in the industrial regions of Istanbul," *Journal of Residuals Science & Technology*. 4 (4), 89–94.
16. Hakanson L. 1980. "An ecological risk index for aquatic pollution control. a sedimentological approach," *Water Research*. 14, 975–1001. [http://dx.doi.org/10.1016/0043-1354\(80\)90143-8](http://dx.doi.org/10.1016/0043-1354(80)90143-8)

GUIDE TO AUTHORS

1. Manuscripts shall be sent electronically to the Editor-in-Chief, Dr. P. Brent Duncan at pduncan@unt.edu using Microsoft Word in an IBM/PC format. If electronic submission is not possible, three paper copies of double-spaced manuscripts may be sent to Dr. P. Brent Duncan, (Editor of the *Journal of Residuals Science & Technology*, University of North Texas, Biology Building, Rm 210, 1510 Chestnut St., Denton, TX 76203-5017) (Tel: 940-565-4350). Manuscripts should normally be limited to the space equivalent of 6,000 words. The editor may waive this requirement in special occasions. As a guideline, each page of a double-spaced manuscript contains about 300 words. Include on the title page the names, affiliations, and addresses of all the authors, and identify one author as the corresponding author. Because communication between the editor and the authors will be electronic, the email address of the corresponding author is required. Papers under review, accepted for publication, or published elsewhere in journals are normally not accepted for publication in the *Journal of Residuals Science & Technology*. Papers published as proceedings of conferences are welcomed.
2. Article titles should be brief, followed by the author's name(s), affiliation, address, country, and postal code (zip) of author(s). Indicate to whom correspondence and proofs should be sent, including telephone and fax numbers and e-mail address.
3. Include a 100-word or less abstract and at least six keywords.
4. If electronic art files are not supplied, submit three copies of camera-ready drawings and glossy photographs. Drawings should be uniformly sized, if possible, planned for 50% reduction. Art that is sent electronically should be saved in either a .tif or .JPEG files for superior reproduction. All illustrations of any kind must be numbered and mentioned in the text. Captions for illustrations should all be typed on a separate sheet(s) and should be understandable without reference to the text.
5. DEStech uses a numbered reference system consisting of two elements: a numbered list of all references and (in the text itself) numbers in brackets that correspond to the list. At the end of your article, please supply a numbered list of all references (books, journals, web sites etc.). References on the list should be in the form given below. In the text write the number in brackets corresponding to the reference on the list. Place the number in brackets inside the final period of the sentence cited by the reference. Here is an example [2].
Journal: 1. Halpin, J. C., "article title", *J. Cellular Plastics*, Vol. 3, No. 2, 1997, pp. 432–435.
Book: 2. Kececioglu, D. B. and F.-B. Sun. 2002. *Burn-In Testing: Its Quantification and Optimization*, Lancaster, PA: DEStech Publications, Inc.
6. Tables. Number consecutively and insert closest to where first mentioned in text or type on a numbered, separate page. Please use Arabic numerals and supply a heading. Column headings should be explanatory and carry units. (See example at right.)
7. Units & Abbreviations. Metric units are preferred. English units or other equivalents should appear in parentheses if necessary.
8. Symbols. A list of symbols used and their meanings should be included.
9. Page proofs. Authors will receive page proofs by E-mail. Proof pages will be in a .PDF file, which can be read by Acrobat Reader. Corrections on proof pages should be limited to the correction of errors. Authors should print out pages that require corrections and mark the corrections on the printed pages. Pages with corrections should be returned by FAX (717-509-6100) or mail to the publisher (DEStech Publications, Inc., 439 North Duke Street, Lancaster, PA 17602, USA). If authors cannot handle proofs in a .PDF file format, please notify the Editor, Dr. P. Brent Duncan at pduncan@unt.edu.
10. Index terms. With proof pages authors will receive a form for listing key words that will appear in the index. Please fill out this form with index terms and return it.
11. Copyright Information. All original journal articles are copyrighted in the name of DEStech Publications, Inc. All original articles accepted for publication must be accompanied by a signed copyright transfer agreement available from the journal editor. Previously copyrighted material used in an article can be published with the *written* permission of the copyright holder (see #14 below).
12. Headings. Your article should be structured with unnumbered headings. Normally two headings are used as follows:
Main Subhead: DESIGN OF A MICROWAVE INSTALLATION
Secondary Subhead: Principle of the Design Method
If further subordination is required, please limit to no more than one (*Third Subhead*).
13. Equations. Number equations with Arabic numbers enclosed in parentheses at the right-hand margin. Type superscripts and subscripts clearly above or below the baseline, or mark them with a caret. Be sure that all symbols, letters, and numbers are distinguishable (e.g., "oh" or zero, one or lowercase "el," "vee" or Greek nu).
14. Permissions. The author of a paper is responsible for obtaining releases for the use of copyrighted figures, tables, or excerpts longer than 200 words used in his/her paper. Copyright releases are permissions to reprint previously copyrighted material. Releases must be obtained from the copyright holder, which is usually a publisher. Forms for copyright release will be sent by the editor to authors on request.

Table 5. Comparison of state-of-the-art matrix resins with VPSP/BMI copolymers.

Resin System	Core Temp. (DSC peak)	T _E	Char Yield, %
Epoxy (MY720)	235	250	30
Bismaleimide (H795)	282	>400	48
VPSP/Bismaleimide copolymer			
C379: H795 = 1.9	245	>400	50
C379: H795 = 1.4	285	>400	53

General: The *Journal of Residuals Science & Technology* and DEStech Publications, Inc. are not responsible for the views expressed by individual contributors in articles published in the journal.